

Isotachophoresis and zone electrophoresis in narrow bore tubes

Citation for published version (APA):

Mikkers, F. E. P. (1980). *Isotachophoresis and zone electrophoresis in narrow bore tubes*. [Phd Thesis 1 (Research TU/e / Graduation TU/e), Chemical Engineering and Chemistry]. Technische Hogeschool Eindhoven. <https://doi.org/10.6100/IR80187>

DOI:

[10.6100/IR80187](https://doi.org/10.6100/IR80187)

Document status and date:

Published: 01/01/1980

Document Version:

Publisher's PDF, also known as Version of Record (includes final page, issue and volume numbers)

Please check the document version of this publication:

- A submitted manuscript is the version of the article upon submission and before peer-review. There can be important differences between the submitted version and the official published version of record. People interested in the research are advised to contact the author for the final version of the publication, or visit the DOI to the publisher's website.
- The final author version and the galley proof are versions of the publication after peer review.
- The final published version features the final layout of the paper including the volume, issue and page numbers.

[Link to publication](#)

General rights

Copyright and moral rights for the publications made accessible in the public portal are retained by the authors and/or other copyright owners and it is a condition of accessing publications that users recognise and abide by the legal requirements associated with these rights.

- Users may download and print one copy of any publication from the public portal for the purpose of private study or research.
- You may not further distribute the material or use it for any profit-making activity or commercial gain
- You may freely distribute the URL identifying the publication in the public portal.

If the publication is distributed under the terms of Article 25fa of the Dutch Copyright Act, indicated by the "Taverne" license above, please follow below link for the End User Agreement:

www.tue.nl/taverne

Take down policy

If you believe that this document breaches copyright please contact us at:

openaccess@tue.nl

providing details and we will investigate your claim.

ISOTACHOPHORESIS AND ZONE ELECTROPHORESIS IN NARROW BORE TUBES

PROEFSCHRIFT

ter verkrijging van de graad van doctor in de
technische wetenschappen aan de Technische
Hogeschool Eindhoven, op gezag van de
rector magnificus, prof. ir. J. Erkelens, voor
een commissie aangewezen door het college
van dekanen in het openbaar te verdedigen op
dinsdag 28 oktober 1980 te 16.00 uur

door

FRANCISCUS EDMUNDUS PETRUS MIKKERS

Geboren te Valkenswaard

© 1980 by F.E.P. Mikkers, The Netherlands

Dit proefschrift is goedgekeurd
door de promotoren

Prof. dr. in. C.A.M.G. Cramers
en

Prof. dr. in. F.M. Everaerts

aan mijn ouders

Cover design

Frans E.P. Mikkens , 1970

Thysigeni multi, paucos adflavit iacchus!

CONTENTS

	GENERAL INTRODUCTION	9
	REFERENCES	10
PART 1	THEORY	11
CHAPTER 1	ELECTROPHORESIS	13
	1.0 Introduction	13
	1.1 Electrophoresis a regulated process	16
	<i>The Kohlrausch functions</i>	17
	<i>The moving boundary equation</i>	20
	<i>The criterion for separation</i>	22
	1.2 Electrophoretic principles	24
	<i>Zone electrophoresis</i>	25
	<i>Moving boundary electrophoresis</i>	26
	<i>Isotachophoresis</i>	27
	<i>Isoelectric focusing</i>	28
	REFERENCES	29
CHAPTER 2	ZONE ELECTROPHORESIS	33
	2.0 Introduction	33
	2.1 General equations	35
	2.2 Concentration distributions	38
	2.3 Electric-field-strength profiles	42
	2.4 Retention behaviour	44
	REFERENCES	48
CHAPTER 3	ISOTACHOPHORESIS	51
	3.0 Introduction	51
	3.1 The separation process	53
	3.2 Resolution	59
	<i>The influence of the counter consti-</i>	62
	<i>tuent</i>	
	<i>The influence of the pH of the lea-</i>	63
	<i>ding electrolyte</i>	

	<i>The influence of the pH of the sample</i>	66
3.3	Time of detection and load capacity	68
3.4	Current efficiency	71
	REFERENCES	76
PART 2	EXPERIMENTAL	79
CHAPTER 1	HIGH PERFORMANCE ZONE ELECTROPHORESIS	81
	1.0 Introduction	81
	1.1 Experimental	83
	1.2 Results and discussion	85
	1.3 Conclusions	96
	REFERENCES	97
CHAPTER 2	THE TRANSIENT-STATE CHARACTERISTICS OF ISOTACHOPHORESIS	99
	2.0 Introduction	99
	2.1 Experimental	101
	2.2 Results and discussion	101
	2.3 Conclusions	120
	REFERENCES	121
CHAPTER 3	COLUMN-COUPLING IN ISOTACHOPHORESIS	123
	3.0 Introduction	123
	3.1 Column-coupling	126
	<i>Instrumentation</i>	128
	<i>Automation of the coupled column system</i>	133
	3.2 Experimental performance	135
	3.3 Conclusions	143
	REFERENCES	143
CHAPTER 4	SEPARATION OF UREMIC METABOLITES	145
	4.0 Introduction	145
	4.1 Experimental	149
	4.2 Results and discussion	151
	4.3 Conclusions	170
	REFERENCES	170

CHAPTER 5	DETERMINATION OF VALPROIC ACID IN	
	HUMAN SERUM	175
	5.0 Introduction	175
	5.1 Experimental	176
	5.2 Results and discussion	177
	5.3 Conclusions	181
	REFERENCES	181
CHAPTER 6	DETERMINATION OF URIC ACID IN HUMAN	
	SERUM	183
	6.0 Introduction	183
	6.1 Experimental	184
	6.2 Results and discussion	185
	6.3 Conclusions	190
	REFERENCES	190
ABBREVIATIONS OF CHEMICAL SUBSTANCES		193
SYMBOLS		193
SUMMARY		197
SAMENVATTING		201
AUTHOR'S PUBLICATIONS ON ELECTROPHORESIS		205
ACKNOWLEDGEMENTS		209
CURRICULUM VITAE		211

GENERAL INTRODUCTION

For an adequate assessment of the structure or properties of a chemical substance it is often of decisive importance that the substance can be isolated from its native environment. All branches of chemistry and biochemistry therefore require separation methods for analytical and preparative purposes. Most appropriate the Dutch word for the entire science of chemistry, *Scheikunde*, means the art of separation. During the last fifty years separation techniques have evolved in a rather spectacular way and have become a self-evident factor in analytical chemistry. Numerous separation methods have been developed and fortunately for the analytical chemist, with interest in separation, there is no straightforward and simple answer to the question: "which separation method is the best?".

Electrophoresis can be used as a method for achieving separation of ionic substances in solution using an electric field. Furthermore the term electrophoresis is loosely applied to a number of industrial processes involving particle precipitation onto a surface. Like all separation methods, whether they involve dilution or concentration of the solutes, electrophoresis aims to produce a relative increase of concentration in a mixture of one solute with respect to another, at least one solute being ionic.

The fundamental phenomenology of electrophoresis has been described already in 1897 by Kohlrausch¹ and numerous different techniques and procedures have been developed. As a result electrophoresis proved to be a useful method for the separation of many ionic solutes, especially for large bio-

polymers. Whereas after World War II chromatography developed quite spectacular, electrophoresis remained at about the same level of utility as that of paper- and thin layer chromatography. In the early nineteen sixties, however, there has been an accumulation of new impulses in electrophoresis: *disc electrophoresis* ², *isoelectric focusing* ³ and *isotachopheresis* ⁴. Especially for the latter technique there has been a continuous effort in improving the instrumental conditions and the theoretical knowledge ⁵. This thesis and the authors further work on electrophoresis aims to fit within this frame work as it was started with the second generation of isotachopheretic instruments ⁶ and ended with a third generation ⁷.

Nowadays isotachopheresis can compete with other analytical separation techniques. It has found its its applications in many fields, especially with low molecular weight substances, and has advantages due to its high resolving capabilities, accuracy and flexibility.

REFERENCES

1. F. Kohlrausch, *Ann. Phys. Chem.*, 62 (1897) 209.
2. L. Ornstein, *Ann. N.Y. Acad. Sci.*, 121 (1964) 321.
3. H. Svensson, *Acta Chem. Scand.*, 15 (1961) 325.
4. A. Martin and F. Everaerts, *Anal. Chim. Acta.*, 38 (1967) 233.
5. F. Everaerts, J. Beckers and Th. Verheggen, *Isotachopheresis*, J. Chromatogr. Libr. Vol VI, Elsevier, Amsterdam-Oxford-New York, 1976
6. F. Everaerts, M. Geurts, F. Mikkers and Th. Verheggen, *J. Chromatogr.*, 119 (1976) 129.
7. F. Everaerts, Th. Verheggen and F. Mikkers, *J. Chromatogr.*, 169 (1979) 21.

PART 1

THEORETICAL PART

CHAPTER 1

Electrophoresis

Electrophoresis is an electric field induced transport process of electrically charged particles. It is a strongly regulated process, governed by the Kohlrausch regulating function concept. Basically four electrophoretic migration modes suffice to describe all electrophoretic separation techniques.

1.0. INTRODUCTION

As early as 1808 von Reuss¹ observed two important electrokinetic effects. He inserted two vertical glass tubes into a lump of moist clay, filled them with water and put an electrode in each. Applying a voltage over the electrodes, the water rose in one tube and sank in the other. Moreover, the water in the latter became turbid, since clay particles were moving in the opposite direction to the water. He thus discovered both electro-osmosis and electrophoresis. Since that time numerous investigations have shown that this electric field induced migration is a general electrokinetic phenomenon shown by colloidal particles. As a result electrophoresis is historically linked with colloid chemistry, where it proved to be a useful method for the measurement of electrophoretic mobilities of colloidal particles.

The concept of ionic migration was suggested by Hittorf²

in 1853, and in the following years the measurement of the Hittorf transference numbers^{3,4} obtained much attention.

At the end of the last century the early physico-chemical interest in electrophoresis diverged into a more analytical one: electrophoresis as a method for achieving separation. In this respect an important discovery was made by Hardy⁵ in 1899, when he noticed that the net electrical charge of proteins could be changed in varying the pH of the protein solution. It was in fact Michaelis⁶ who revealed the potential strength of electrophoresis on the separation and characterization of proteins. Substantial experimental improvements in electrophoretic techniques were introduced by Svedberg and Tiselius in 1926⁷. The real importance of electrophoresis for protein chemistry was stipulated by the work of Tiselius^{8,9} who in 1937 described in detail his moving boundary equipment and for his work he obtained the Nobel Prize. Although Tiselius was convinced of the general applicability of electrophoresis, from that time on a close liaison between electrophoresis and proteins was established. In the early sixties this association was reinforced by the ingenious work of Ornstein¹⁰ and Davies¹¹, with the development of discontinuous electrophoresis. About the same time the development of isoelectric focusing was initiated by Svensson¹², and particularly this technique proved to be extremely well applicable for proteins.

From the start, however, there was a problem which always worried research workers: stabilization in electrophoresis. Already in 1886 Lodge¹³ observed that electrophoresis was very sensitive to convective disturbances and he appears to have been the first to attempt to use an anticonvective medium, gelatine in his case, in order to study the migration characteristics of inorganic ions in an electric field. Since that time numerous substances, such as glass wool, glass beads, cotton gauze, silk fibers, paper, gels of agarose and poly-acrylamide, etc, have been used, with more or less success. In fact the liaison electrophoresis-chromatography was born out of the need for

stabilization. This liaison not only increased the practical applicability of electrophoresis in protein chemistry but also allowed the use of electrophoresis as a practical separation technique for lower molecular weight substances.

A problem of comparable importance to stabilization has been detection. Even nowadays the most generally applied method of detection is based on a specific chemical reaction of the sample constituents with a chromogenic reagent. Numerous staining procedures, for post-run detection, have been developed for proteins as well as for low molecular weight substances. Many of the procedures are familiar with those used in paper- and thin-layer chromatography. Though generally rather elaborate some of these procedures have a high sensitivity and specificity. This is best illustrated by immuno-electrophoresis, in which the highly specific immunochemical precipitation of the antigen-antibody system is used. Various detection systems have been developed for in run detection, of which the Schlieren method proved to be useful for moving boundary electrophoresis with the Tiselius apparatus. This interference method, monitoring a change of refractive index, is useful for electrophoresis in free solution but not in gels and require rather elaborate optics.

In the early sixties both problems, stabilization and detection were again tackled by Konstantinov and Oshurkova¹⁴ and Martin and Everaerts¹⁵, in the development of isotachophoresis. The use of capillary systems (anti-convective carrier) and reliable detection systems (photometric, thermometric and conductimetric) in combination with a superb electrophoretic principle (isotachophoresis) proved to be successful. Whereas most of the earlier work did find its main field of application in proteins and proteinlike substances, this new approach was extremely well applicable to the lower molecular weight substances. The development of detection systems with a fast response and high sensitivity and the use of capillary configurations therefore can be a turning point in the development of electrophoresis.

1.1. ELECTROPHORESIS A REGULATED PROCESS

Electrophoresis can be considered as an electric field induced transport process of electric charge carrying species in a conductor, that consists of a solution of electrolytes with initially arbitrary local concentrations. As early as 1897 Kohlrausch¹⁶ concluded that the change of local electrolyte concentrations cannot be an arbitrary process, but must be strongly regulated. This he formulated in his regulating function concept and its mathematical expression "*die beharrliche Function*". Kohlrausch derived his regulating function not with respect to a specific electrophoretic principle but as a general concept. It comprised the transport phenomena, that occur during electrolysis of electrolyte solutions, without the analytical implications that nowadays are linked with electrophoresis. In his original work he applied his basic concept to several electrophoretic configurations. The experiments of Lodge¹³, Wetham^{17,18} and Nernst¹⁹ were for him the basis to derive a specific function for the electrolyte configuration in which the constituents are electrophoretically displaced by a sharp moving boundary. These experiments can be considered as the onset of moving boundary electrophoresis, which proved to be a useful method for the measurement of mobilities and transference numbers.

When Tiselius⁸ developed his moving boundary method into a quantitative analytical method, a new interpretation of the regulating function concept became desirable. The first attempt was made by Svensson²⁰, when he derived the moving boundary equation, in which the moving boundary velocity is related to local constituent concentrations and mobilities. Some years later the moving boundary equation was given in a more general form by Longworth²¹, Dole²² and Alberty²³. The regulating function concept as well as the moving boundary theory regained their importance with the development of isotachophoresis and discontinuous electrophoresis. These techniques clearly

showed that electrophoresis is a regulated process governed by four basic principles: Ohms law, electroneutrality, chemical equilibrium and balance of mass²⁶.

The Kohlrausch regulating functions

In electrophoresis the migration velocity, v , of a constituent i is given by the product of effective mobility \bar{m}_i and the local electric field strength, E :

$$v_i = \bar{m}_i E \quad (1.1)$$

The electric field strength is vectorial so, the effective mobilities can be taken as signed quantities, positive for constituents that migrate in a cathodic direction and negative for those migrating anodically. As a constituent may consist of several forms of subspecies in rapid equilibrium, the effective mobility represents an average ensemble. Not considering constituents consisting of both positively and negatively charged subspecies in equilibrium, we can take concentrations with a sign corresponding to the charge of the subspecies. Thus the total constituent concentration, \bar{c}_i , is given by the summation of all subspecies concentrations:

$$\bar{c}_i = \sum_n c_n \quad (1.2)$$

where c_n is the subspecies concentration.

Following the mobility concept of Tiselius²⁴, the effective mobility is given by

$$\bar{m}_i = \frac{\sum_n \frac{c_n m_n}{\bar{c}_i}}{\bar{c}_i} \quad (1.3)$$

where m_n is the ionic mobility of the sub-species. The effective mobility of the constituent can be influenced by several parameters, such as temperature, solvation, dissociation, complex-formation and permeability. Considering only dissociation equilibria the effective mobility can be evaluated using the degree of dissociation, α :

$$\bar{m}_i = \sum_n \alpha_n m_n \quad (1.4)$$

The degree of dissociation can be calculated once the equilibrium constants, K_n , for the subspecies and the pH of the solution are known. Neglecting activity effects it follows:

$$\alpha_n = \left\{ \frac{K_n}{(c_H)^n} \right\}^{+n} \left\{ 1 + \sum_n \frac{K_n}{(c_H)^n} \right\}^{-n} \quad (1.5)$$

where c_H is the proton concentration and K_n is the protolysis constant for the n^{th} subspecies.

For monovalent weakly ionic constituents this equation can be transformed to the well known Henderson-Hasselbalch²⁵ relation

$$pH = pK \pm \log \left(\frac{1}{\alpha} - 1 \right) \quad (1.6)$$

where pK is the negative logarithm of the protolysis constant; the positive sign holds for cationic subspecies and the negative sign for anionic sub-species.

In electrophoresis we are dealing with the migration of electrically charged species in a solvent. This means that it is essentially a charge transport process and that Ohm's law is valid. In electrophoresis this law is most conveniently expressed in terms of electrical current density, J , specific conductance, κ , and electric field strength, E :

$$J = \kappa E \quad (1.7)$$

The advantage of this modified law of Ohm²⁶ is that the electric field strength, an electrophoretic important parameter, can easily be converted into a more chemical one, i.e. the specific conductance. In general, the electric conductance of a solution is the summation of contributions from all charged subspecies present. In spite of the fact that it is a non specific property, conductance gives useful information of the charged species present in a solution and the interactions with the solvent. The spe-

cific conductance is given by the individual subspecies concentrations:

$$\kappa = F \sum_i \sum_n m_n c_n |z_n| \quad (1.8)$$

where F is the Faraday constant and $|z_n|$ is the absolute value of the subspecies valency.

The equation of continuity states for the electrophoretic process that

$$\frac{\partial}{\partial t} c_n = - \frac{\partial}{\partial x} \left(\frac{\partial}{\partial x} D_n c_n - v_n c_n \right) \quad (1.9)$$

where t and x are time and place coordinates, respectively and D is the diffusion coefficient. Assuming the presence of monovalent weakly ionic constituents eqn. 1.9 can be applied for each subspecies. Since the non-charged subspecies do not contribute in the migrational term and if the diffusion coefficient can be considered to be independent of the subspecies we obtain.

$$\frac{\partial}{\partial t} \bar{c}_i = - D_i \frac{\partial^2}{\partial x^2} \bar{c}_i + \frac{\partial}{\partial x} E m_i c_i \quad (1.10)$$

where m_i and c_i are the mobility and the concentration of the charged species i . Neglecting diffusional dispersion we can apply eqn. 1.10 for each constituent and the overall summation of the constituents gives

$$\frac{\partial}{\partial t} \sum_i \bar{c}_i = \frac{\partial}{\partial x} E \sum_i m_i c_i \quad (1.11)$$

In combination with the specific conductance and the modified Ohm's law it follows that

$$\frac{\partial}{\partial t} \sum_i \bar{c}_i = 0 \quad \text{or} \quad \sum_i \bar{c}_i = \text{constant} \quad (1.12)$$

A function of the same constraint can be derived from eqn. 1.10. Division by m_i and application of the resulting relationship for each constituent and overall summation gives

$$\frac{\partial}{\partial t} \sum_i \frac{\bar{c}_i}{m_i} = \frac{\partial}{\partial x} E \sum_i c_i \quad (1.13)$$

Electroneutrality, however, demands $\sum_i c_i = 0$, so

$$\frac{\partial}{\partial t} \sum_i \frac{\bar{c}_i}{m_i} = 0 \quad \text{or} \quad \sum_i \frac{\bar{c}_i}{m_i} = \text{constant} \quad (1.14)$$

Eqn. 1.14 is well known as the Kohlrausch regulating function.

Both regulating functions can be used for the calculation of local constituent concentrations in electrophoresis. The success of such an operation will largely depend on the complexity of the problem and the nature of the constituents involved. Only in one particular case the regulating functions will result in a direct solution: i.e. when an electrolyte solution of two constituents is displaced by a solution of two other constituents. In all other cases a further knowledge of the etiology of the electrophoretic process is required.

The moving boundary equation

In an electrophoretic system different zones can be present, in which a zone is defined as a homogeneous solution demarcated by moving and/or stationary boundaries²⁷. We can apply the continuity principle to a boundary, Fig. 1.1, and derive the general form of the moving boundary equation²³.

$$\bar{m}_i \bar{c}_i E - \bar{m}_i^{-K+1} \bar{c}_i^{-K+1} E^{K+1} = v^{K/K+1} (\bar{c}_i^K - \bar{c}_i^{K+1}) \quad (1.15)$$

where $v^{K/K+1}$ represents the drift velocity of the separating boundary between the zones K and $K+1$.

In the case of a stationary boundary, the boundary velocity is zero and eqn. 1.15 reduces to

$$\frac{\bar{m}_i^{-K+1} \bar{c}_i^{-K+1}}{\bar{m}_i^K \bar{c}_i^K} = \frac{E^K}{E^{K+1}} = \text{constant} \quad (1.16)$$

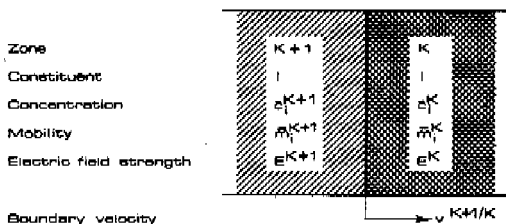


Fig. 1.1 A moving boundary.

From eqn. 1.16 it follows directly that for monovalent weak and strong electrolytes all ionic species are diluted or concentrated over the stationary boundary to the same extent because

$$\frac{c_i^{K+1}}{c_i^K} = \text{constant} \quad (1.17)$$

It should be noted that this phenomenon holds only when the constituent mobilities are relatively insensitive to temperature and concentration effects, which generally holds for dilute solutions over a limited temperature range. The dilution or concentration over the stationary boundary is directly related to the fact that the Kohlrausch functions are locally invariable with time. Hence a concentration boundary, with all constituents present at each side of the boundary, will not be displaced by electrophoresis.

A moving boundary will be present if at least one constituent disappears over the boundary. From Fig. 1.1 it follows that essentially two configurations are possible. If the disappearing constituent is present in the zone K but not in the zone $K+1$ the criterion for boundary stability is given by

$$v_j^{K+1} > v_j^K \quad (1.18)$$

where v_j^K is the constituent velocity in the zone K and v_j^{K+1} is the constituent velocity if the constituent j

might turn on in the $K+1$ zone. A similar relation is found if the disappearing constituent is present in the zone $K+1$ but not in the zone K .

It should be emphasized that the boundary velocity need not to be constant, but may vary as a function of time. The sharpness and structure of the transition boundary is dependent on the local values of the electric field strength, the mobility of the constituents and of the dispersive factors such as diffusion and uneven temperature distributions. As long as an inhomogeneity in the electric field exists any dispersion will be optimally levelled by the selfsharpening effect, but always a finite transition boundary will be present^{34,39}.

The criterion for separation

As in all differential migration methods, the criterion for separation in electrophoresis depends simply on the effect that two ionic constituents will separate whenever their migration rates in the mixed state are different. For two constituents i and j , this means that their effective mobilities in the mixed state must be different:

$$\frac{\bar{m}_i}{\bar{m}_j} \neq 1 \quad (1.19)$$

When the effective mobility of i is higher than that of j the latter constituent will lag behind the former. Consequently, two monovalent weakly anionic constituents will fail to separate when the pH of the mixed state, pH^M , is given by

$$pH^{MO} = pK_j + \log \left(\frac{1 - \frac{m_j K_j}{m_i K_i}}{\frac{m_j}{m_i} - 1} \right) \quad (1.20)$$

where K_i and K_j are the protolysis constants for the subspecies of the constituents i and j and pK is the negative logarithm of the protolysis constant.

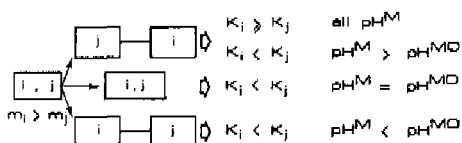


Fig. 1.2 Possible migration configurations for anionic constituents.

When the more mobile constituent has the larger protolysis constant the migration configuration will be independent of pH. If the more mobile constituent has the smaller protolysis constant the migration configuration is a function of pH, as can be seen from Fig. 1.2.

For two monovalent weakly cationic constituents the critical pH is given by

$$pH^{MO} = pK_j - \log \left(\frac{1 - \frac{K_i m_j}{K_j m_i}}{\frac{m_j}{m_i} - 1} \right) \quad (1.21)$$

It should be recognized that the criterion for separation gives only an academic answer to the question of whether constituents can be separated or not. Dealing with actual separability other parameters, such as time for resolution, resolution and load capacity, can be of decisive importance. Moreover, dealing with separability in its limiting case, i.e. $\bar{m}_i/\bar{m}_j + 1$, dispersive factors become important and should be incorporated into the equation of continuity and its resulting relationships. Dispersion may have several causes, e.g. temperature distributions, hydrodynamic flow and density gradients, and they may exceed diffusional dispersion largely. This overall dispersion is closely related to the chosen operating conditions and the design of the equipment. Allowance can be made for such dispersive factors but the resulting uncertainty in the criterion for separation would cause this to remain academic²⁸. The merit of the criterion for separation is that it gives the experimental conditions that should not be used if separation is pursued.

1.2. ELECTROPHORETIC PRINCIPLES

In 1909 Michaelis⁶ suggested that the migration of colloidal particles in an electric field should be called electrophoresis. The discrimination between the migration of colloidal particles and ions was reemphasized by Martin and Synge²⁹ designating the latter effect with the name ionophoresis. Though there may exist a difference, at least in the quantitative description of the two effects, they do not differ qualitatively. Noting that electric field induced migration in solution is applicable to ions, cells, biopolymers irrespective their size as well as colloids, it is obvious that the discrimination between electrophoresis and ionophoresis offers no real advantage. As a result the name electrophoresis nowadays is generally accepted.

TABLE 1.1

THE ELECTROPHORETIC CABOODLE

Agarophoresis	Ion focusing
Cataphoresis	Ionophoresis
Cons electrophoresis	Isoelectric focusing
Continuous flow electrophoresis	Isotachophoresis
Density gradient electrophoresis	Moving boundary electrophoresis
Deviation electrophoresis	Multi phasic zone electrophoresis
Dielectrophoresis	Omegaphoresis
Disc electrophoresis	Paper electrophoresis
Displacement electrophoresis	Paper ionography
Electrochromatography	Preparative electrophoresis
Electrorheophoresis	Pore gradient electrophoresis
Endless beld electrophoresis	Micro electrophoresis
Gel electrophoresis	Transphoresis
High voltage electrophoresis	Zone electrophoresis
Immuno electrophoresis	Slab gel electrophoresis

During its historical development numerous electrophoretic principles, methods and techniques have been developed. From Table 1.1, where a selection is given, it follows that this has resulted in a babylonian confusion. There are, however, several criteria that can be chosen to classify the various electrophoretic methods^{28,30}, but only one allows a systematic and simple classification. In his Nobel lecture Tiselius³¹ pointed out that in chromatography basically three differential migration modes can be

distinguished: zonal, frontal and displacement. Surprisingly, however, Tiselius preferred to distinguish in electrophoresis only between boundary and zonal separations^{32,33}. Martin and Everaerts^{15,34}, noting the analogy between electrophoresis and chromatography used again the differential migration criterion and distinguished three main principles.

Zone electrophoresis: which can be compared with the elution principle in chromatography.

Moving boundary electrophoresis: as the analogon of chromatographic frontal analysis.

Isotachophoresis: the electrophoretic displacement principle.

These three main principles suffice to describe every migration configuration but need the addition of *Isoelectric focusing*.

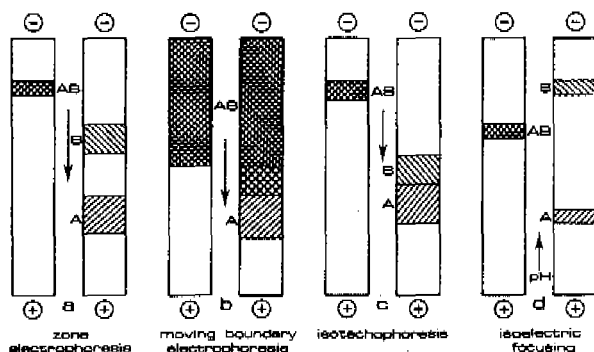


Fig. 1.3 The electrophoretic principles.

Combinations of these principles with one another can be made, e.g. disc electrophoresis¹⁰ is a combination of isotachophoresis and zone electrophoresis. Moreover, additional force fields, multiple dimensions, additional separation mechanisms and methods of detection can be used.

Zone electrophoresis

In zone electrophoresis the separands are allowed to migrate in spatially separated zones. Such a separation

configuration, Fig. 1.3a, is most conveniently obtained by filling all the compartments of the equipment with one kind of electrolyte, the so-called carrier electrolyte. The sample containing the separands, is introduced as a small discrete band in the carrier electrolyte, Fig. 1.3a. Applying a voltage all constituents will migrate with their own velocity depending on the local experimental conditions, such as pH, conductance and driving current. After an appropriate time of analysis the various separands will migrate in different zones, spatially separated by the carrier electrolyte. Each separand zone migrates with its own velocity in a superimposed configuration with the carrier electrolyte. Zone electrophoresis can be performed on anticonvective media, such as paper, cellulose acetate, thin layers of silica or sephadex and in gels of starch, agar and polyacrylamide. Special chromatographic effects can be introduced through the use of ion exchange or pore gradient media. This principle of electrophoresis is comparable with the elution techniques in chromatography and probably the most popular technique in use^{35,36}.

Moving boundary electrophoresis

If moving boundary electrophoresis is considered as the analogon of frontal analysis the method should be depicted as shown in Fig. 1.3b. One part of the electrophoretic equipment is filled with the sample. In order to guarantee a constant sample feed, the sample compartment should be large. The other part of the electrophoretic equipment is filled with a so-called leading electrolyte, consisting of a leading constituent, which has the same sign of charge as the separands, and a counter constituent to preserve electroneutrality. The effective mobility of the leading constituent should be higher than that of the separands and the polarity of the electric field should be chosen in such a way that the separands migrate towards the leading electrolyte. Applying a voltage the moving boundary separation process begins, characterized by the separation of the most mobile separand and mixed zones for

all other separands. Depending on the sample composition and the characteristics of the leading electrolyte, the zone boundaries can be very sharp^{26,34,37}. As an analytical method moving boundary electrophoresis has only limited value, but it should be emphasized that the moving boundary principle is operative in almost every electrophoretic separation process in its initial phase. A classical example of this is given by the Tiselius boundary electrophoresis, which is in fact zone electrophoresis in its early stage, when the zones are not yet fully separated.

Isotachophoresis

Moving boundary electrophoresis fails as an analytical technique since no complete separation can be obtained, due to the fact that the amount of sample is unlimited. As a result the rationale for achievement of complete separation is straightforward: limitation of the amount of sample.

In isotachophoresis this is realized by displacement of a limited amount of the separands by a suitable constituent, the terminator, Fig. 1.3c. In order to obtain an isotachophoretic configuration some stringent requirements have to be met³⁸. These comprise the application of a discrete amount of sample at the interface of two different electrolytes: the leading electrolyte and the terminating electrolyte. In its most simple configuration, both the leading electrolyte and the terminating electrolyte contain only one ionic constituent of the same charge sign as the separands and a counter constituent to preserve electroneutrality. The effective mobility of the leading constituent should be higher than that of any of the separands. The terminating constituent must have an effective mobility smaller than that of any of the separands. The electric field is applied in such a way that the direction of separand migration is towards the leading electrolyte. Applying the electric field a moving boundary separation process will begin and after sufficient time of migration

the separands will be completely separated. All separands will then be arranged in contiguous zones, generally in order of their mobilities. Provided that the current density is constant all zones will migrate at equal and constant velocity without further changes. The velocity of each separand zone is equal to the velocity of the leading electrolyte zone and as a result the electric field strength in each zone is inversely proportional to the effective separand mobility. Since mobilities are constituent dependent quantities, measurement of the electric field strength, or its related parameters, can be used for identification purposes. According to the Kohlrausch regulating function concept and the moving boundary phenomenon, the concentration within each zone is strictly regulated and the zone boundaries have self-sharpening capabilities against convective disturbances^{34,39}. Within a zone the separand concentration is constant and measurement of zone length therefore provides quantitative information. Though the principle of isotachopheresis had been known for many years⁴⁰⁻⁴⁶, it took until the late sixties before the basic instrumental requirements for isotachopheresis were developed by Everaerts³⁴.

Isoelectric focusing

In isoelectric focusing the migration behaviour of ampholytic molecules in a pH gradient is used to obtain their condensation in narrow zones that are stationary in an electric field. Depending on the pH of the solution ampholytic substances, such as proteins, can be positively and/or negatively charged. Hence an ampholyte in solution may electrophoretically migrate as a cationic or an anionic constituent or it may not migrate at all. In the latter configuration the ampholyte is called isoelectric. The pH value, at which this isoelectric state occurs is called the isoelectric point, *pI*. Generally the *pI* value coincides or is nearly equal to the isoprotonic point, at which the molecule carries no net electric charge. Since many ampholytes have different *pI* values, isoelectric

focusing can be used as a separation principle. A basic requirement for this is the availability of a stable pH-gradient. By exposing a mixture of ampholytic substances with different pI values to an electric gradient in a convection free medium a natural pH gradient is formed by the electric transport process itself. The most acidic ampholyte, with the lowest pI , will condense in the most anodically position and the most basic ampholyte, with the highest pI , will condense in the most cathodic position. Ampholytes with intermediate pI values will condense in intermediate positions. A mixture of proteins can be superimposed in the pH gradient and the various proteins will migrate towards their respective pI values. During this migration process their electrophoretic velocity gradually decreases. As a result the time for reaching the condensed state will be rather long. Moreover, the decrease in electrophoretic velocity also implies a decrease in electric conductance, and as a result local temperature regimes may occur, that sometimes can be deleterious for proteins. Since its introduction in biochemistry isoelectric focusing has become very popular. The main field of application is the separation of proteins. The resolved proteins can be identified through their pI value. Detection by means of a staining procedure is the most commonly used method. UV-absorption, autoradiography and zymogram methods are other possibilities for detection.

REFERENCES

1. F. von Reuss, *Comment. Soc. Phys. Univ. Mosquensem*, 1 (1808) 141.
2. J. Hittorf, *Ann. Phys. Chem.*, 89 (1853) 177.
3. J. Hittorf, *Ann. Phys. Chem.*, 98 (1856) 1.
4. G. Wiedemann, *Pogg. Ann.*, 99 (1856) 197.
5. W. Hardy, *J. Physiol.*, 24 (1899) 288.
6. L. Michaelis, *Biochem. Z.*, 16 (1909) 81.
7. T. Svedberg and A. Tiselius, *J. Amer. Chem. Soc.*, 48 (1926) 227.

8. A. Tiselius, *Thesis*, University of Uppsala, Uppsala (Sweden) 1930.
9. A. Tiselius, *Trans. Faraday Soc.*, 33 (1937) 524.
10. L. Ornstein, *Ann. N.Y. Acad. Sci.*, 121 (1964) 321.
11. B. Davies, *Ann. N.Y. Acad. Sci.*, 121 (1964) 404.
12. H. Svensson, *Acta Chem. Scand.*, 15 (1961) 325.
13. O. Lodge, *Brit. Assoc. Adv. Sci. Rept.*, 38 (1886) 389.
14. B. Konstantinov and V. Oshurkova, *Doklad. Akad. Nauk. SSSR.*, 148 (1963) 1110.
15. A. Martin and F. Everaerts, *Anal. Chim. Acta*, 38 (1967) 233.
16. F. Kohlrausch, *Ann. Phys. Chem.*, 62 (1897) 209.
17. W. Wetham, *Proc. Roy. Soc. London*, 52 (1893) 283.
18. W. Wetham, *Phil. Trans. A*, 184 (1893) 337.
19. E. Nernst, *Z. Electrochem.*, 12 (1896) 308.
20. H. Svensson, *Arkiv. Kem. Mineral. Geol.*, 14 (1943) A17.
21. L. Longworth, *J. Amer. Chem. Soc.*, 67 (1945) 1169.
22. V. Dole, *J. Amer. Chem. Soc.*, 67 (1945) 1119.
23. R. Alberty, *J. Amer. Chem. Soc.*, 73 (1951) 517.
24. A. Tiselius, *Nova Acta Regiae. Soc. Sci. Uppsaliensis*, Ser. IV, Vol. 7, no. 4, (1930).
25. H. Hasselbalch, *Biochem. Z.*, 78 (1916) 112.
26. J. Beckers, *Thesis*, Eindhoven University of Technology, Eindhoven (The Netherlands) 1973.
27. T. Jovin, *Biochemistry*, 12 (1973) 871.
28. J. Vačik, in *Electrophoresis*, Z. Deyl Ed., J. Chromatogr. Lib. Vol. 18, Elsevier, Amsterdam-New York-Oxford (1979).
29. A. Martin and L. Syngé, *Adv. Prot. Chem.*, 2 (1945) 32.
30. F. Everaerts, F. Mikkers and Th. Verheggen, *Separ. Pur. Methods*, 6 (1977) 287.
31. A. Tiselius, in *Nobel Lectures Chemistry 1948-1962*, Elsevier, Amsterdam-London-New York, 1964.
32. H. Haglund and A. Tiselius, *Acta Chem. Scand.*, 4 (1950) 957.
33. A. Tiselius, *Far. Soc. Disc.*, 13 (1953) 29.

34. F. Everaerts, *Thesis*, Eindhoven University of Technology, Eindhoven (The Netherlands) 1968.
35. J. Sargent and S. George, *Methods in zone electrophoresis*, BDH Chemical Ltd., Poole, England, 1975.
36. L. Vámos, *Electrophoresis auf Papier and anderen Trägern*, Akademie Verlag, Berlin, 1972.
37. M. Bier (ed.), *Electrophoresis; theory, methods and applications*, Academic Press Inc., N.Y. USA, 1959.
38. F. Everaerts, *Chem. Listy*, 67 (1973) 9.
39. G. Moore, *J. Chromatogr.*, 106 (1975) 1.
40. J. Kendall, *Science*, 67 (1928) 163.
41. D. MacInnes and L. Longworth, *Chem. Rev.*, 11 (1932) 171.
42. A. Martin, unpublished results, 1942.
43. A. Vestermark, *Thesis*, University of Stockholm, Stockholm (Sweden) 1966.
44. E. Schumacher and T. Studer, *Helv. Chim. Acta*, 47 (1964) 957.
45. W. Preetz, *Talanta*, 13 (1966) 1649.
46. B. Konstantinov and O. Oshurkova, *Dokl. Akad. Nauk. SSSR*, 148 (1963) 1110.

CHAPTER 2

Zone electrophoresis

Non symmetrical concentration distributions in zone electrophoresis are inherent to the separation principle. The mobility of the separand relative to that of the carrier constituent determines whether the concentration distribution is leading or tailing. Only at very low sample loads an independent retention behaviour can exist.

2.0. INTRODUCTION

Zone electrophoresis is the commonest and most widely applied electrophoretic principle. Numerous zone electrophoretic techniques and procedures have been developed, mainly on an empirical basis.

Being a zonal separation principle, zone electrophoresis allows a separand to form a zone, separated from other zones by separand free regions. When in zone electrophoresis longitudinal diffusion is the only mechanism of band spreading and migration occurs at a constant velocity, Gaussian concentration distributions are obtained^{1,2}.

The actual broadening, however, may exceed the diffusional broadening due to convection, electrodiffusion, electro-osmosis and reversible adsorption. Such non-idealities have been discussed in detail by Wieme³ and Boyack and Giddings⁴ and are collectively responsible for what has been called "electrophoretic dispersion". They can be dealt with by using a pseudo-diffusion coefficient, that combines the adverse effects of this additional spreading³.

In zone electrophoresis, however, frequently non-symmetrical concentration distributions are obtained. When adsorption processes can occur, non linear adsorption isotherms can explain the asymmetry⁵⁻⁹. The effect of an inhomogeneity of the electric field on the zone profile has been discussed by several workers¹⁰⁻¹⁵. This phenomenon is closely related to the fact that in electrophoresis one frequently encounters "boundary anomalies", i.e. stationary or moving boundaries, in which the migration velocity is a function of concentration¹⁶⁻¹⁸. It is generally assumed that in view of electrophoretic performance these "boundary anomalies" have to be avoided. This seems to be the result of the chromatographic tenet that any effect which improves the definition of the one boundary invariably causes deterioration of the other boundary. Thus, in chromatographic zonal separations generally the best resolution is obtained when these effects are absent and the zone boundaries are symmetrical.

Although there is a close analogy between chromatographic and electrophoretic separation principles, some important methodological differences exist. Probably the most profound difference is that in electrophoresis Ohm's law must hold and that the resulting Kohlrausch relations¹⁶⁻²¹ govern the electrophoretic process. Any changing of concentrations during an electrophoretic process are ruled by these relationships. As a result, on the one hand the occurrence of "boundary anomalies" can be used in a favourable way, while on the other hand problems in retention behaviour arise.

2.1. GENERAL EQUATIONS

In all electrophoretic separation techniques changes of electrolyte constituent concentrations will occur owing to the action of an externally applied electric field. In zone electrophoresis a discrete sample zone is eluted by the so-called carrier electrolyte. Although gradient configurations (dimensional, thermal or electrolytic) are possible, we shall assume a separation compartment of uniform dimensions, operated at a constant temperature and filled with a homogeneous carrier electrolyte. This electrolyte basically consists of a carrier constituent A , which has the same sign of electrical charge as the separand(s) J , and a counter constituent B , to preserve electroneutrality.

A small-volume element of the separation compartment, Fig. 2.1, that originally was filled with the carrier electrolyte AB , will contain after an appropriate time of analysis a mixture of the carrier constituent and one or even more separands.

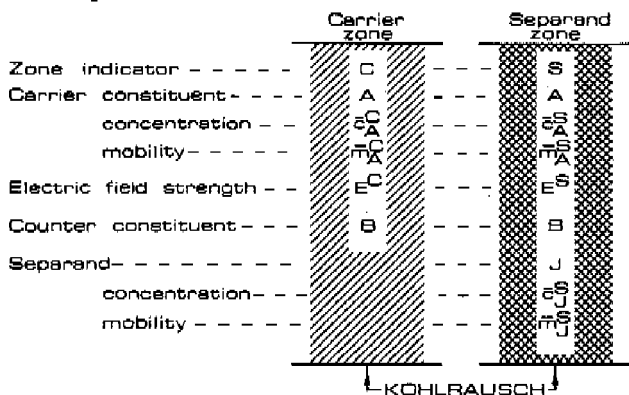


Fig. 2.1 A zone electrophoretic configuration.

After a even longer time, the sample will have left the volume-element and the original situation will be restored again. Assuming the presence of only monovalent weak ionic constituents, two important Kohlrausch functions can be derived, Part 1 chapter 1:

$$\sum_i \bar{c}_i = \omega_1 \quad \text{and} \quad \sum_i \frac{\bar{c}_i}{r_i} = \omega_2 \quad (2.1)$$

where \bar{c}_i represents the molar concentration of the constituent i and r_i is its ionic mobility relative to an appropriate reference constituent. Obviously the carrier constituent offers the best reference mobility. It should be noted that both the concentrations and the mobilities can most conveniently be taken as signed quantities and that the summation should be applied to all constituents, including the common counter constituent. The use of relative mobilities will reduce the influence of temperature and activity effects.

The numerical values of the *Kohlrausch* functions, ω_1 and ω_2 , are locally invariable with time. Thus, taking the carrier electrolyte as a frame of reference, it follows for the configurations of Fig. 2.1

$$\bar{c}_A^C(x,t) = \bar{c}_A^S(x,t) + \sum_j k_j \bar{c}_j^S(x,t) \quad (2.2)$$

where

$$k_j = \left(\frac{r_j - r_B}{1 - r_B} \right) \cdot \frac{1}{r_B}$$

The summation indicates that within the volume-element several separands J can be present. If a constant electric driving current and the presence of only strong ionic constituents is assumed, it follows for the specific electrical conductance κ , that

$$\kappa^S(x,t) = \kappa^C + \sum_j b_j \bar{c}_j^S(x,t) \quad (2.3)$$

where

$$b_j = F m_A (r_j - r_B) \left(1 - \frac{1}{r_j} \right)$$

F is the Faraday constant, m_A is the ionic mobility of the carrier constituent and $\bar{c}_j^S(x,t)$ is the total concentration of the separand J .

Applying Ohm's law, we obtain for the electric field strength E :

$$E^S(x,t) = \frac{E^C}{1 - \sum_j a_j c_j^S(x,t)} \quad (2.4)$$

where

$$a_j = \frac{k_j}{c_A} (1 - r_j)$$

When only separand is present in the volume-element, an important conclusion can be drawn from eqns. 2.2 and 2.4. The electric field strength in the separand zone will always be smaller than that in the carrier electrolyte, when the separand has a mobility higher than that of the carrier constituent, i.e. when $r_j > 1$. For other mobility configurations analogous conclusions can be drawn:

$$\begin{aligned} r_j > 1 & \quad E^S(x,t) < E^C \\ r_j = 1 & \quad E^S(x,t) = E^C \\ r_j < 1 & \quad E^S(x,t) > E^C \end{aligned}$$

The inhomogeneity of the electric field strength will influence the concentration distributions of all ionic constituents. The equation of continuity states for the electrophoretic process

$$\frac{\partial}{\partial t} c_j(x,t) = \frac{\partial}{\partial x} (D_j \frac{\partial}{\partial x} c_j(x,t) - v_j(x,t) c_j(x,t)) \quad (2.6)$$

where D_j is the diffusion coefficient and v_j is the electrophoretic drift velocity of the constituent j . Assuming a constant velocity, Gaussian concentration distributions are obtained, in which a symmetrical broadening of the separand zone occurs due to diffusion. The distribution can be described by

$$c_j(x,t) = \frac{c_j(0,0)}{\sqrt{4\pi D_j t}} \cdot \exp\left(-\frac{(x - v_j t)^2}{4 D_j t}\right) \quad (2.7)$$

In electrophoresis, however, one frequently encounters "boundary anomalies", in which the migration rate is a function of concentration. Virtanen¹⁰ indicated that the electrophoretic velocity is not constant and gave an analytical solution of the equation of continuity, assuming that the drift velocity is linearly related to the separand concentration. According to eqn. 2.4 this can only be approximate. The equations describing this effect are non-linear and the description of non-linear migration in which diffusional dispersion occurs is laboursome. The effect of "boundary anomalies", however, can easily be deduced if one assumes that diffusional dispersion can be neglected. Eqn. 2.6 then reduces to

$$\frac{\partial}{\partial t} c_j(x, t) = - \frac{\partial}{\partial x} v_j(x, t) c_j(x, t) \quad (2.8)$$

If the presence of only one strong ionic separand J is assumed, combination of eqns. 2.4 and 2.6 gives

$$\frac{\partial}{\partial t} c_j^S(x, t) = - m_{\Lambda} r_j E^C \frac{\partial}{\partial x} \left\{ \frac{c_j^S(x, t)}{1 - a_j c_j^S(x, t)} \right\} \quad (2.9)$$

Introducing $\psi(x, t) = 1 - a_j c_j^S(x, t)$ this differential equation can easily be solved to give

$$\psi(x, t) = (\alpha x + \beta)^{-\frac{1}{a_j}} (t + \gamma)^{\frac{1}{a_j}} \quad (2.10)$$

The constants α , β and γ are determined by the actual boundary conditions.

2.2. CONCENTRATION DISTRIBUTIONS

During the migration process, several discontinuities can occur that are restricted both in place and time. A complete mathematical treatment of all possible configurations has been given elsewhere²¹. After an appropriate time of migration the concentration distributions have a characteristic form. Fig. 2.2 gives the distributions for three possible cases of the separand mobilities.

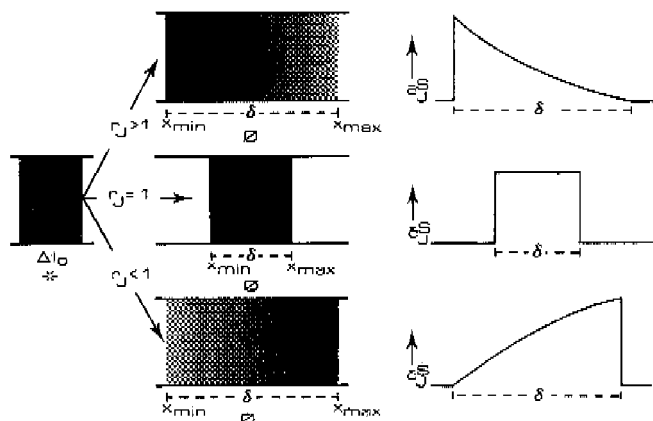


Fig. 2.2 Concentration distributions in zone electrophoresis as a function of the relative separand mobility.

*-sampling compartment, \emptyset separation compartment.

When the separand has a higher mobility than that of the carrier constituent, $r_j > 1$, the leading side of the separand zone will be diffuse, whereas the rear will be sharp. This is caused by the fact that at the rear a stable moving boundary can be formed, whereas at the leading side the criterion for stability cannot be met. Although several time restrictions can occur during the initial phase of the migration process²¹, the final concentration distribution will be given by

$$c_J^S(x, t) = \frac{1}{a_J} \left(1 - \sqrt{\frac{x_{max} - \Delta l_0}{x - \Delta l_0}} \right) \quad (2.11)$$

where Δl_0 is the initial width of the sample pulse and x_{max} is the maximal distance that the separand has migrated in the given time interval. It follows that this maximal distance is given by

$$x_{max} = m_A r_J E^C t + \Delta l_0 \quad (2.12)$$

It should be noted that for this mobility configuration the maximal distance is linearly related with time, whereas the minimal distance that the separand has migrated,

x_{min} , is a rather complex function of all parameters involved. For the zone-width $\delta(t)$ it can be derived that

$$\delta(t) = x_{max} - x_{min} = -a_J \Delta l_0 c_J^{S*} + 2 \sqrt{-m_A r_J E^C t a_J \Delta l_0 c_J^{S*}} \quad (2.13)$$

where c_J^{S*} is the concentration of the separand in the original sample. Figure 2.3 shows the electrophoretic development as a function of time. From the concentration distribution after one sec it can be seen that the separand concentrates over the boundary between the sampling and the separation compartment. After five sec of migration the zone still contains a homogeneous part, but the

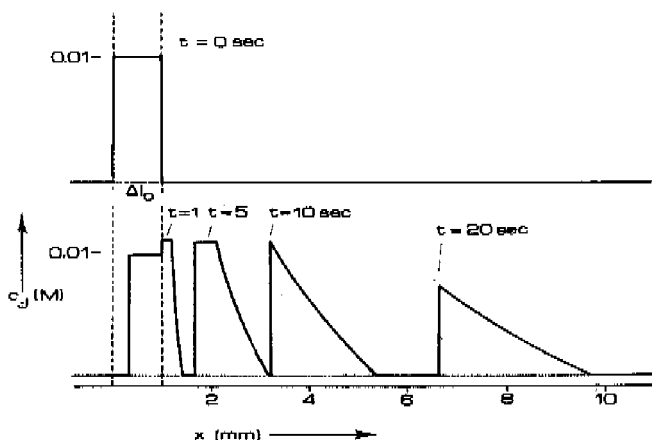


Fig. 2.3 Development of a zone electrophoretic process for a $r_J > 1$ configuration. c_J is the concentration of the separand, x is the migration coordinate (mm). t is the migration time (sec).

"diffuse" region is already clearly visible. After 10 sec the homogeneous part has just disappeared and complete elution starts. From this moment on the concentration distribution according to the eqn. 2.11 is present. It should be emphasized that the boundary velocity during the first ten sec is constant. The moment that true elution starts, the velocity of the moving boundary will gradually

increase until it has reached the maximal migration velocity v_{max} . During this increase the sharpness of the boundary decreases.

When the mobility of the separand is equal to the mobility of the carrier constituent, $r_J = 1$, the sample constituent is only diluted or concentrated over the stationary boundary between the sampling and the separation compartment. If the sample again has been introduced as a block pulse, the concentration distribution will be given by

$$c_J^S = \frac{c_A^C}{c_A^{C^*}} c_J^{S^*} \quad (2.14)$$

where $c_A^C/c_A^{C^*}$ is the dilution factor over the stationary boundary between the sampling and the separation compartment. It follows that the concentration of the separand is independent of time and that the maximal distance that the separand has migrated is given by eqn. 2.12. Moreover, it must be concluded that, after an initial elongation or shortening, the zone width δ is independent of time

$$\delta = \frac{c_A^{C^*}}{c_A^C} \Delta l_0 \quad (2.15)$$

When the separand has a smaller mobility than that of the carrier constituent, $r_J < 1$, the leading side of the separand zone will be sharp, whereas the rear will be diffuse. The final concentration distribution will be given by

$$c_J^S(x, t) = \frac{1}{a_J} \left\{ 1 - \sqrt{\frac{x_{min} + \Delta l_0 (c_A^{C^*}/c_A^C - 1)}{x + \Delta l_0 (c_A^{C^*}/c_A^C - 1)}} \right\} \quad (2.16)$$

For the zone width $\delta(t)$ it follows that

$$\delta(t) = a_J c_J^{S^*} \Delta l_0 + 2 \sqrt{m_A r_J E^C t a_J \Delta l_0 c_J^{S^*}} \quad (2.17)$$

The minimal migrated distance, x_{min} , is given by

$$x_{\min} = m_A r_J E^C t - \Delta l_0 \left\{ \frac{c_A^{C^*}}{c_A^C} - 1 \right\} \quad (2.18)$$

2.3. ELECTRIC FIELD STRENGTH PROFILES

Electric field strength profiles and concentration distributions have different forms and there is a distinct difference between time-based and distance-based distributions. According to eqn. 2.4 the electric field strength readily can be calculated once the local constituent concentrations are known. Distance-based electric field strength profiles can be obtained by substitution of the appropriate concentration distribution in eqn. 2.4. When a fixed point electric gradient detection system is used, time-based distributions will be measured and it can easily be shown that for a $r_J \neq 1$ configuration it must hold that

$$\frac{E^S(x_{\det}, t)}{E^C} = \sqrt{\frac{t_{\det}}{t}} \quad (2.19)$$

where E^S and E^C are the electric field strengths in the separand zone and in the carrier electrolyte respectively and x_{\det} is the distance at which the electric gradient detector is located. For a $r_J > 1$ configuration t_{\det} is given by the time interval at which the first separand ion reaches the point of detection. For $r_J < 1$ configurations, however, t_{\det} is given by the time interval at which the last separand ion reaches the point of detection. The moment at which the last separand ion, for $r_J > 1$, or the first separand ion, $r_J < 1$, reaches the point of detection, i.e. t_{stop} , is related to the sampled amount, since

$$n_J = 0 \int_{t_{\det}}^{t_{\text{stop}}} c_J^S(x_{\det}, t) dt \quad (2.20)$$

where n_J is the sampled amount of the separand J and 0 is the cross-sectional area of the separation compartment. So to describe the generated distribution function requi-

res only the knowledge of t_{det} from either theoretical calculations or experimental observations. The sampled amount should be used to know the time interval during which the generated distribution function is applicable. Combining the eqns. 2.19 and 2.20 a very useful relation for quantitative determinations is found

$$n_J = \frac{0}{a_J} \left(t_{stop} - \frac{2}{3} \sqrt{\frac{t_{stop}^3}{t_{det}}} - \frac{1}{3} t_{det} \right) \quad (2.21)$$

So for quantitative measurements it is not necessary to measure the exact form of the distribution, since the measurement of both t_{stop} and t_{det} will suffice.

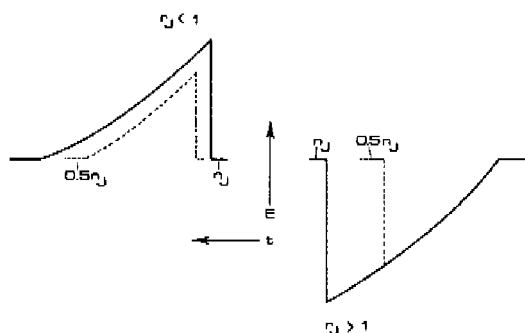


Fig. 2.4 Electric field strength profiles as a function of the sampled amount. E = electric field strength, t = migration time, n_J = sampled amount.

According to eqn. 2.12, t_{det} for a $n_J > 1$ configuration is independent of the sampled amount and is constant for a given separand and carrier electrolyte. For a $n_J < 1$ configuration however both t_{det} and t_{stop} are a function of the sampled amount. As can be seen from Fig. 2.4, not only the shape of the distribution but also its position is influenced by the sample load. Whereas it is possible to define a retention time for the $n_J > 1$ configuration, i.e. t_{det} , this is not possible for the $n_J < 1$ configuration. As mentioned already a $n_J = 1$ configuration will result in a constant electric field strength.

2.4. RETENTION BEHAVIOUR

The separation of multicomponent samples will develop in a complicated manner, since the concentration distributions and the migration velocities of almost each separand is influenced by the physico-chemical characteristics and concentrations of all constituents present. The effect of mutual interactions in electrophoretic separation techniques is more pronounced than in chromatographic separation techniques. This adverse effect of Ohm's law can be suppressed only by the application of very small amounts of sample. The complexity is further increased as generally weak electrolytes will be applied.

It has been shown that, in isotachopheresis and moving boundary electrophoresis²², the ratio of separand mobilities in the mixed state is important when separability and current efficiency are considered. The same holds for zone electrophoresis and generally the same optimization rationales can be followed. In anionic separations a low pH of the carrier electrolyte is preferable, whereas for cationic separations a high pH will give the better results. The current efficiency in zone electrophoresis, however, will be low in comparison with that in isotachopheresis owing to the continuous transport of carrier electrolyte.

In zone electrophoresis the zone characteristics will be determined by the carrier electrolyte and the separands. Using a fixed-point detection system, the time-interval that a separand needs to reach the detector, i.e. the retention behaviour, is strongly affected by the proper choice of operational conditions. Considering retention behaviour it can be concluded that the difference in the separand mobilities is important. In experimental practice, a compromise between current efficiency and retention behaviour has to be found. Obviously, pH and complex formation have a great influence on the retention behaviour. Assuming a well buffered electrolyte system and the application of a small amount of sample, pH deviations and inhomogeneities in the electric field can be neglected.

For the retention time t_R it follows that

$$t_R = t_0 / \bar{r}_J$$

where \bar{r}_J is the effective mobility of the separand relative to that of the carrier constituent and t_0 is the retention time of the carrier constituent. Effective mobilities are strongly influenced by pH and the dissociation constants. Fig. 2.5 shows the relative retention as a function of the relative ionic mobility of the separand. The difference between the pK_a value of the separand and the pH of the carrier electrolyte has been used as a parameter.

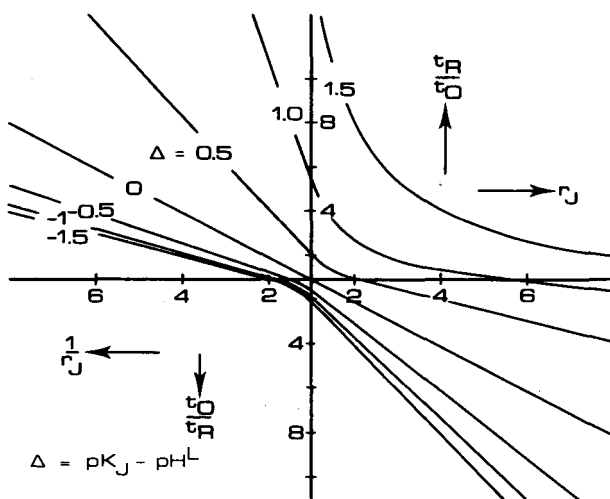


Fig. 2.5 The relative retention as a function of the relative ionic mobility of the separand. The difference between the pK_a of the separand and the pH of the carrier electrolyte has been used as a parameter.

The carrier constituent has been chosen for its optimal buffering capacity, i.e. $pH^C = pK_C$. A separand with a relative ionic mobility of 2 and a low pK value compared with the pH of the carrier electrolyte will have an inverse relative retention, t_0/t_R , of 4. This means that the sample constituent will migrate at a higher velocity than the carrier constituent. A separand with a relative ionic mobility of 0.5, i.e. $1/r_J = 2$, has an inverse relative retention of unity. Obviously this separand cannot be detected by

measurement of the electric gradient.

2.5. THE INFLUENCE OF DIFFUSION

In the given approach, diffusional effects were purposely neglected in order to emphasize the important influence of the electrophoretic process on the concentration distributions. In this way the asymmetry, that frequently occurs in zone electrophoresis can easily be explained as the result of the electrophoretic process. In experimental practice, however, the diffusional effect cannot be neglected and for the calculation of concentration distributions the diffusional effect should be incorporated in the equation of continuity. The importance of diffusional and migrational dispersion, however, can be evaluated rather easily. Using the appropriate relationships, the eqns. 2.13 and 2.17 can be written in a somewhat more practical form:

$$\delta(t) = \frac{c_J^{S^*}}{c_A} \Delta l_0 f(x) + 2 \sqrt{\frac{c_J^{S^*}}{c_A} \Delta l_0 f(x) v_J t} \quad (2.22)$$

where $f(x)$ is a function of the ionic mobilities and v_J is the migration velocity of the separand in the carrier electrolyte. Both $f(x)$ and Δl_0 will commonly show only a limited degree of freedom and both should be minimized. Neglecting the initial discontinuities, band-spreading due to diffusion and to electrophoretic migration is of the same order of magnitude when

$$D_J \approx 0.1 \frac{c_J^{S^*}}{c_A} f(x) \Delta l_0 v_J \quad (2.23)$$

Taking a diffusion coefficient, D_J , of 10^{-5} cm²/sec at a migration rate of 1 mm/sec and an initial band width of 1 mm, diffusion and electrophoretic migration will have a comparable adverse effect at a concentration ratio $c_J^{S^*}/c_A^C$ of 10^{-2} . Below this value band spreading is due mainly to diffusion and above this value electrophoretic migration

will mainly contribute. Assuming that the zone electro-separations are carried out in a capillary system with an inner diameter of 0.2 mm and using a carrier electrolyte at a concentration of 10 mM, the migrational effect will be appreciable when more than 3×10^{-12} mole of the separand is injected. Obviously the detection of such a low amount will put very high demands on the detection systems. Generally a higher sample load will be used and consequently the migrational effect will dominate.

Other forms of dispersion, through which the effective diffusion coefficient may exceed the thermal one, will obscure the migrational dispersion and should be minimized. It should be noted, however, that the occurrence of "boundary anomalies" counteracts the influence of non migrational dispersion. This has been shown to be especially true for isotachopheresis²⁴, but holds also for zone electrophoresis, although to a minor extent. The selfrestoring capabilities, a direct result of the "boundary anomalies", are decreasing when r_j approaches the critical value of unity. This configuration will be particularly sensitive for non-migrational dispersion.

The adverse effect of a relatively large sampling width, Δl_0 , can be counteracted by the concentrating capabilities of the electrolyte system. Choosing the condition $c_J^{S*} \ll c_A^C$ and a high sampling ratio, i.e. $c_J^{S*} \gg c_A^{S*}$, the separand will be concentrated over the stationary boundary between the sampling and the separation compartment. This concentrating effect is the result of the fact that in electrophoresis the *Kohlrausch* regulating function concept cannot be overruled by the electrophoretic process (Part 1 Chapter 1). It seems that this forms the most profound difference between chromatographic and electrophoretic separation principles. In experimental practice this means that, in order to take full advantage of the concentrating capabilities, the sample should not be equilibrated with the carrier electrolyte.

REFERENCES

1. Q. Peniston, H. Agar and J. McCarthy, *Anal. Chem.*, 23 (1951) 994.
2. J. Giddings, *Separ. Sci.*, 4 (1969) 181.
3. R. Wieme, in E. Heftmann (ed.), *Chromatography*, Reinhold, New York, 2nd ed., 1967, p. 228.
4. J. Boyack and J. Giddings, *J. Biol. Chem.*, 235 (1960) 1971.
5. C. Morris and P. Morris, *Separation methods in Biochemistry*, Pitman, London, 1963. p. 639.
6. J. Vacik, *Collect. Czech. Chem. Commun.*, 36 (1971) 1713.
7. J. Vacik and V. Fidler, *Collect. Czech. Chem. Commun.*, 36 (1971) 2123.
8. J. Vacik and Z. Fidler, *Collect. Czech. Chem. Commun.*, 36 (1971) 2342.
9. W. Preetz and H. Homborg, *J. Chromatogr.*, 54 (1971) 115.
10. R. Virtanen, *Thesis*, Helsinki University of Technology. Otaniemi, (Finland) 1974.
11. J. Vacik and J. Dvorák, *Collect. Czech. Chem. Commun.*, 31 (1966) 863.
12. E. Richards and R. Lecanidou, *Anal. Biochem.*, 40 (1971) 43.
13. R. Mills, *Arch. Biochem. Biophys.*, 138 (1970) 171.
14. R. Mills, *Arch. Biochem. Biophys.*, 140 (1970) 425.
15. R. Mills, *Arch. Biochem. Biophys.*, 140 (1970) 439.
16. V. Dole, *J. Amer. Chem. Soc.*, 67 (1945) 1119.
17. H. Svensson, *Ark. Kemi. Min. Geol.*, 22 (1946) 22A.
18. J. Nichol, E. Dismukes and R. Alberty, *J. Amer. Chem. Soc.*, 80 (1958) 2610.
19. F. Kohlrausch, *Ann. Phys. Chem.*, 62 (1897) 209.
20. T. Jovin, *Biochemistry*, 12 (1973) 871.
21. F. Mikkers, *Internal Report ELCEF. THE/TI 1976*, Eindhoven University of Technology, Eindhoven (The Netherlands).
22. F. Mikkers, F. Everaerts and J. Peek, *J. Chromatogr.*, 168 (1979) 293.

23. F. Mikkers, F. Everaerts and Th. Verheggen, *J. Chromatogr.*, 169 (1979) 11.
24. F. Everaerts, J. Beckers and Th. Verheggen, *Isotachophonesis*, *J. Chromatogr. Libr.* Vol. 6, Elsevier, Amsterdam, New York, 1976.

CHAPTER 3

Isotachophoresis

A model for the separation process of isotachophoresis is given. The influence of operational parameters on the separation process is described in terms of time for resolution, load capacity and current efficiency. Optimization favoured by a high driving current, a low mobility of the counter constituent and a low pH for anionic separations, whereas for cationic separations a high pH will be favourable.

3.0. INTRODUCTION

In isotachophoresis a steady state configuration is obtained as the results of a separation process that proceeds according to the moving boundary principle¹. Though this has been recognized for many years most attention has been paid to the development of theoretical models that describe the steady state of isotachophoresis. These theoretical approaches have resulted in different computer programs, that have shown to be in good agreement with one another and with experimental data²⁻⁵. Though the steady

state, representing the pursued target, is important, additional features are decisive dealing with the practical applicability of a used isotachophoretic procedure. Most of these features are related to the separation process. Although the separation process is a transient state, it is governed by the same regulating function concept as the steady state. A quantitative description of the transient state provides information on the time needed for an isotachophoretic separation. Moreover, such a description requires the definition of resolution and separability in isotachophoresis and shows the results that can be expected from optimization procedures.

In the transient state model we will neglect several secondary effects, such as temperature distribution and activity effects. Although these effects are not always marginal, they will generally not have a drastic impact on the transient state model and its resulting guidances for optimization. With regard to uneven temperature distributions, either longitudinal or transversal⁶, it should be emphasized that their effect will be deleterious only under extreme operating conditions. Working at moderate current densities, without excessive cooling, convective disturbances are negligible and temperature differences can be well controlled⁷. In special cases, temperature effects can have a favourable influence on separation, but so far temperature programming has not been studied in isotachophoresis.

The transient state model and its resulting implications will be developed for a sample containing two monovalent weakly ionic separands. The relative simplicity of such a model allows a fundamental understanding of the isotachophoretic separation process and provides a realistic view on what results can be expected from optimization procedures. It is obvious that the model can be extended to multivalent weak electrolytes. The efficiency of such considerations, however, will be poor as no other guidances will be found. Concerning multi-component samples it should be emphasized that the mathematical intricacy in-

increases very rapidly with increase in the number of separands. For strong electrolytes extension of the model is not difficult but is laborious and monastic for practical purposes^{3,8,14-16}. The major advantage of relatively simple model is that it clearly indicates the importance of physico-chemical, operational and instrumental parameters.

3.1. THE SEPARATION PROCESS

Although essentially immaterial, we shall consider a separation compartment of uniform dimensions operated at a constant electric driving current and a constant temperature. We shall deal with the case where all constituents involved are monovalent weak electrolytes. The development of the separation process is shown in Fig. 3.1. In the initial situation, t_0 , the sampling compartment has been

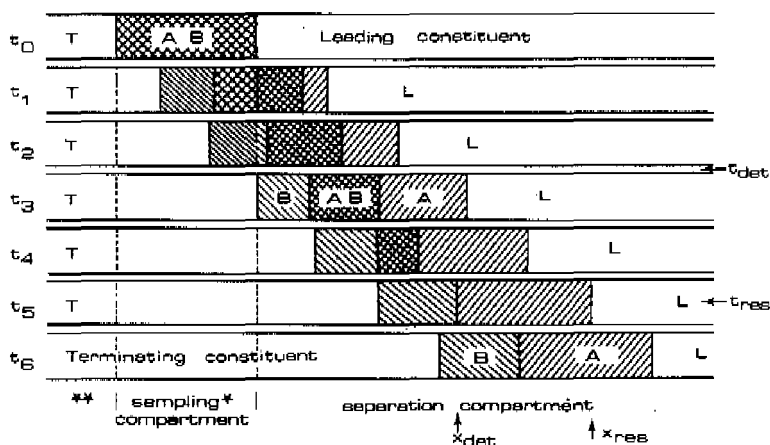


Fig. 3.1 The separation process.

filled with a homogeneous mixture of the two separands A and B. The separation compartment contains the leading constituent L and the terminating compartment is filled with the terminating constituent T. A counter constituent C, to preserve electroneutrality, is common to both the sample constituents, the leading and the terminating constituents. Electrolyte changes in the electrode compart-

ments, temperature effects and activity effects are neglected. Each compartment has its own regulating function, due to the initial composition of the electrolytes. Starting from t_0 the separation of the sample will occur according to the moving boundary principle. All zone characteristics are, as long as they exist, constant with time. At different times several moving boundaries can be present: A/L , AB/A , B/AB , B/A , T/B , B^*/AB^* , T^*/B^* . Boundary velocities are given by local conditions. The sampling compartment causes the stationary boundaries: AB^*/AB , B^*/B , T^*/T , T^{**}/T^* . At t_3 the sample is leaving the sampling compartment and from this time on the total zone length of the sample zone is constant. The properties of the mixed zone in the separation compartment will be in agreement with the local regulating function and the nature of the sample. At t_5 resolution is obtained and from this moment on the individual zone lengths will be constant. Resolution was obtained at t_{res} with a resolution length of x_{res} . Using a fixed point detector, detection could have been started at t_{det} with the detection system located at x_{det} . It should be emphasized that within the separator three different regions are present and each has its own regulating behaviour. The regulating functions, eqns. 1.12 and 1.14, are the mathematical expression of this regulating behaviour and locally they cannot be overruled by the electrophoretic process⁹. All changes in electrophoretic parameters, e.g. concentration, pH and conductance, will be in agreement with the local regulating function. Applying eqn. 1.17 it follows that for monovalent weak and strong separands all ionic subspecies are diluted or concentrated to the same extent over the stationary boundary between the separation and the sampling compartment

$$\phi = \frac{c_B^{M*}}{c_A^{M*}} = \frac{c_B^M}{c_A^M} = \text{constant} \quad (3.1)$$

where the asterisk marks the mixed zone properties in the sampling compartment. Hence the sampling ratio ϕ for the

charged sub-species is invariable. Taking the leading electrolyte as a frame of reference, the regulating functions will result in

$$\bar{c}_L^L + \bar{c}_C^L = \bar{c}_A^M + \bar{c}_B^M + \bar{c}_C^M \quad (3.2)$$

and

$$\frac{\bar{c}_L^L}{r_L} + \frac{\bar{c}_C^L}{r_C} = \frac{\bar{c}_A^M}{r_A} + \frac{\bar{c}_B^M}{r_B} + \frac{\bar{c}_C^M}{r_C} \quad (3.3)$$

where C is the counter constituent common to all separands and r_I is the mobility of the constituent I relative to that of an appropriate reference constituent, in this case the leading constituent. Chemical equilibrium and electro-neutrality imply that

$$\begin{aligned} \bar{c}_A^M &= c_A^M (1 + 10^{+(pK_A - pH^M)}) \\ \bar{c}_B^M &= \phi c_A^M (1 + 10^{+(pK_B - pH^M)}) \\ \bar{c}_C^M &= - (1 + \phi) c_A^M (1 + 10^{+(pH^M - pK_C)}) \end{aligned} \quad (3.4)$$

Combining the eqns. 3.2, 3.3 and 3.4 we obtain

$$\bar{c}_L^L + \bar{c}_C^L = c_A^M \left\{ \frac{1}{\alpha_A^M} + \frac{\phi}{\alpha_B^M} - \frac{(1 + \phi)}{\alpha_C^M} \right\} \quad (3.5)$$

and

$$\bar{c}_L^L (1 - r_C) = c_A^M \left\{ \frac{(r_A - r_C)}{r_A \alpha_A^M} + \frac{(r_B - r_C)}{r_B \alpha_B^M} \right\} \quad (3.6)$$

We now introduce the relative leading concentration ρ and the reduced mobility k_I

$$\rho = \frac{\bar{c}_C^L}{\bar{c}_L^L} \quad \text{and} \quad k_I = \frac{1 - r_C}{r_I - r_C} \quad (3.7)$$

Elimination of c_A^M gives a quadratic equation for the proton concentration in the mixed zone. Only one root will have physical significance.

$$a 10^{2\text{pH}^M} + b 10^{\text{pH}^M} + c = 0 \quad (3.8)$$

The constants a , b and c for the equation are given in Table 3.1. Once the pH in the mixed zone has been calculated, all dynamic process variables can be calculated by using the appropriate equations. Moreover, steady-state configurations are obtained by using a zero sampling ratio.

TABLE 3.1

CONSTANTS FOR THE pH OF THE MIXED ZONE (EQN. 3.8)

Anionic constituents	Cationic constituents
$a = (1+\phi)10^{-\text{PK}_C}$	$a = \left(\frac{1+\rho}{r_A k_A} - 1\right)10^{-\text{PK}_A} + \phi \left(\frac{1+\rho}{r_B k_B} - 1\right)10^{-\text{PK}_B}$
$b = (1+\phi) \left(\frac{1}{r_A k_A} + \frac{\phi}{r_B k_B} \right)$	$b = (1+\rho) \left(\frac{1}{r_A k_A} + \frac{\phi}{k_B k_B} \right)$
$c = \left(\frac{1+\phi}{r_A k_A} - 1\right)10^{\text{PK}_A} + \phi \left(\frac{1+\phi}{r_B k_B} - 1\right)10^{\text{PK}_B}$	$c = (1+\phi)10^{\text{PK}_C}$

Moving boundary experiments can be simulated by the introduction of a high sample load. Computerization allows multiple calculations of all dynamic process variables¹⁰. As the criterion for separation, Part 1 Chapter 1, has to be satisfied, the pH of the mixed zone is of decisive importance. According to eqn. 3.8, this pH is influenced by the physico-chemical characteristics of the separands and of the common counter constituent, by the sampling ratio, ϕ , and the relative leading concentration, ρ . The last parameter is closely related to the pH of the leading electrolyte and the former one to the pH of the sample. We shall consider anionic separations, but equivalent relationships and conclusions can be made for cationic separations.

In isotachopheresis the leading constituent generally must have a high effective mobility, so strong ionic constituents like chloride are commonly used¹¹. In this instance it follows that

$$-\infty < \rho = -\frac{1}{\alpha_C^L} < -1 \quad (3.9)$$

At $\rho \rightarrow -1$ the counter constituent is used far below its pK value and it behaves like a strongly ionic species. In this case the leading electrolyte has no buffering capacity. At $\rho = -2$ the counter constituent is used at its pK value, $pH^L = pK_C$, and therefore exhibits its full buffering capabilities. High negative values for the relative leading concentration again imply a low buffering capacity. Moreover, in this case the concentration of the counter constituent will be high in comparison with that of the leading constituent, which can be favourable in complex formation. It is easily shown that for increasing $pK_J - pH^L$, i.e. the separands are only partially dissociated at the pH of the leading electrolyte, the difference in pH between the mixed zone and the leading electrolyte will increase. Separands that are already completely ionized at the pH of the leading electrolyte will induce only a slight elevation of pH^M and therefore will be separated as strong electrolytes. Counter constituents with a low pK value in comparison with the pH of the leading electrolyte show a tendency to diminish this increase in pH^M . When the leading constituent is a strongly ionic species the pH of any following zone will be higher than the pH of the leading zone. If however, a weak constituent is chosen as the leading constituent negative pH steps can occur under the appropriate conditions¹¹.

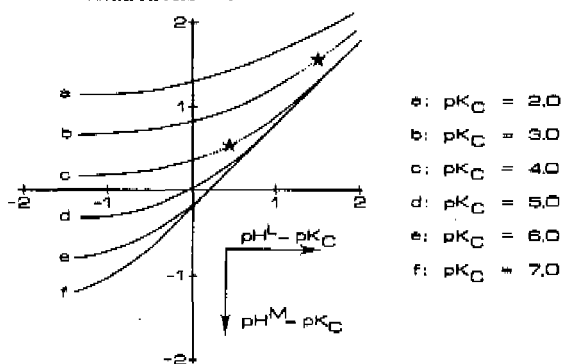


Fig. 3.2 The influence of the pH of the leading electrolyte on the pH of the mixed zones. Constituent data: Table 3.2.

Obviously, problems in separation generally occur when both the pK values and the mobilities of the separands show only little differences. An example of such a pair is given in Fig. 3.2. When the more mobile constituent has the larger dissociation constant, the criterion for separation will always be satisfied. Optimization in this instance is very straightforward: low pH^L and low pK_C . However, when the more mobile constituent has the smaller equilibrium constant, the criterion for separation need not always be satisfied. It will depend on the proper choice of pH^L and pK_C whether the critical pH , as indicated in Fig. 3.2 with an asterisk, will be obtained.

TABLE 3.2

CONSTITUENT DATA FOR FIG. 3.2 AND FIG. 3.3

constituent	mobility $cm^2/Vsec$	pK_a value
Leading, L	-77×10^{-5}	$pK_L = -2$
Counter, C	$+30 \times 10^{-5}$	pK_C variable
Separand, A	-45×10^{-5}	$pK_A = 4.5$
B	-30×10^{-5}	$pK_B = 4.0$

Sampling ratio: Fig. 3.2 $\phi = 1$, Fig. 3.3 variable.

From eqn. 1.20, it follows that the given pair will not separate at $pH^M = 4.52$. If a counter constituent is chosen with $pK_C = 4$, there will be no separation at $pH^L = 4.40$. Above this pH^L , constituent B will migrate behind A, whereas the order will be reversed at low pH^L . It is easily shown that the lower pH of the leading electrolyte will give a more favourable ratio of effective mobilities. It should be emphasized that the mobilities of the separands have only a marginal influence owing to their limited numerical extension.

The influence of the sampling ratio is shown in Fig. 3.3, where limiting values of ϕ are given. At zero sampling ratio the pH of the "mixed" zone will be that of the isotachophoretic A zone, whereas at very large sampling ratio the pH^M will be governed by the separand B.

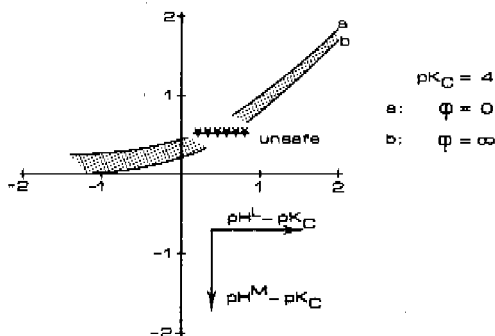


Fig. 3.3 The influence of the sampling ratio on the pH of the mixed zone. Constituent data: Table 3.2.

Hence, whatever the pH of the sample or its molar concentration ratio, the pH of the mixed zone will always lie between the pH values of the completely resolved zones. In common practice sampling ratios can show appreciable fluctuations due to the sample pH or the molar concentrations. Fig. 3.3 therefore gives an indication of the "unsafe" margin, which in this particular case extends over 0.4 pH unit. It is obvious that the pH of the leading electrolyte must be chosen well out of this "unsafe" region. Sampling ratios can show an even larger influence, when the pK values of the separands show more distinct differences.

3.2. RESOLUTION

Once the criterion for separation, $m_i/m_j \neq 1$, has been satisfied, the time needed for resolution becomes important. When a separand zone contains all of the sampled amount, resolution has been obtained for that constituent. We therefore define the resolution, R , as the separated fractional amount of the constituent:

$$R_i = \frac{\text{separated amount of I}}{\text{sampld amount of I}} \quad (3.10)$$

From this definition, it follows that during the separation process the resolution increases from zero to its maximal value, unity. Constituents that fail to separate,

remain at zero resolution and can be termed ideally mixed zones¹².

Complete separation of a sample requires the resolution values of all separands to be unity. As expected the resolution and its time derivative are complex functions of the constituents involved and the driving forces applied. Moreover, the mathematical intricacy involved in calculating optimal process variables increases rapidly with increasing number and complexity of the separands. For strong electrolytes relevant mathematical formulations have been published⁸ but most separations nowadays concern weak electrolytes. In this case dissociation equilibria, and therefore a proper choice of pH, are tools in the control and optimization of the separation process. When dealing with complex formation, association equilibria should be involved. It has been suggested¹³ that the difference in migration rates, i.e. $v_i - v_j$, is of decisive importance in separation. However, in isotachopheresis and moving boundary electrophoresis this does not apply, and in these instances it is more beneficial to optimize the ratio of the migration rates, i.e. v_i/v_j . Whereas the velocity difference will reach a maximal value as a function of pH, the ratio shows no such optimum. As the local electric field strength for both separands in the mixed zone will be the same, it follows directly that the mobility ratio must be maximized or minimized, depending on the migration configuration, Part 1 Chapter 1. Introducing equilibrium constants and ionic mobilities it follows that in anionic separations the lowest pH will give the better mobility ratio, and *mutatis mutandis* holds for cationic separations. It should be emphasized however, that pH extremes have only limited experimental applicability and that practical considerations often govern the proper choice of pH. Moreover, a low numerical value of the effective mobility will require a high electric field strength in order to obtain an appreciable migration rate and other electrokinetic effects may then prevail.

From Fig. 3.1 it can be concluded that the time

needed to reach the maximal resolution for the constituent A can be expressed as a function of the boundary velocities:

$$t_{res} = \frac{l_A}{v_{L/A} - v_{A/A+B}} \quad (3.11)$$

where l_A is the steady state zone length of the separand zone A and $v_{L/A}$ is the boundary velocity.

Using the appropriate relationships, we obtain

$$t_{res} = \frac{n_A F}{I} \left\{ \frac{1 + \phi \frac{k_A}{k_B}}{1 - \frac{\alpha_B^M r_B}{\alpha_A^M r_A}} \right\} \left\{ 1 - \frac{r_C}{r_A} \right\} \quad (3.12)$$

Hence it follows that the time of resolution is a complex function of the concentration and the pH of both the leading electrolyte and the sample, of the sampled amount, the sampling ratio, the electric driving current and all ionic mobilities and dissociation constants. It should be noted that in eqn. 3.12 it is the ratio of the effective separand mobilities and not their difference that is important. Further this equation emphasizes the importance of the pH of the mixed zone.

For the length of the separation compartment, needed to contain the completely resolved state, x_{res} , it follows that

$$x_{res} = \frac{n_A}{O c_L} \left\{ \frac{1 + \phi \frac{k_A}{k_B}}{1 - \frac{\alpha_B^M r_B}{\alpha_A^M r_A}} \right\} \frac{1}{k_A r_A} \quad (3.13)$$

where O is the cross sectional area of the separation compartment.

For a given sample and electrolyte system, the resolution length, x_{res} , is independent of the applied electrical driving current, whereas the time of resolution, t_{res} , is inversely related to the driving current. From the eqns.

3.12 and 3.13 it follows that the separation of a given sample load requires a definite amount of coulombs and column volume. Taking limiting values for eqn. 3.12, it follows that

$$\frac{n_A F}{I} < t_{res} < \infty \quad (3.14)$$

The relationship between the sampled amount and the time of resolution is obviously a linear one. Moreover, for a two-separand sample, resolution for both separands will be obtained simultaneously.

The influence of the counter constituent

From eqns. 3.12 and 3.8 it can be concluded that both the time of resolution and the pH of the mixed zone are affected by the mobility of the common counter constituent. Fig. 3.4 shows the variation of the time of resolution as a function of the mobility of the counter constituent relative to that of the leading constituent. It follows that a low mobility favours the time of resolution, partly because of its influence on the pH of the mixed zone and partly because it increases the efficiency of the current transport.

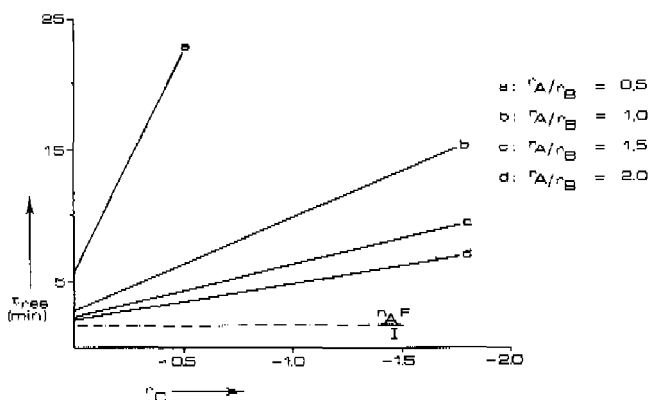


Fig. 3.4 The time of resolution as a function of the relative counter constituent mobility. Constituent data: Table 3.3.

TABLE 3.3

CONSTITUENT DATA FOR FIG. 3.4

Constituent	mobility cm^2/Vsec	pK_a value
Leading, L	-70×10^{-5}	$\text{pK}_L = 0$
Counter, C	variable	$\text{pK}_C = 4.0$
Separand, A	variable	$\text{pK}_A = 4.0$
B	-30×10^{-5}	$\text{pK}_B = 5.0$

Leading electrolyte: $\text{pH}^L = 4.0$, $\bar{c}_L^L = -0.01 \text{ M}$
Sample: $\text{pH}^{M*} = 4.0$, $n_A = n_B = 10^{-7} \text{ mole}$, $\frac{-M^*}{c_A} = \frac{-M^*}{c_B} = -0.05 \text{ M}$
Driving current: $I = 100 \mu\text{A}$, $O = 0.002 \text{ cm}^2$.

The influence of the mobility of the counter constituent on the pH of the mixed zone is, however, marginal. For the lower limiting value of zero it follows that the pH of the mixed zone becomes independent of the constituent mobilities.

As eqn. 3.12 is a function of the effective separand mobilities in the mixed zone, the pH of this zone is of decisive importance. Recognizing that all mixed zone characteristics are determined by the leading electrolyte as well as by the sample, it is obvious that the relative leading concentration, ρ , and the sampling ratio, ϕ , can be used in optimization procedures. Both ρ and ϕ are functions of pH and can be chosen arbitrarily within practical limitations.

The influence of the pH of the leading electrolyte

From the practical point of view the choice of the pH of the leading electrolyte offers the best possibilities in optimization procedures. In Fig. 3.5 the influence of the pH of the leading electrolyte, for different mobilities of the separands, on the time of resolution is shown. The counter constituent has been chosen for its maximal buffering capacity at the pH of the leading electrolyte. Dealing with monovalent anionic constituents it follows that, whenever the more mobile separand has the larger

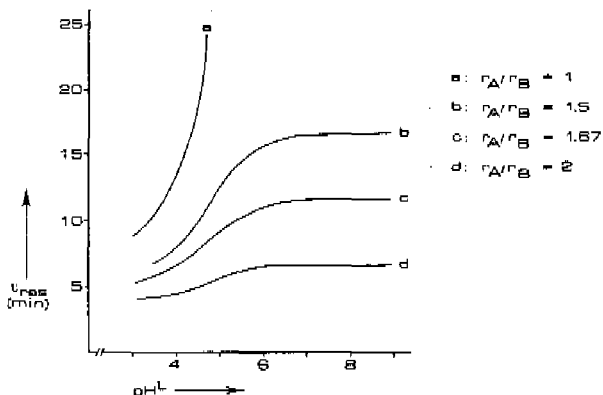


Fig. 3.5 Time of resolution as a function of the pH of the leading electrolyte. Constituent data: Table 3.5.

dissociation constant, resolution is favoured by a low pH of the leading electrolyte. Mutatis mutandis holds for cationic separands, for which a high pH will be favourable. It should be noted that the effect on the time of resolution can be quite appreciable. When the ionic mobilities are equal only a low pH^L will result in an acceptable time of resolution. For separands that have already large differences in their ionic mobilities, the effect of decreasing the pH of the leading electrolyte is much less pronounced. The flattening of the sigmoidal curves at high pH indicates that the sample constituents are being separated as monovalent strong ions, in which event there is, of course, no influence of pH^L .

Though the rationale for optimization of the separation process is rather straightforward, care should be taken in choosing extreme pH values for the electrolyte systems. Electrolyte systems that induce a low effective mobility of the constituents, e.g. smaller than $10^{-4} \text{ cm}^2/\text{Vsec}$, will require the use of high electric gradients, e.g. larger than 200 V/cm. In analytical practice such electrolyte systems have only limited value¹¹. At low high pH the contribution of protons or hydroxylions, being rather mobile species, to the conductance can not be neglected and their deleterious effects will be dealt with in Chapter 3.4.

TABLE 3.4

CONSTITUENT DATA FOR FIGS. 3.5 AND 3.6

Constituent	mobility cm^2/Vsec	pK_a value	
		Fig. 3.5	Fig. 3.6
Leading, L	-77×10^{-5}	$\text{pK}_L = -2$	$\text{pK}_L = -2$
Counter, C	$+30 \times 10^{-5}$	$\text{pH}^L = \text{pK}_C$	$\text{pH}^L = \text{pK}_C$
Separand, A	variable	$\text{pK}_A = 4.0$	$\text{pK}_A = 4.5$
B	-20×10^{-5}	$\text{pK}_B = 4.5$	$\text{pK}_B = 4.0$

Leading electrolyte: pH^L variable, $\bar{C}_L^- = -0.01 \text{ M}$

Sample: $\text{pH}^{M*} = 4.0$, $n_A = n_B = 10^{-7}$ mole, $\bar{C}_A^{M*} = \bar{C}_B^{M*} = -0.05 \text{ M}$

Driving current: $I = 100 \mu\text{A}$, $O = 0.002 \text{ cm}^2$.

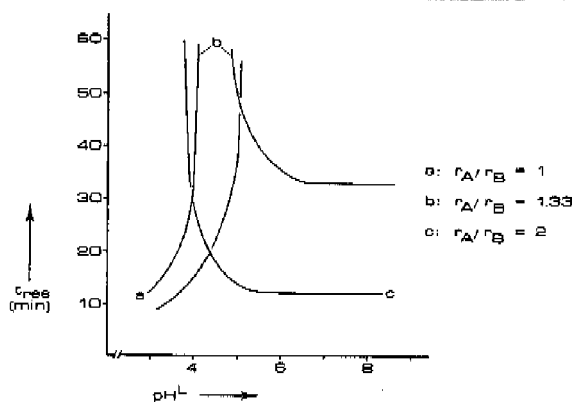


Fig. 3.6 Time of resolution as a function of the pH of the leading electrolyte. Constituent data: Table 3.4.

If the more mobile separand has the lower dissociation constant, the situation becomes more complex. The pH of the mixed zone, at which, in this case, no separation occurs and its relation to the pH of the leading electrolyte, have already been discussed. From Fig. 3.6 it follows that the pH of the leading electrolyte must be at least one pH unit different from the critical pH^L in order to obtain an acceptable time of resolution. The question of whether a high or a low pH must be chosen depends on the

physico-chemical characteristics of the separands. Nevertheless, the tendency that a low pH^L is favourable still holds. For example, with the mobility ratio of 1.33 resolution will be obtained at $\text{pH}^L = 7$, but a higher resolution rate will be obtained at $\text{pH}^L = 3$. At high pH the separands will migrate in order of ionic mobilities, whereas at low pH they will migrate in order of dissociation constants.

The influence of the pH of the sample

Although in practice the pH of the sample can not be varied arbitrarily, its influence can nevertheless be substantial, as can be seen from Fig. 3.7.

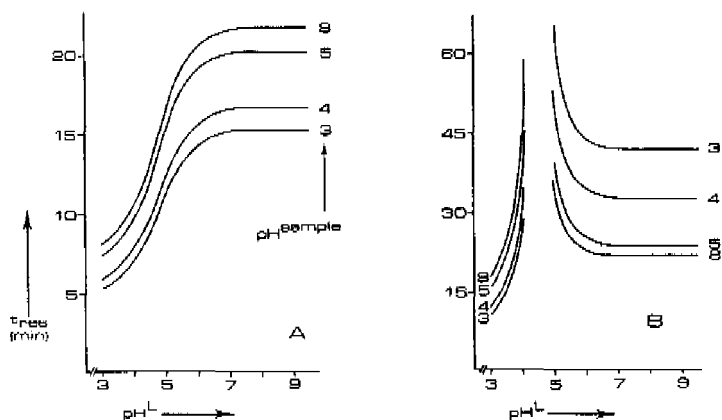


Fig. 3.7 The influence of the pH of the sample on the time of resolution. Constituent data: Table 3.5.

Again, resolution is favoured by a low pH of the sample. When the more mobile constituent has the larger dissociation constant, Fig. 3.7A, the effect is straightforward. Resolution is favoured by a low pH of both the sample and the leading electrolyte. From Fig. 3.7B where $r_A > r_B$ and $K_A < K_B$, the guidance for this "reversed pair" of separands can be deduced. When running such a sample at a high pH of the leading electrolyte it is also preferable to use a sample with a high pH.

TABLE 3.5
 CONSTITUENT DATA FOR FIG. 3.7

Constituent	mobility cm ² /Vsec	pK _a value	
		Fig. 3.7A	Fig. 3.7B
Leading, L	-70 × 10 ⁻⁵	pK _L = -2	pK _L = -2
Counter, C	+30 × 10 ⁻⁵	pH ^L = pK _C	pH ^L = pK _C
Separands, A	-40 × 10 ⁻⁵	pK _A = 4.0	pK _A = 4.5
B	-30 × 10 ⁻⁵	pK _B = 4.5	pK _B = 4.0

Leading electrolyte: pH^L variable, $\bar{c}_L^{-L} = -0.01$ M
 Sample: pH^{M*} variable, $n_A = n_B = 10^{-7}$ mole, $\bar{c}_A^{M*} = \bar{c}_B^{M*} = -0.05$ M
 Driving current: I = 100 μA, O = 0.002 cm².

Optimal conditions are obtained, however, at a low pH of both the sample and the leading electrolyte. In both cases the migration configuration of the separands in the sampling compartment and the separation compartment will be the same. If, however, a low pH of the leading electrolyte is combined with a high pH of the sample, B will separate as well in the sampling compartment as in the separation compartment.

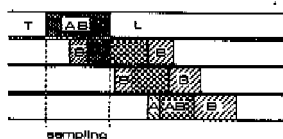


Fig. 3.8 The dual separation phenomenon.

As soon as the sample train has left the sampling compartment, Fig. 3.8, a zone-electrophoretic elution of the mixed zone in the separation compartment will start. As soon as the terminating constituent has reached the rear side of the zone-electrophoretic concentration distribution, a new discontinuity, the separand zone A, will start to grow. This phenomenon of zone-electrophoretic rearrangement, has no other influence on the separation process, as

has been discussed already.

3.3. TIME OF DETECTION AND LOAD CAPACITY

Eqn. 3.13 suggests that a fixed-point detector must be located at x_{res} from the sampling compartment and that detection can be started at t_{res} . From Fig. 3.1, however, it follows that this is not always the case, as detection can already have commenced before the sample has been resolved completely. The criterion for detection states, that only resolved separands must be detected, i.e. the mixed zone should resolve the moment reaches the point of detection. Hence, for the minimal length at which the detector must be located, x_{det} , it follows that

$$x_{det} = t_{res} v_{A/A+B} \quad (3.15)$$

and, for the moment at which detection must be started, t_{det}

$$t_{det} = x_{det}/v_L \quad (3.16)$$

It follows directly that the time of resolution will be larger than or equal to the time of detection, as holds for the resolution distance and the detection distance. Using the appropriate relationships we obtain

$$\frac{x_{det}}{x_{res}} = \frac{t_{det}}{t_{res}} = \frac{\phi \frac{k_A}{k_B} + \frac{\alpha_B^M r_B}{\alpha_A^M r_A}}{1 + \phi \frac{k_A}{k_B}} \quad (3.17)$$

For a fixed point detector it is important to minimize both x_{det} and t_{det} , and optimization procedures are analogous to the minimization of the time of resolution. Fig. 3.9 shows the influence of the sampling ratio on the ratio of detection time and resolution time. Depending on the actual parameters, the effect can be considerable. For a low sampling ratio and a low mobility ratio, the time of detection will be very small compared with the time of resolution. In practical terms this means that,

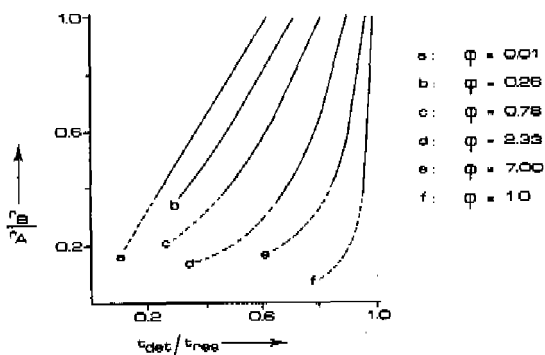


Fig. 3.9 Relationship between the time of detection and the time of resolution. Constituent data Table 3.6.

TABLE 3.6

CONSTITUENT DATA FOR FIG. 3.9 AND FIG. 3.10

Constituent	mobility cm^2/Vsec	pK_a value	
		Fig. 3.10	Fig. 3.9
Leading, L	-77×10^{-5}	-77×10^{-5}	$\text{pK}_L = -2$
Counter, C	30×10^{-5}	30×10^{-5}	$\text{pK}_C = 4$
Separand, A	variable	variable	$\text{pK}_A = 4$
B	-30×10^{-5}	-30×10^{-5}	$\text{pK}_B = 4.5$

Leading electrolyte: $\text{pH}^L = 4$, $\bar{C}_L^- = -0.01 \text{ M}$

Sample: Fig. 3.9 $\text{pH}^{M^+} = 4$, ϕ variable, $n_A = 10^{-7}$ mole

Fig. 3.10 pH^{M^+} variable, $n_A = n_B$

Driving current: Fig. 3.9 $I = 100 \mu\text{A}$, $O = 0.002 \text{ cm}^2$.

whenever the more mobile separand has a high concentration compared with that of the less mobile separand, detection can be started early and only a short separation compartment is needed. At high sampling ratios, the time of detection will be almost equal to the time of resolution.

In common practice, however, the detector will be located at a fixed position in the separation compartment,

x_{detfix} , so it is impossible to choose the actual length of the separation compartment. For the maximal sample load, n^{max} , for the column we obtain

$$n_A^{\text{max}} = n_L^{\text{load}} r_A k_A \left\{ \frac{1 - \frac{\alpha_B^M r_B}{\alpha_A^M r_A}}{\phi \frac{k_A}{k_B} + \frac{\alpha_B^M r_B}{\alpha_A^M r_A}} \right\} \quad (3.18)$$

where n_L^{load} is the amount of the leading constituent filling the separation compartment, from the sampling compartment to the detector.

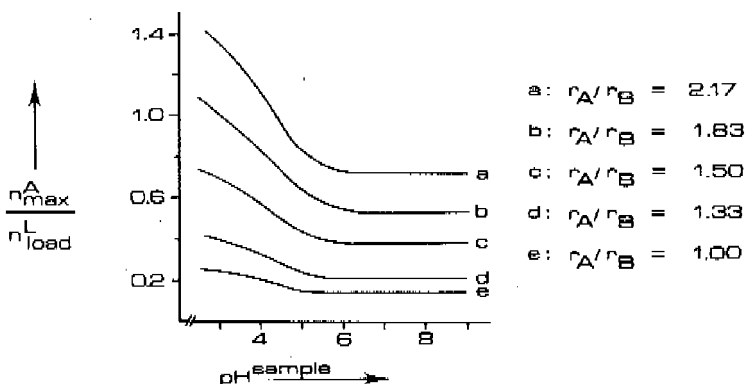


Fig. 3.10 Influence of the sample pH on the load capacity. Constituent data: Table 3.6.

The maximal sample load for the second separand follows directly from the given definitions. Moreover, eqn. 3.18 can be transformed directly into a time-based or distance-based form, using

$$n_L^{\text{load}} = x_{\text{detfix}} \bar{c}_L^L = t_{\text{detfix}} \frac{I}{F(1 - r_C)} \quad (3.19)$$

Eqn. 3.19 is very useful, since it gives directly the amount of the leading electrolyte, n_L^{load} , once the product of time and driving current, i.e. the amount of Coulombs used, is measured and the transference number of the leading constituent is known. Since the amount of leading constituent can be arbitrarily chosen, we define for the load capacity C

$$C_{load} = \frac{n_A^{max}}{n_L^{load}} \quad (3.20)$$

A maximal load capacity is obtained by optimization of the separation process. For anionic separations a low pH of both the sample and the leading electrolyte will favour the load capacity, as can be seen from Fig. 3.10. For cationic separations a high pH of the leading electrolyte will be preferable.

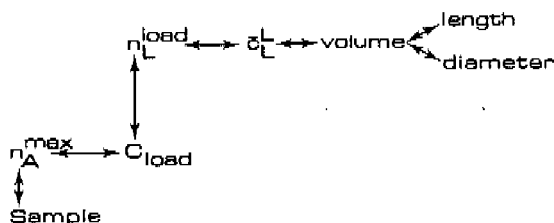


Fig. 3.11 Column evaluation.

The load capacity can be used for defining the required column dimensions or vice versa. The evaluation procedure is schematically given in Fig. 3.11.

3.4. CURRENT EFFICIENCY

In the previous sections it was shown how important parameters, such as time of resolution and load capacity, are related with operational and instrumental conditions. In addition, however, it is important to know how efficient the applied electric driving current is used for separation. Eqn. 3.12 offers a unique possibility to derive the dimensionless separation number S . The advantage of this

separation number is that it is essentially independent of the amount of sample, column geometry and the electric driving current. Differentiation of the separated amount of the constituent *A* with respect to time and multiplication by F/I gives

$$S_A = \frac{F}{I} \frac{\partial}{\partial t} n_A = \left\{ \frac{1 - \frac{\alpha_B^M r_B}{\alpha_A^M r_A}}{1 + \phi \frac{k_A}{k_B}} \right\} \left\{ \frac{r_A}{r_A - r_C} \right\} \quad (3.21)$$

The physical significance of the dimensionless separation number is that it gives the relative part of the driving current, that is actually used for the separation of the separand *A*. It should be noted that the separation number is not equivalent with the transference number T . For the transference number of the constituents *A* and *B* in the mixed zone it follows that:

$$T_A^M = \frac{1}{1 + \phi \frac{k_A}{k_B}} \left\{ \frac{r_A}{r_A - r_C} \right\} \quad \text{and} \quad T_B^M = \frac{\frac{k_A}{k_B}}{1 + \phi \frac{k_A}{k_B}} \left\{ \frac{r_B}{r_B - r_C} \right\} \quad (3.22)$$

In the limiting cases, where $\phi = 0$ or $\phi = \infty$, the transference numbers are equal to those in the separated zones. Combining the eqns. 3.21 and 3.22 we obtain for the separation number

$$S_A = \left\{ 1 - \frac{\alpha_B^M r_B}{\alpha_A^M r_A} \right\} T_A^M \quad (3.23)$$

Taking limiting conditions for the pH of the mixed zone and the sampling ratio into consideration it follows that:

$$0 < S_A < T_A \quad (3.24)$$

The separation number of the second separand, *B*, is closely related to that of *A*, as

$$S_B = \left\{ \frac{\alpha_{ArA}^M}{\alpha_{BrB}^M} - 1 \right\} \cdot T_B^M = \frac{S_A T_B^M}{T_A^M - S_A} = \chi S_A \quad (3.25)$$

where χ is the molar concentration ratio \bar{c}_B/\bar{c}_A in the sample. The relationship between χ , ϕ and the pH of the sample is straightforward:

$$\phi = \chi \cdot \frac{(1 + 10^{+(pK_A - pH^{M*})})}{(1 + 10^{+(pK_B - pH^{M*})})} \quad (3.26)$$

In Fig. 3.12 the influence of the sampling ratio on the separation number is shown for various separands. The counter constituent again has been chosen for its optimal buffering capacity in the leading electrolyte.

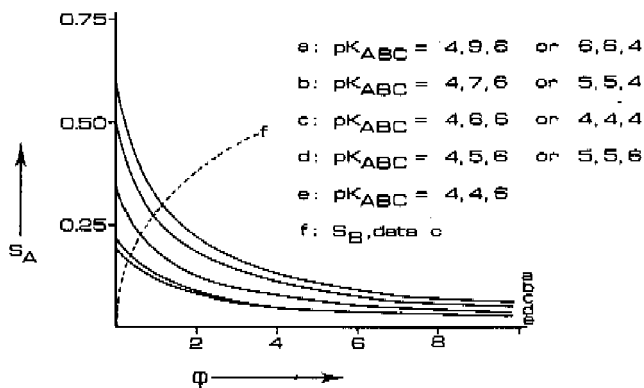


Fig. 3.12 The influence of the sampling ratio on the dimensionless separation number.

$$pH^L = pK_C, \quad r_A = 0.6, \quad r_B = 0.4, \quad r_C = -0.4.$$

It follows that the separation number decreases rapidly with increasing sampling ratio. Numerical calculations have shown¹⁰ that many of the curves, that are obtained when the dissociation constants and mobilities are varied, show congruent behaviour. It should be recognized that generally exact data for the separands are not known and therefore a variation in the input data has to be taken into consideration. Reasons for these variations are

obvious: lack of data, unreliable data, temperature and activity effects. The influence of parameter fluctuations is however marginal¹⁰, as many of them are counter active. From the curve f in Fig. 3.12 it follows that the separation number for the second separand increases with increasing sampling ratio.

Eqn. 3.22 again gives the optimization rationale for anionic separations. As long as the transference number in the mixed zone is independent of pH, a low pH will have a favourable influence on separation. At a low pH, however, the contribution of protons in the transport process cannot be neglected and the transference number for the separand A can be written as:

$$T_A^M = \frac{r_A}{r_A - r_C} \cdot \left\{ \frac{1}{1 + \phi \frac{k_A}{k_B} + \frac{c_H^M}{c_A^M} \cdot \frac{k_A}{k_H}} \right\} \quad (3.27)$$

where c_H^M and c_A^M are the proton concentration and the separand concentration in the mixed zone. From eqn. 3.27 it follows that the ratio of the proton and the separand concentration may have a large influence on the transference number. At a relatively high proton concentration the favourable influence of the low pH on the ratio of effective

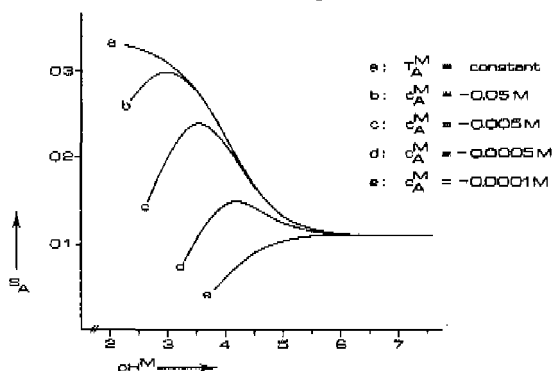


Fig. 3.13 The influence of a relatively high proton concentration on the separation number.

$r_A = 0.6$, $r_B = 0.4$, $r_C = 0.4$, $r_H = 6$, $\phi = 1$, $pK_A = -3$, $pK_B = 4$.

separand mobilities is counteracted by the deleterious effect of pH on the transference number. Depending on the actual conditions the separation number can show an optimum. In Fig. 3.13 an example is shown. The sampling ratio was chosen to be unity and the concentration of the separand A was chosen as a parameter. It follows that, at a low separand concentration and a low pH of the mixed zone, the effect can be appreciable.

The optimal pH of the mixed zone is influenced by all the physico-chemical constants of the constituents in the mixed zone. A small difference in dissociation constants and/or mobilities will make the separation number rather insensitive for pH, but it should be remembered that such separands, per se, will have a low separation number. Separand pairs that have a large difference in pK values will be more sensitive in this respect and the optimum in pH increases with increasing pK values. It should be recognized, however, that a low separand concentration and low pH of the mixed zone, at this sampling ratio, cannot be generated by an arbitrarily chosen leading electrolyte.

Curve e of Fig. 3.13 can only be generated by using a rather low concentration of the constituent. Such electrolyte systems are known to have only a rather small range of pH applicability¹¹. Depending on the concentration of the leading constituent the transference number of the leading constituent is influenced by the pH of the leading

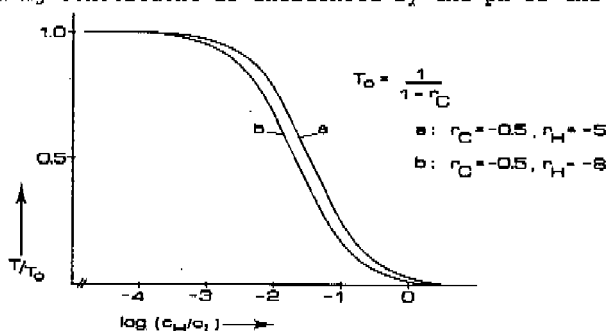


Fig. 3.14 The transference number of leading constituent as a function of pH.

electrolyte, as can be seen from Fig. 3.14. If the ratio of the proton concentration and leading constituent concentration is small, the transference number is constant. With increasing ratio, however, it decreases rapidly, and almost the total electric driving current is carried by the rather mobile protons. In practice, the concentration ratio will be chosen smaller than 0.1. Therefore, working at a leading constituent concentration of 10 mM, the pH of the leading electrolyte should be chosen higher than pH = 3. Working at a concentration of 1 mM the lower limit of pH is already 4, which emphasizes the limited applicability of very dilute electrolyte systems. Though we did consider only the deleterious influence of protons at low pH, similar considerations can be done for the influence of hydroxyl ions at a high pH.

REFERENCES

1. F. Everaerts, *Graduation Report*, Eindhoven University of Technology, Eindhoven (The Netherlands) 1963.
2. R. Routs, *Thesis*, Eindhoven University of Technology, Eindhoven (The Netherlands) 1971.
3. J. Beckers, *Thesis*, Eindhoven University of Technology, Eindhoven (The Netherlands) 1973.
4. T. Jovin, *Biochemistry*, 12 (1973) 871, 879, 890.
5. P. Ryser, *Thesis*, University of Bern, Bern (Switzerland) 1976.
6. J. Hinckley, *J. Chromatogr.*, 109 (1975) 209.
7. Th. Verheggen, F. Mikkers and F. Everaerts, *J. Chromatogr.*, 132 (1977) 205.
8. G. Brouwer and G. Postema, *J. Electrochem. Soc. Electrochem. Sci.*, 117 (1970) 874.
9. F. Kohlrausch, *Ann. Chem. Phys.*, 62 (1897) 14.
10. J. Peek, *Graduation Report*, Eindhoven University of Technology, Eindhoven (The Netherlands) 1977.
11. F. Everaerts, J. Beckers and Th. Verheggen, *Isotachopheresis*, *J. Chromatogr. Libr. Vol. 6*, Elsevier, Amsterdam-Oxford-New York, 1976.

12. J. Wielders and F. Everaerts, in B. Radola and D. Graesslin (Editors), *Electrofocusing and Isotachopheresis*, Walter de Gruyter, Berlin-New York, 1977, 527.
13. R. Conson, A. Gordon and A. Martin, *Biochem. J.*, 40 (1946) 33.
14. L. Arlinger, *J. Chromatogr.*, 91 (1974) 785.
15. P. Bocek, M. Deml, B. Kaplanova and J. Janak, *J. Chromatogr.*, 160 (1978) 1.
16. J. Wielders, *Thesis*, Eindhoven University of Technology, Eindhoven (The Netherlands), 1978.

PART 2

EXPERIMENTAL PART

CHAPTER 1

High performance zone electrophoresis

An experimental approach is given to high performance zone electrophoresis. The asymmetric concentration distributions are the result of migration dispersion and asymmetry can be only suppressed by the application of very low amounts of sample. Non migrational dispersion can be well controlled by the use of narrow bore tubes. Plate heights smaller than 10 μm can easily be obtained. The practical applicability of HPZE is discussed.

1.0. INTRODUCTION

Many of the problems in the development of electrophoresis are caused by convection and detection. In experimental practice there are three alternative approaches to alleviate the problem of convection. One approach emphasizes the use of additional force fields, e.g. gravitational or electromagnetic, to eliminate the disturbing influence of convection^{1,2}. In a second, somewhat more practical approach, stabilizing media such as paper,

cellulose acetate or gels are used³. Although in this way convection can be effectively suppressed, it inherently introduces an interaction between the solutes of interest and the anticonvective medium. Such interactions may well be beneficial in many applications, but are generally not desirable. The third approach, which has proven to give a satisfactory solution to obtain a stable electrophoretic performance, is the use of the anticonvective "wall-effect"⁴. Hence stability can be obtained by decreasing the diameter of circular columns or decreasing the gap distance for flat columns. In moving boundary electrophoresis and isotachopheresis such configurations have been applied successfully, mainly by using narrow-bore tubes of chemically and electrically non conducting materials⁵⁻¹², such as glass and PTFE.

In conventional zone electrophoresis generally "off-line" detection methods, such as colour reactions and subsequent optical scanning, are used. A prerequisite for high performance zone electrophoresis in narrow-bore tubes is however the availability of a reliable, fast responding and sensitive detection system. Until now only the conductimetric and UV detection systems¹² seems to have some compatibility with the required demands.

Zone electrophoresis in narrow bore tubes has attracted less attention, although several suggestions about its feasibility have been made¹³⁻¹⁵. Hjertén¹³ performed zone electrophoresis in tubes of quartz glass coated with methyl cellulose and used UV detection. The adverse effect of the relatively large inner diameter of the separation compartment was reduced by rotating it about its longitudinal axis. Although the operating conditions seem somewhat complex, he clearly showed the feasibility of the technique.

Everaerts and Hoving Keulemans¹⁴ used an isotachopheretic instrument equipped with a thermometric detector. The separation compartment was of PTFE tubing and with instrument they were able to perform zone electrophoretic separations and they detected highly asymmetric zones.

A detailed study was made by Virtanen¹⁵, who used a glass capillary with an inner diameter of 0.21 mm and potentiometric detection. The performance of the equipment however was poor as the experiments were extremely sensitive for disturbances.

Giddings¹⁶ evaluated theoretically the ultimate capabilities of zone electrophoresis by introducing the HETP concept. Provided that a low dispersive performance can be achieved, he suggested that plate heights down to 10 μm should be possible. Until recently this limit of performance had never been reached, but the use of capillary configurations seemed to be promising in this respect. In analogy with modern chromatographic methods, the low load capacity of capillary systems will put high demands on detection. For moving boundary electrophoresis and isotachopheresis a satisfactory solution has been found. In zone electrophoresis however, a higher selectivity is needed. Moreover, there are some methodological problems, that may hamper the development of high performance zone electrophoresis.

1.1. EXPERIMENTAL

All chemicals used were of analytical reagent grade or additionally purified by conventional methods. The operational systems and conditions are given in Table 1.1. Counter constituents were chosen for their optimal buffering capacity at the operative pH, whereas the carrier constituent was chosen according to the specific requirements of the analytical problem.

In all cases a viscous additive was used to increase the electrophoretic performance. Driving currents were chosen in such a way that an acceptable compromise was found between the time for analysis, heat production and required voltage.

The major part of the experiments were performed in the electrophoretic equipment developed by Everaerts et al.¹². The separation compartment was formed by PTFE narrow

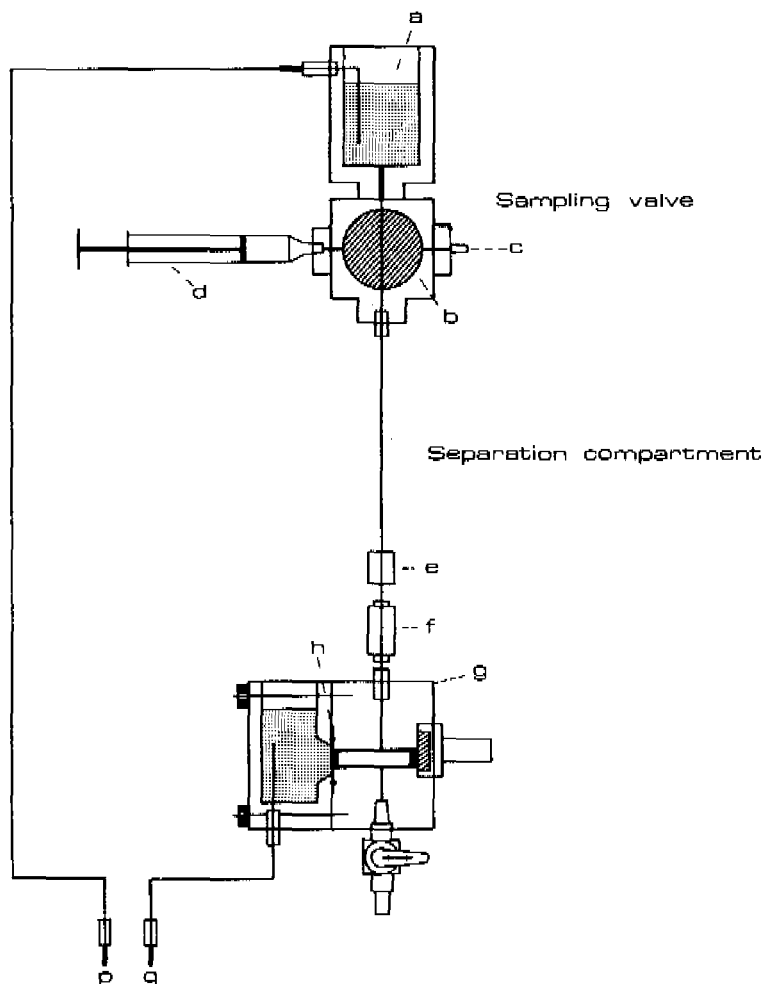


Fig. 1.7 Zone electrophoretic equipment.

a: electrode compartment, b: sampling valve, c: drain, d: sampling syringe, e: UV detector, f: conductimeter, g: electrode compartment, h: membrane, p and q: leads to power supply.

TABLE 1.1
OPERATIONAL SYSTEMS

Parameter	System No.			
	1	2	3	4
Carrier constituent	MES	Acetid acid	Acetid acid	HEPES
Concentration (M)	0.01	0.005	0.1	0.1
Counter constituent	HIST	HIST	GABA	TRIS
pH	6.05	6.02	4.00	6.00
Additive	0.1% HEC	0.1% HEC	0.1% HEC	0.1% HEC
Inner diameter (mm)	0.2	0.2	0.2	0.45
Driving current (μ A)	20	30	100	150
Temperature ($^{\circ}$ C)				20

bore tube with an inner diameter of 0.2 mm and an outer diameter of 0.35 mm. Samples were introduced by means of a microliter syringe or a specially constructed four-way injection valve with a volume of 0.7 μ l and an inner diameter of 0.3 mm. Electric gradient detectors were used in the conductance mode¹² and UV absorption signals (254 nm) were converted electronically into absorbance. The direct and constant driving current was taken from a modified Brandenburg (Thornton Heath, Great Britain) high voltage power supply.

A schematic representation of the experimental set up is given in Fig. 1.1. Additional experiments were performed with the LKB Tachophor (LKB Bromma, Sweden), equipped with a 0.45 I.D. narrow bore tube. Only the experiments with the LKB Tachophor were performed at a constant temperature of 20 $^{\circ}$ C, in all other experiments the temperature was ambient.

1.2. RESULTS AND DISCUSSION

According to our theoretical considerations, Part 1 Chapter 2, the effective mobility of the separand, relative to that of the carrier constituent, determines the concentration distribution of the separand. A separand with an effective mobility smaller than that of the carrier

constituent must migrate with a sharp leading side, whereas the back side of the zone must be "diffuse". From Fig. 1.2b it can be seen that the electric gradient profile of propionate conforms with theory when acetate is used as the carrier constituent. In this case a stable moving boundary is formed at the leading side of the zone, whereas at the back side the criterion for stability can not be met. The steepness of the voltage gradient, of course, determines the actual sharpness of the moving boundary.

On the other hand the electric gradient profile of a separand with an effective mobility larger than that of the carrier constituent must migrate with a sharp back side and a "diffuse" leading side. In Fig. 1.2a the distribution of formate detected under the same operational conditions, (system 2, Table 1.1) is given.

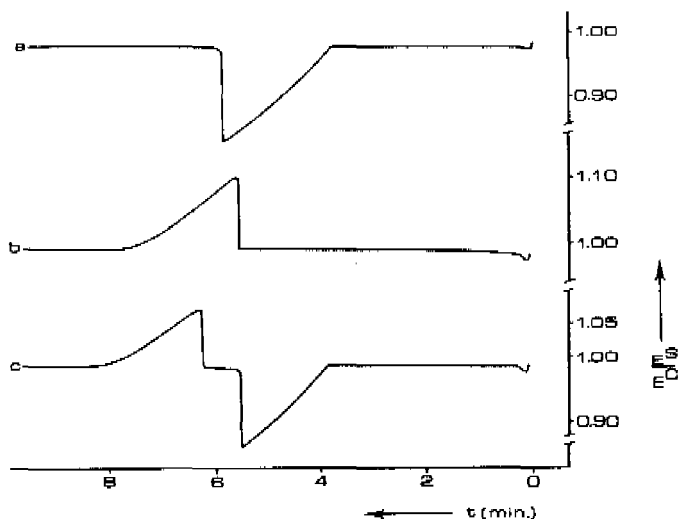


Fig. 1.2 Zone electrophoretic separation of formate and propionate in the operational system 2 (Table 1.1). a) formate, 3.5×10^{-9} mole; b) propionate, 3.5×10^{-9} mole; c) formate + propionate, each 2.33×10^{-9} mole. E^G/E^C = electrical field strength in the separand zone relative to the carrier electrolyte; $t(\text{min})$ = time of analysis.

Again the actual gradient profile conforms with theory. The result of the analysis of a mixture of the two separands is shown in Fig. 1.2c. It can be seen that neither the retention behaviour nor the distribution function of the more mobile separand, i.e. formate, is affected by the presence of the second separand, whereas the opposite is clearly not true. This is caused by the fact that for a $r_j > 1$ configuration the time needed for the first separand ion to reach the point of detection, t_{det} , is independent of the sampled amount and the presence of other separands, whereas for a $r_j < 1$ configuration no independence exists. Therefore Fig. 1.2 not only proves theory but also emphasizes the complex nature of retention in zone electrophoresis. This complexity may hamper the handling of multicomponent samples in which large concentration differences occur.

When an fixed point detection system is used, the electric gradient profile for a $r_j > 1$ is given by:

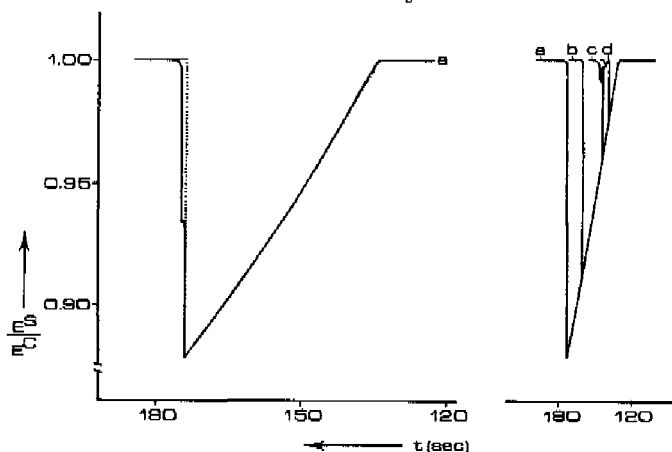


Fig. 1.3 Electric gradient profile of a chloride zone, migrating in the operational system 1 of Table 1.1.

a) 707×10^{-12} mole Cl^- ; b) 354×10^{-12} mole Cl^- ; c) 70.7×10^{-12} mole Cl^- ; d) 21.1×10^{-12} mole Cl^- ; E^S/E^C relative electric field strength; $t(sec)$ = time of analysis.

$$E^S(x_{\text{det}}, t)/E^C = \sqrt{t_{\text{det}}/t} \quad (1.1)$$

In Fig. 1.3 an electric gradient profile of a chloride zone migrating in the operational system 1 of Table 1.1 is shown. From the theoretical profile, given in Fig. 1.3 by the dotted line, and the experimental profile it must be concluded that the theoretical profile is in close agreement with experimental practice. It should be emphasized that the theoretical model, Chapter 2 Part 1, essentially was developed for monovalent strong electrolytes. The operational system 1 of Table 1.1, however, is well buffered, as both the carrier constituent and the counter constituent have pK values that are close to the pH of the carrier electrolyte. Any pH shift in this electrolyte system is unlikely and therefore the theoretical considerations will apply. From Fig. 1.3 we conclude that dispersive factors, other than electrophoretic migration, are well controlled and have a negligible influence on the concentration distributions. Owing to the high relative mobility of the separand and its local concentration, an appreciable inhomogeneity in the electric field occurs, resulting in stable boundaries. It can be calculated that under the given operational conditions diffusional dispersion becomes important at the picomole level for the sampled amount.

TABLE 1.2
RETENTION DATA

c.v. coefficient of variation								
No. of deter- minations	Sample load (mole x 10 ⁻¹²)	Peak width		Peak height		t _{stop} sec	t _{det} sec	t _{gr} sec
		sec	C.V.(%)	mm	C.V.(%)			
3	707	39.1	1.5	1230	0	172.4	133.3	159.2
4	500	32.4	2	1094	0.4	166.1	133.7	155.0
4	354	27.4	2	908	0.2	162.2	134.8	153.0
4	225	21.8	2	732	0.5	154.9	133.1	147.6
4	70.7	11.8	6	427	1.0	146.2	134.4	142.3
4	21.2	7.53	12	243.5	1.0	140.7	133.2	138.2
3	7.07	6.14	5	165.2	3.0	138.7	132.6	136.7

Theoretically, it has been shown, Part 1, Chapter 1, that t_{det} is independent of the sampled amount, as is experimentally confirmed by the right hand side of Fig. 1.3 and the data of Table 1.2. Decreasing the sample load has no effect on the shape of the concentration distribution and only the moment the last sample ions are reaching the point of detection, t_{stop} , is determined by the sampled amount and the generated distribution function.

From the data in Table 1.2, it follows that neither the peak height nor the peak width is linearly related to the amount sampled. For quantitative determinations we derived:

$$n_s = k \left(t_{stop} - \frac{2}{3} \sqrt{\frac{t_{stop}^3}{t_{det}}} - \frac{1}{3} t_{det} \right) \quad (1.2)$$

where k is a calibration constant depending on the cross-sectional area, the current density and the mobilities. The data of Table 1.2 fit this eqn. with a correlation coefficient of 0.9997. Again it must be concluded that the experiments performed were essentially non-diffusional.

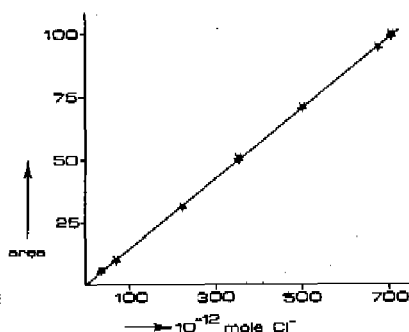


Fig. 1.4 Calibration graph for chloride determinations.

In those instances in which somewhat blurred concentration distributions are obtained, e.g. when injection is made with a microliter syringe, it is necessary to use the peak area. As the difference in specific conductance between a sample zone and the carrier electrolyte is directly related to the concentration of the separand concentra-

tion, it is obvious that the conductance-based peak area must be used. Though the applied detection system is of the electric gradient or resistance type¹², the electric gradient peak-area, in a triangle approximation, proved to be linearly related with the sampled amount. Figure 1.4 shows the calibration graph for the separand chloride.

For identification purposes a retention time has to be defined. Both the time-based centre of gravity, t_{gr} , and the time of the peak maximum, t_{stop} , are affected by the sample load as can be seen from Table 1.2. For practical reasons, generally the time of the peak maximum will be preferred.

At high sample loads probably an appropriate empirical correction function can be used. The use of a constant voltage instead of a constant driving current may well be favourable in this respect. From the Fig. 1.3 it can be seen that the sample did not only contain chloride, but also an impurity, which was identified as sulphate. At a high sample load it is difficult to decide whether separation is complete or not. Although asymmetric concentration distributions are frequently encountered in free zone electrophoresis, they also occur when anticonvective media such as gels or cellulose acetate are used¹⁸. Using capillary systems, however, they seem to be more pronounced because most forms of non migrational dispersion can be well controlled. In fact the high asymmetry of the separations shown in Figs. 1.2 and 1.3 gives an indication of the low dispersive performance of the equipment. Working with syringe injection also very reproducible and low dispersive separations can be done, as can be seen from Fig. 1.5. Manual injection must be done with great care in order to ensure that the sample is introduced in the ideal plug-form. The use of a sampling valve obviously is superior in this respect but has the disadvantage of a relatively large and invariable volume. The adverse effect of a relatively large sampling volume can often be decreased by the concentrating capabilities of the electrolyte system. The left hand side of Fig. 1.6 shows a separation of three

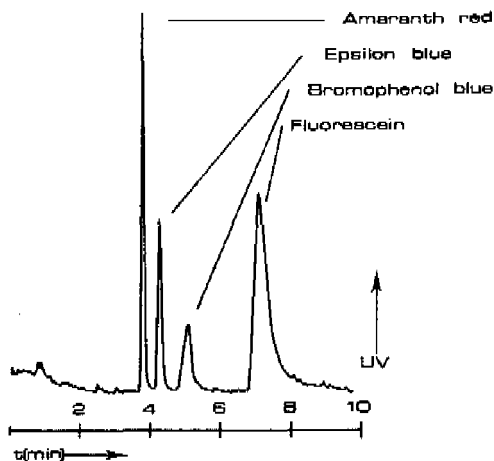


Fig. 1.5 Separation of some anionic dyes on the LKB Tachophor, t = time of analysis, UV = UV absorption at 254 nm Operational system 4 of Table 1.1.

separands, analysed in the operational system 3 of Table 1.1, when the four-way sample valve is used. The relatively high concentration of the carrier constituent and the fact that the separands were not dissolved in the carrier electrolyte guarantees a concentration of the sample over the stationary boundary between the sampling and the separation compartment, Part 1 Chapter 2.

Irrespective the long sample width, i.e. 10 mm, a good separation is obtained. A comparable result can be obtained by disc electrophoresis^{19,20}, by choosing a suitable stacking electrolyte or by using a two dimensional coupled column system²¹. The right hand side of Fig. 1.6 shows the same separation, but now the separands are dissolved in the carrier electrolyte. In this instance the electrolyte system has no concentrating effect and the adverse effect of the relatively long sample width is clearly visible. Therefore, in experimental practice the sample should not be equilibrated with the carrier electrolyte. Selective removal of any separand, in which one is not interested,

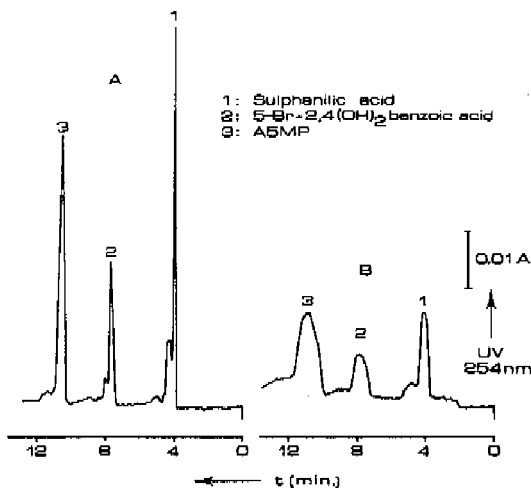


Fig. 1.6 The influence of the sampling width.

Operational system 3, Table 1.1; t (min) = time of analysis; UV = UV absorbance at 254 nm; A) Separands dissolved in water; B) Separands dissolved in carrier electrolyte.

or replacement of it by a less mobile constituent, will enhance resolution. Theoretically it is possible to obtain peak widths that are smaller than the sample width. Another important consequence of the concentrating capabilities should be mentioned. Since local separand concentrations depend on the concentration of the carrier constituent, Part 1, Chapter 2, a high concentration of the latter one involves a relatively high concentration of the separand. Working with concentration dependent detection systems, such as UV, this may have a favourable effect on the signal to noise ratio. For non specific detection systems, such as the conductimeter, no direct advantage is obtained from highly concentrated electrolyte systems. In order to obtain a comparable time of analysis the driving current should be taken proportional to the concentration of the carrier constituent. The resulting increase in heat production may well have a deleterious effect on separation.

As mentioned already quantification in zone electro-

phoresis is not straightforward. Especially with UV detection, being a concentration dependent detector, some care should be taken. At a large peak width, e.g. the separations of Fig. 1.2, appreciable velocity differences exist within the concentration distribution, that is passing the detection system. As a result the integrated peak area can not be linearly related to the sampled amount. At small peak widths however, deviations will be small.

The applicability of a non specific detection system follows from Fig. 1.7, where a separation of a 16-component sample is shown in the operational system 1 of Table 1.1. Because only 17.5 pmole of each constituent were injected, reasonably symmetric distributions are obtained. From the separation shown in Fig. 1.7, it follows that the respons of the conductimetric detector¹⁷ decreases with increasing retention time. Moreover, divalent separands have a considerable higher respons than monovalent separands. For a quantitative evaluation at this low concentration level, the integrated peak area can be used directly.

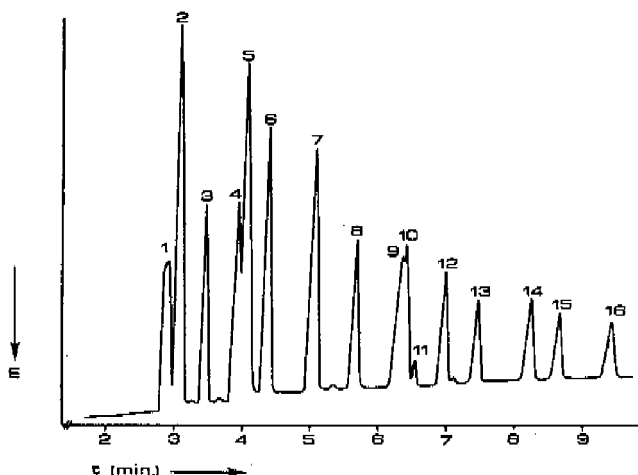


Fig. 1.7 Zone-electrophoretic separation of a 16 component sample. $t(\text{min})$ = time of analysis; E = increasing electrical field strength, sample load: each separand 17.5×10^{-18} mole. Operational system: system 1 Table 1.1 separands: Table 1.3.

The peak maxima can be used most conveniently for retention purposes, because at this low sample load they are fairly independent of the amount sampled. As their repeatability is very high, as can be seen from Table 1.3, they can be used for identification.

Column efficiency is generally expressed as the theoretical plate number N or the related quantity H , the height equivalent to a theoretical plate:

$$N = \left(\frac{t_R}{\sigma_t} \right)^2 \quad \text{and} \quad H = \frac{L}{N}$$

where t_R is the retention time, σ_t is the standard deviation of the concentration distribution and L is the column length. Though there is still some asymmetry left we used the well known chromatographic relation, $N = 5.53 (t_R/w_{1/2})^2$, where $w_{1/2}$ is the peak width at half height. Giddings¹⁶ predicted that the minimal plate height that can be obtained in zone electrophoresis is about 10 μm . According to Fig. 1.7 and the data of Table 1.3, this minimal value is easily obtained for several sample constituents.

As there is still some asymmetry left, it must be concluded that at a lower sample load even better HETPs can be obtained. This, however, will place even higher demands on the detection system, which essentially was developed for isotachopheresis and moving boundary electrophoresis¹². Using the appropriate equations and the data of Table 1.2, it follows that 1 pmole of chloride, analysed in the operational system 1 of Table 1.1, will cause a maximal deviation of the baseline signal of 0.5%. As most separands will have a lower response than chloride, an even higher stability is required. At a very high sensitivity, e.g. 0.01% of the conductance of the carrier electrolyte, the conductivity signal often shows a poor reproducibility and time dependent instabilities, that are not of electronic origin. As a result an irreproducible drift of the baseline, signal wander and ghost peaking occur. These effects are mainly due to electrochemical effects at the micro

TABLE 1.3
PERFORMANCE CHARACTERISTICS

Separand	No	Retention time HETP			N
		sec	cv%	μm	
Chloride	1				
Sulphate	2	185.3	0.8	38	5300
Chlorate	3	208.2	0.8	20	10000
Malonate	4	236.3	0.2	--	-
Chromate	5	244.1	0.6	22	9200
Pyrazole-3,5-dicar-					
boxylate	6	262.6	0.8	18	11000
Adipate	7	304.2	0.9	18	11000
Acetate	8	339.4	0.9	8.7	23000
Propionate	9	376.9	0.9	-	-
β -Chloropropionate	10	382.7	0.6	-	-
Benzoate	12	416.4	0.6	7.1	28000
Naphtalene-2-mono					
sulphonate	13	443.2	0.9	5.6	36000
Glutamate	14	486.9	1.3	6.3	32000
Enanthate	15	514.0	1.0	5.6	36000
Benzylaspartate	16	558.0	1.0	5.9	34000

Length of the separation compartment: L = 20 cm

HETP = Height equivalent to a theoretical plate

N = theoretical plate number

cv. = coefficient of variation $n = 6$.

sensing electrodes, adsorption and the presence of impurities in the electrolytes. Temperature effects seem to have only a minor influence¹⁸. Signal stability causes less problems when UV detection is used. Noting that in the conventional equipment¹² and optical path-length of only 0.2 mm is present, a proportional increase in sensitivity can be achieved by increasing this length. Other advantages of UV detection are the selectivity and its compatibility with electrophoretic gradient elution techniques by pH programming.

1.3. CONCLUSIONS

Concentration distributions in free zone electrophoresis are strongly influenced by the effective mobility of the separand relative to that of the carrier constituent. Leading distributions will be obtained whenever the effective mobility of the separand is larger than that of the carrier constituent. Tailing distributions will result when the relative mobility of the separand is smaller than unity.

High performance zone electrophoresis at a low concentration level is possible and gives reproducible results. Adequate design of the equipment¹² and the use of narrow bore tubes guarantees a low dispersive performance and allows a simple and easy operation.

The retention mechanism in zone electrophoresis is complex, especially when large concentration differences in the separands occur. The retention behaviour is strongly affected by the nature of the sample.

A high stability and of the detection systems is required. UV detection seems to be most promising in this respect.

A fundamental question is whether zone electrophoresis is superior to isotachopheresis or not. It should be noticed that the separation processes of both electrophoretic principles mainly proceed according to the moving boundary principle. In isotachopheresis a high current efficiency is coupled with the need for a relatively high sample load. In zone electrophoresis the current efficiency is rather low, due to the continuous transport of carrier electrolyte, but fortunately only a low sample load is required. The overall result is that both principles differ not appreciable in their time of analysis. Problems considering separability with the two principles are not very likely to be different. Since the retention behaviour in zone electrophoresis is dependent on the presence of other sample constituents, isotachopheresis has a small advantage considering qualitative aspects.

REFERENCES

1. A. Kolin, *J. Appl. Phys.*, 23 (1954) 1442.
2. S. Hjertén, *Ark. Kemi*, 13 (1958) 151.
3. J. Sargent and S. George, *Methods in Zone electrophoresis*, BHD Chemicals, Poole, Great Britain, 3rd edn., 1975.
4. Th. Verheggen, F. Mikkers and F. Everaerts, *J. Chromatogr.*, 132 (1977) 205.
5. B. Konstantinov and O. Oshurkova, *Soc. Phys. Tech. Phys.*, 11 (1966) 693.
6. F. Everaerts, *Thesis*, Eindhoven University of Technology, Eindhoven (The Netherlands), 1968.
7. L. Arlinger and R. Routs, *Sci. Tools*, 17 (1970) 1.
8. J. Vacík and J. Zuska, *Chem. Listy*, 66 (1972) 416.
9. T. Haruki and J. Akiyama, *Anal. Letters*, 6 (1974) 24.
10. S. Stankoviansky P. Cicmanec and D. Kaniansky, *J. Chromatogr.*, 106 (1975) 131.
11. P. Bocek, M. Deml and J. Janak, *J. Chromatogr.*, 106 (1975) 283.
12. F. Everaerts, J. Beckers and Th. Verheggen, *Isotachopheresis*, *J. Chromatogr. Libr.*, Vol. 6, Elsevier, Amsterdam-Oxford-New York, (1976).
13. S. Hjerten, *Thesis*, University of Uppsala, Uppsala (Sweden) 1967.
14. F. Everaerts and W. Hoving-Keulemans, *Sci. Tools*, 17 (1970) 25.
15. R. Virtanen, *Thesis*, Helsinki University of Technology, Helsinki (Finland) 1974.
16. J. Giddings, *Separ. Sci.*, 4 (1969) 181.
17. M. Vervoordeldonk, *Graduation report*, Eindhoven University of Technology, Eindhoven (The Netherlands), 1977.
18. F. Mikkers, F. Everaerts and Th. Verheggen, *J. Chromatogr.*, 169 (1979) 1.
19. L. Ornstein, *Ann. N.Y. Acad. Sci.*, 121 (1964) 321.
20. T. Jovin, *Biochemistry*, 12 (1973) 871.
21. Th. Verheggen, F. Mikkers and F. Everaerts, *Prot. Biol. Fluids 27th coll.*, 27 (1979) 723.

CHAPTER 2

The transient-state characteristics of isotachopheresis

Resolution, load capacity and current efficiency are experimentally evaluated. The pH of the leading electrolyte gives the best rationale for optimization, whereas the pH of the sample has only restricted possibilities. The dimensionless separation number and the load capacity can be used for determination and standardization of experimental performance. Steady state configurations in which the separands are not migrating in order of decreasing effective mobilities are shown and discussed.

2.0. INTRODUCTION

Resolution in isotachopheresis has been defined as the fractional separated amount of the separands under investigation. According to this definition, its numerical value may vary between the limiting values of unity and

zero. At zero resolution no separation has occurred and the constituent forms an ideally mixed zone with at least one other constituent. Obviously the maximal resolution value of unity should be reached in the shortest time possible and with the most convenient experimental conditions.

Basically the three optimization rationales are given by the electric driving current, the mobility of the counter constituent and the chemical equilibria of the electrolytes¹.

The electric driving current acts directly on the time needed to resolve a sample. It should be recognized, however, that for the separation of a given sample a definite amount of coulombs is necessary, but that the time interval in which this amount must be delivered is immaterial². The time needed for resolution and the electric driving current are inversely related, so minimization of the former involves maximization of the latter. High driving currents result in an appreciable temperature effect, which can be deleterious for the separation. The use of flat columns^{3,4} works favourable in this respect, since they allow a better removal of the heat produced. Neglecting differential temperature effects, the driving current has no influence on the current efficiency of the separation process. It follows that for a given sample the volume of the separation compartment, required for the separation is independent of the driving current.

The mobility of the counter constituent acts directly on the transference number and should be as low as possible. The mobility of the counter constituent has only a small influence on the pH of the mixed zone.

For an optimal current efficiency both the ratio of effective separands mobilities and their transference numbers should be optimized. A well known mechanism influencing effective mobilities selectively is given by dissociation and complex formation⁵⁻⁷. In the former instance the pH can be used in optimization procedures, and until now it has been the most frequently used parameter⁵.

The direct result of optimal current efficiency will

be a favourable time of resolution and an optimal load capacity. The current efficiency is best expressed by the dimensionless separation number, Part 1 Chapter 3, which has its maximal value at unity. This separation number is neglecting temperature effects, independent of various operational conditions, such as the electric driving current and the column geometry. It is, however, strongly affected by the nature of the electrolytes and therefore can be used to compare the efficiency of different analyses. The load capacity gives direct information on the amount of separand that can be separated in a given operational system. The load capacity can be optimized by following the same rationales as for the current efficiency. Both parameters can be used to evaluate the experimental performance of an isotachophoretic separation.

2.1. EXPERIMENTAL

All experiments were performed using the isotachophoretic equipment developed by Everaerts et al⁵. The separation compartment, Fig. 2.1, consisted of PTFE narrow bore tubing with inner diameters of 0.45, 0.2 or 0.15 mm and corresponding outer diameters of 0.75, 0.4 and 0.3 mm. The direct constant electric driving current was obtained from a modified Brandenburg (Thornton Heath, Great Britain) high voltage power supply. Electric gradient detectors, applied in either the electric gradient or resistance mode, were used for the measurement transient- state and steady state characteristics. UV detection was performed in the absorption mode at 254 nm.

2.2. RESULTS AND DISCUSSION

Transient-state characteristics can be easily obtained experimentally and several important parameters can be evaluated directly as most are interrelated. For isotachophoretic analyses it is most convenient to use a separation compartment of well defined and constant volume and to apply a constant electric driving current. Using a fixed

TABLE 2.1

OPERATIONAL SYSTEMS

Parameter	System No.				
	1	2	3	4	5
pH of leading electrolyte	3.60	4.03	4.60	5.04	6.02
Leading constituent	Cl ⁻	Cl ⁻	Cl ⁻	Cl ⁻	Cl ⁻
Concentration (M)	0.01	0.01	0.01	0.01	0.01
Counter constituent	BALA	GABA	EACA	CREAT	HIST
Terminating constituent	C ₂ H ₅ COOH	C ₂ H ₅ COOH	C ₂ H ₅ COOH	C ₂ H ₅ COOH	MES ^{**}
Concentration (M)	0.005	0.005	0.005	0.005	0.005
Additive to leading electrolyte	0.05%	0.05%	0.05%	0.05%	0.05%
	MOWIOL	MOWIOL	MOWIOL	MOWIOL	MOWIOL
Temperature	Ambient	Ambient	Ambient	Ambient	Ambient
Current density (A/cm ²)					
d _i = 0.45 mm	0.0503	0.0503	0.0503	0.0503	0.0503
d _i = 0.20 mm	0.0796	0.0796	0.0796	0.0796	0.0796
d _i = 0.14 mm	0.1415	0.1415	0.1415	0.1415	0.1415

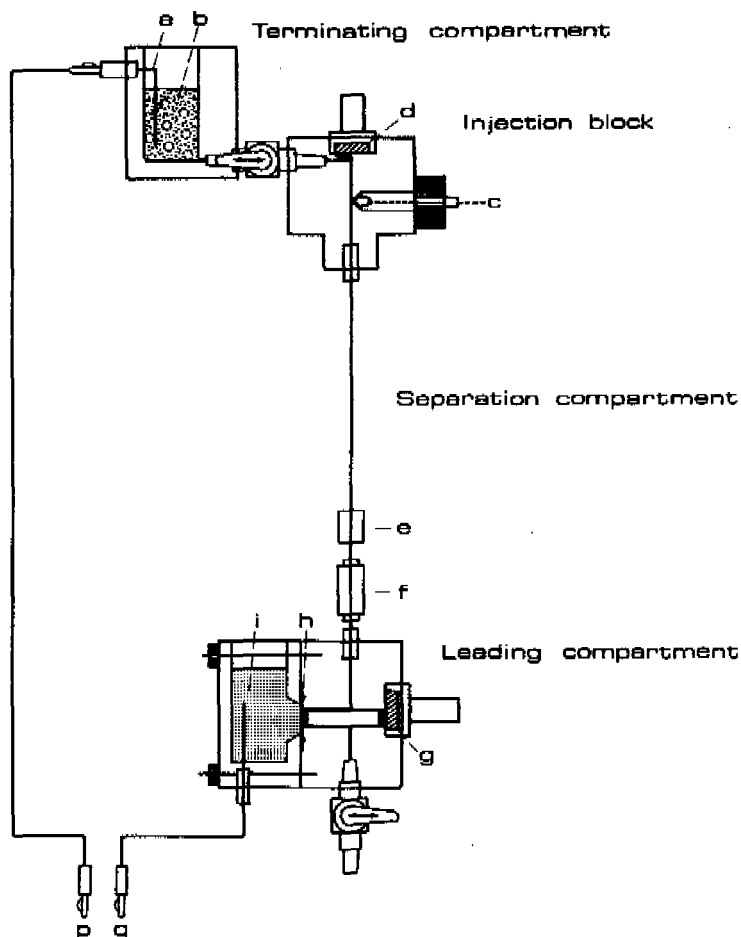


Fig. 2.1 Isotachophoretic equipment.

a: Pt-electrode, b: terminating electrolyte, c: drain, d: septum, e: UV detector, f: conductimeter, g: septum, h: membrane, i: Pt-electrode, p and q leads to power supply.

point detector and a given electrolyte system, all characteristics can be evaluated by injection of known amounts of sample and accurate measurement of all electric gradient and time events.

TABLE 2.2
CHARACTERISTICS OF THE LEADING ELECTROLYTE, SYSTEM 2 TABLE 2.1.

Parameter	value
Leading Constituent, chloride concentration	$n_{Cl^-} = -77 \times 10^{-5} \text{ cm}^2/\text{Vsec}$ $\bar{c}_L^L = -0.01 \text{ M}$
Counter constituent, GABA	$n_{GABA} = 30 \times 10^{-5} \text{ cm}^2/\text{Vsec}$ $pK_{GABA} = 4.03$
Electric driving current	$I = 80 \mu\text{A}$
Diameter of the sep. compartment	$d_i = 0.45 \text{ mm}$
Appearance of 1 st boundary	$t_{\text{detfix}} = 1112 \text{ sec}$
Response leading constituent	$\Delta n_L/\Delta t = 0.592 \text{ nmole/sec}$
Leading load	$n_L^{\text{load}} = 658 \text{ nmole}$
Transference number: experimental	$T_{\text{exp}} = 0.714$
theoretical	$T_{\text{theor}} = 0.720$

In this case, the amount of the leading constituent filling the separation compartment, n_L^{load} , is constant. Provided the sample did not contain the leading constituent, the first boundary, that reaches the detector, will always be registered after the same time interval, t_{detfix} :

$$t_{\text{detfix}} = n_L^{\text{load}} \frac{F}{I} (1 - r_C) \quad (2.1)$$

where F is the Faraday constant, I the applied current and r_C the ionic mobility of the counter constituent, relative to the mobility of the leading constituent. Experimentally the amount of the leading constituent can be determined by the injection of a known amount of the leading constituent Δn_L , and the measurement of the resulting time delay, Δt ,

with respect to t_{detfix} :

$$n_L^{\text{load}} = t_{\text{detfix}} \frac{\Delta n_L}{\Delta t} \quad (2.2)$$

Moreover, because for a one-constituent monovalent weakly ionic constituent zone the dimensionless separation number S , is identical with the transference number, T , the experimental and theoretical transport efficiency can be compared:

$$T_L = \frac{F}{I} \cdot \frac{n_L^{\text{load}}}{t_{\text{detfix}}} = \frac{m_L}{\sum_i m_i} \quad (2.3)$$

where m_i is the ionic mobility of the constituent i . It should be noted that the transference number of monovalent weakly ionic constituents does not contain effective mobilities, but rather ionic mobilities, because, owing to electroneutrality, the degree of dissociation cancels out. Some experimental results are given in Table 2.2.

Eqn. 2.3 is useful, as it provides a practical procedure for the determination of the amount of the leading constituent, once the ionic mobilities and t_{detfix} are known. It also provides a method for the determination of counter constituent mobilities from experimental results, as

$$r_C = 1 - \frac{1}{T_{\text{exp}}} \quad (2.4)$$

It should be emphasized, however, that at extreme values of pH the contribution of hydroxyl-ions and protons should be taken into consideration.

Obviously, a high transport efficiency due to a low ionic mobility of the counter constituent, is always favourable as it guarantees an efficient use of the current applied. For the operational systems given in Table 2.1 we can expect transport efficiencies between 70 and 75%.

As already mentioned, the characteristics of the separation process can be evaluated, by the injection of known amounts of sample. An example of such a procedure is

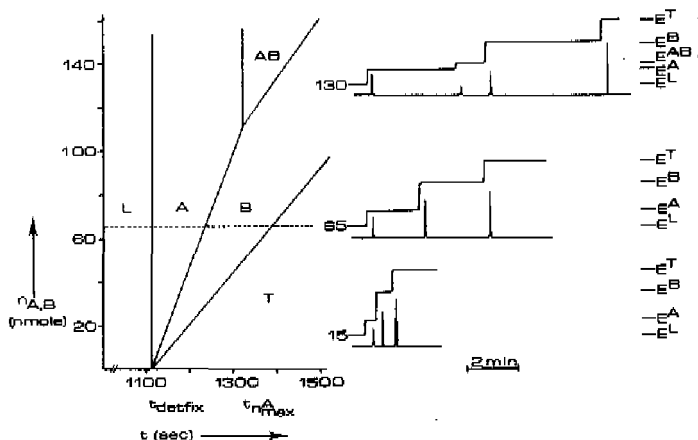


Fig. 2.2 Resolution lines for a two separand sample. Operational system: Table 2.1, system no 2 and Table 2.2 $L = \text{chloride}$, $A = \text{formate}$, $B = \text{glycolate}$, $T = \text{propionate}$; $E^{L,A,B,T} = \text{electric field strength}$; $n = \text{sampld amount}$. Sample: $c_{\text{formate}} = -0.05 \text{ M}$, $c_{\text{glycolate}} = -0.05 \text{ M}$, $\text{pH} = 3.0$.

given in Fig. 2.2 and relevant parameters are summarized in Table 2.3. The fact that, at a constant load of the leading constituent, the first boundary will always be detected at the same time interval, t_{detfix} , is illustrated in Fig. 2.2 by the resolution line L/A . The low coefficient of variation, Table 2.3, confirms the excellent performance of the equipment. Injection of a small amount of sample will cause two zones, stacked between the leading constituent L and the terminating constituent T . A sample load of $1.3 \mu\text{l}$ of the separand sample, see Fig. 2.2, where $n_A = 85$, will give a time based zone length of 124.4 sec for constituent A and detection must be started 1112 sec after injection. The zone length of the second separand, B , will be 148.1 sec . Other sample loads will give proportional zone lengths. The characteristics of these steady state zones will not be discussed here but the close agreement of the calculated and experimental resolution lines, L/A , A/B , and B/T , indicates the reliability of the calculations.

TABLE 2.3
RESOLUTION DATA

For operational system see Fig. 2.2 and Table 2.2

Resolution line: $n = at - b$ (nmole).

Boundary	No. of deter- minations	a		b		C.v. or C.c.
		Exp.	Theor.	Exp.	Theor.	
L/A	53	0	0	-1112	-1112	0.8%
A/B	13	0.525	0.530	584	590	1.000
B/T	45	0.242	0.251	270	279	1.000
A/AB	6	0	0	-1328	-1317	0.4%
AB/B	6	0.321	0.316	314	312	0.998

Parameter	Experimental	Theoretical
Load of leading constituent (n_L^{load})	658 nmole	647 nmole
Maximal sample load (n_A^{max})	113 nmole	108 nmole
Separation number (S_A)	0.103	0.099
(S_B)	0.103	0.099
Load capacity (C_{load})	0.172	0.167

C.v. = coefficient of variation

C.c. = correlation coefficient

As the separation compartment has a limited load capacity, at a high sample load a mixed zone will be detected. The characteristics of these mixed zones are determined by both the leading electrolyte and the sample and are constant with time, as long as they exist. The time interval $t_{n_A}^{max}$, at which the mixed zone will be detected, is again constant, as illustrated in Fig. 2.2 by the resolution line A/AB:

$$t_{n_A}^{max} = t_{detfix} \cdot \frac{\frac{-I}{m_L} E^L}{\frac{-M}{m_B} E^M} \quad (2.5)$$

The maximal zone length for the resolved separand A on a time base, is given by

$$k_A^{\max} = t_{n_A}^{\max} - t_{\text{defix}} \quad (2.6)$$

The maximal sample load, n_A^{\max} , is given by the intercepts of the resolution lines A/B , A/AB and AB/B . For the given pair of separands, formate and glycolate, the maximal sample load was 113 nmole, which was close to the theoretical value, Table 2.3. From the maximal sample load the load capacity, C_{load} , and the dimensionless separation number, S , can be calculated directly. Optimal column dimensions can be derived from the load capacity, whereas the dimensionless separation number gives the relationship between the amount sampled and the electric driving current or time of resolution. The appropriate procedure is given in Fig. 2.3

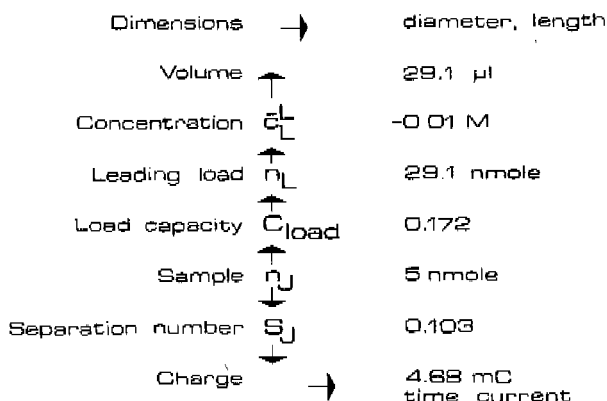


Fig. 2.3 Column evaluation.

From the load capacity, C_{load} , of 0.172, it follows that for a sample that contains 5 nmole of both separands, 29.1 nmole of the leading constituent chloride are necessary. The required volume can now be calculated once the concentration of the leading constituent has been chosen, e.g. $\bar{c}_L = -0.01$ M. If the inside diameter of the separation compartment is 0.2 mm the length must be 9.25 cm. Obviously, if we had chosen a higher concentration of the leading constituent with the same dimensions of the separation compartment, the maximal sample load would have

been proportionally higher. From the dimensionless separation number it follows that for a resolution time of 100 sec, an electric driving current of 46.8 μA must be applied. At a driving current of 25 μA we can expect a resolution time of 187.4 sec, since the sample requires 4.68 mC of electric charge. Although all resolution lines were determined experimentally, the load capacity and the separation number can be obtained with sufficient accuracy from only a few experiments, in which a mixed zone is present. The number of necessary determinations depends largely on the performance of the equipment. A high performance implies that the coefficients of variations in both t_{detfix} and t_{nA}^{max} are low. It should be emphasized that the column evaluation of Fig. 2.3 applies only to one specific sample. Generally, a sample will show fluctuations in composition and an appropriate safety margin should be used. In analytical practice the fluctuations in composition may be due to concentration and/or to pH. Once the extreme values of these fluctuations are known, the safety margin can easily be calculated.

In the experimental determinations, not only time events are being registered, but also electric gradients. As eqn. 2.5 contains only one unknown quantity, \bar{m}_B^M , the effective mobility of the trailing constituent in the mixed zone can be obtained from the experimental results. For the glycolate constituent in the mixed zone of Fig. 2.2 it follows that

$$\frac{\bar{m}_{\text{glycolate}}^{\text{Mixed}}}{\bar{m}_{\text{chloride}}^{\text{Leading}}} = \frac{1112}{1328} \cdot 0.481 = 0.403$$

Provided that the ionic mobility of glycolate is known, the pH of the mixed zone can be derived. Using the appropriate relationships it follows that $\text{pH}^M = 4.28$, which is very close to the theoretically expected value of 4.30, that can be calculated with the transient state model. From this we can evaluate how much the ratio of effective mobilities in the mixed state differs from the critical

value of unity at which no separation occurs.

$$\frac{\bar{m}^{\text{Mixed}}_{\text{glycolate}}}{\bar{m}^{\text{Mixed}}_{\text{formate}}} = 0.73$$

In combination with the separation number, $S = 0.103$, we find for the transference number of formate in the mixed zone: $T_{\text{formate}} = 0.38$.

From Fig. 2.2 and the data of Table 2.3 we conclude that even in the presence of a mixed zone, the relationship between the total zonelength of the sample and the sample load is perfectly linear. Deviations^{12,13,14} from this rule are the result of experimental inaccuracies, such as hydrodynamic flow, improper injection and mixing of leading electrolyte with sample and/or terminating electrolyte.

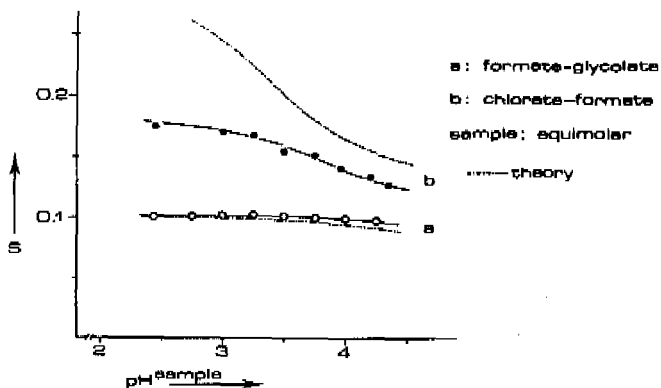


Fig. 2.4 The influence of the pH of the sample on the dimensionless separation number.

Operational system: Table 2.1, system no 2.

As the separation process is strongly dependent on the pH of both the sample and the leading electrolyte, optimization by choosing suitable electrolyte conditions should be possible. The effect of the pH of the sample has been given in Fig. 2.4. Owing to the small difference in the dissociations constants of the separands glycolic acid

and formic acid, $\Delta pK = 0.08$, the effect of the pH of the sample on the current efficiency is minimal. For the given pair of separands the theoretical and experimental results show good agreement. When the difference in the dissociation constants is larger, the effect of the sample pH is much more pronounced, as is confirmed by the constituent pair chlorate-formate. In the instance a low pH of the sample clearly favours resolution. Although the theoretical considerations suggest a rapid, continuous increase in efficiency, decreasing the pH of the sample, the experimental curve indicates only a moderate increase. In the transient state model, Part 1 Chapter 3, we made no allowance for the influence of a relatively high proton concentration at low pH. Functioning as a mobile counter constituent, protons, at a relatively high concentration will decrease the efficiency of the transport process, and as such the current efficiency of the separation process. When the separands have only a small difference in their dissociation constants, such as formic acid and glycolic acid, the theoretical and experimental results will show only small differences. When the pK values of the separands differ substantially, higher pH shifts can be expected and larger deviations will result. Irrespective the numerical discrepancy for anionic separations a low pH of the sample favours resolution. Appropriate incorporation of the hydrogen and/or hydroxyl constituent into the mathematical formulations will improve the theoretical results.

In common practice the pH of the sample shows only a small degree of freedom and the most useful optimization parameter is the pH of the leading electrolyte. As long as the pH has no influence on the transference number the lower pH of the leading electrolyte will increase the current efficiency for anionic separations. Table 2.4 gives some experimental results for the separands of Fig. 2.4. From both the theoretical and the experimental results it follows that, for constituents that have only a small difference in their pK values, the pH of the leading electro-

lyte is not very useful for optimization. According to theory the ratio of effective separand mobilities in the mixed state should be optimized. In case of only small pK differences, the pH of the leading electrolyte will have only a minor influence, as can be seen from the Fig. 2.5.

TABLE 2.4

INFLUENCE OF THE pH OF THE LEADING ELECTROLYTE ON THE DIMENSIONLESS SEPARATION NUMBER

Parameter	Separands			
	Chlorate-Formate		Formate-Glycolate	
Concentration (M)	-0.05	-0.05	-0.05	-0.05
pH ^{sample}	2.41		2.41	
pH ^L Counter Constit.	S _{exp}	S _{theor}	S _{exp}	S _{theor}
3.60 BALA	0.259	0.368	0.095	0.099
4.03 GABA	0.1799	0.275	0.098	0.100
6.02 HIST	0.075	0.105	0.101	0.092

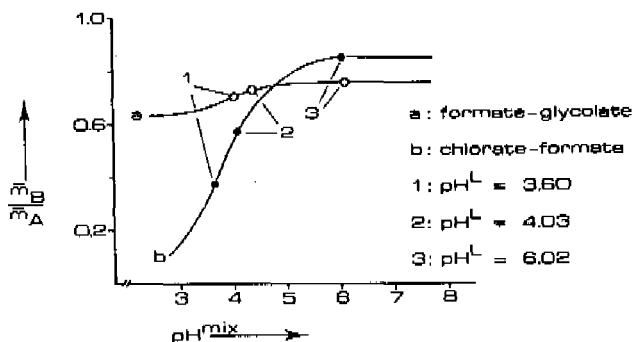


Fig. 2.5 The influence of the pH of the mixed zone on the ratio of effective separand mobilities.

Operational system: Table 2.1.

It can easily be shown that for the limiting values of the mobility ratio it must hold that:

$$10^{(pK_A - pK_B)} \cdot \frac{m_B}{m_A} < \frac{\bar{m}_B}{\bar{m}_A} < \frac{m_B}{m_A} \quad (2.7)$$

As a result, for the separand pair chlorate-formate the ratio of effective mobilities can vary between its maximal value of 0.764 at high pH and its minimal value of 0.365 at low pH. Hence any pH shift, due to either the leading electrolyte or the sample, has hardly any influence on the mobility ratio. Owing to the relatively low mobility of the counter constituent histidine, the separation at pH^L 6.02 has the higher efficiency, although differences are only marginal. When the differences in pK values are more substantial the rationale for optimization is more clear, as can be seen from the second separand pair, chlorate-formate, in Table 2.4 and Fig. 2.5. In this instance the mobility ratio can vary between almost zero at low pH and 0.846 at high pH. A high pH of the leading electrolyte will cause a high pH of the mixed zone, resulting in an unfavourable ratio of the separand mobilities. A low pH of both the leading electrolyte and the sample will result in an optimal ratio and therefore optimal current efficiency.

From the Fig. 2.5 it can also be seen that for small differences in pK values, the difference in the pH values of the mixed zone and the leading zone is relatively high. When the sample contains stronger acids, this difference is considerably smaller, resulting in a relatively low pH in the mixed zone. Whenever the pH of the leading electrolyte is substantially higher than the pK values of the

TABLE 2.5
CONSTITUENT DATA FOR FIG. 2.5

Parameter	Separand	
	Acetate	Naphtalene-2-sulphonate
Mobility (cm^2/Vsec)	-41×10^{-5}	-30×10^{-5}
Concentration (M)	-0.005	-0.005
pK value	4.75	0
$\text{pH}^{\text{sample}}$	4.75	4.75
No separation at $\text{pH}^M = 5.19$		
No separation at $\text{pH}^L = 4.98$ ($\rho = -2, m_C = 30 \times 10^{-5} \text{ cm}^2/\text{Vsec}$)		

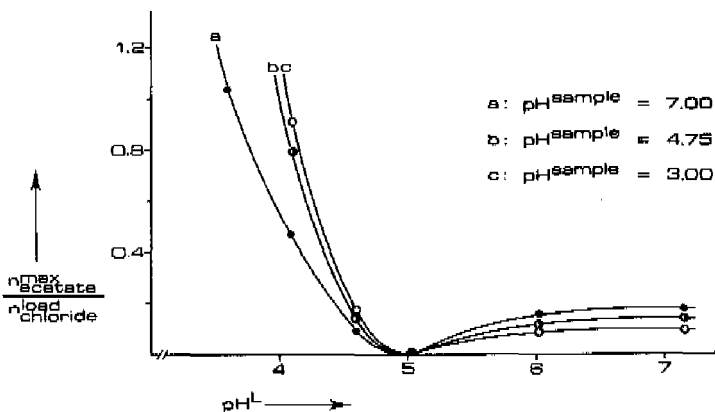


Fig. 2.6 Influence of the pH of the loading electrolyte on the load capacity.

Operational systems: Table 2.1, Constituent Data: Table 2.5.

separands, the difference will be small and the separands will be separated as strongly ionic species. From the example given it follows directly that a separation based on pK values is generally more effective than one based on ionic mobilities.

For pairs of separands, where $m_B < m_A$ and $pK_A < pK_B$, the rationale for optimization is straightforward: low pH. For anionic pairs, where $m_B > m_A$ and $pK_A > pK_B$, the rationale is more complex. It has been shown, Part 1 Chapter 1, that for such pairs a pH will exist, at which no separation occurs. Of course, this pH will cause an infinite time of resolution, zero separation number and zero load capacity. Moreover, at this pH the order in which the separands migrate will be reversed. Experimental results concerning the load capacity of such a pair are given in Fig. 2.6 as a function of the pH of the leading electrolyte and the pH of the sample. The experimental curves confirm the theoretically predicted behaviour. Using the appropriate data, Table 2.5, and relevant mathematical formulations, it follows that the criterion for separation, Part 1 Chapter 1, will not be satisfied at a mixed zone pH of 5.19. Obviously, this pH can be generated by numerous combina-

tions of leading electrolytes and sample compositions. Working at the maximal buffering capacity of the counter constituent, i.e. $\rho = -2$ or $\text{pH}^L = \text{pK}_C$, and introducing an acceptable ionic mobility for the counter constituent, $m_C = 30 \times 10^{-5} \text{ cm}^2/\text{Vsec}$, the critical pH of the leading electrolyte is 4.98. This was confirmed experimentally by the separation at $\text{pH}^L = 5.04$, at which hardly any load capacity was present. At a pH^L higher than the critical value, separands migrate in order of ionic mobilities, and separations can be performed with only moderate efficiency. At low pH^L , however, separands are migrating in order of their pK values and a much higher efficiency can be obtained, resulting in a high load capacity. For example, the resolution of a 1.5 nmole sample, an absolute amount that can be detected without difficulty, would take about 23 sec, $S = 0.28$, at $\text{pH}^L = 4.10$ and $\text{pH}^S = 3.0$, whereas the same sample can be resolved in 133 sec, $S = 0.046$, at $\text{pH}^L = 7.10$. The required length of the separation compartment in the former instance is 5.8 times shorter than in the latter. Obviously, for specific samples rigid optimization procedures can be followed, resulting in very short analysis time, small dimensions of the separation compartment and efficient use of the power applied. It must be emphasized, however, that the success of optimization procedures depends largely on the physico-chemical characteristics of the species to be separated and the performance of the equipment. When there are only small differences in ionic mobility and dissociation constants, optimization procedures are elaborate and result in a rather small increase in efficiency.

Another important conclusion can be drawn from the results shown in Fig. 2.6. It follows that efficient separations can be achieved whenever the sampling ratio ϕ , i.e. the concentration of the charged trailing separand divided by the concentration of the charged leading separand, is small. Biochemical samples often contain substantial amounts of very mobile species such as sodium, chloride or perchlorate. Such samples represent typical low

" ϕ cases", that can be separated in a relatively short column. The time of analysis, however, will increase substantially in the presence of these mobile separands. In very special cases lowering of the sample pH by the addition of, for example, hydrochloric acid will increase the load capacity of the column by the proposed mechanism.

TABLE 2.6

INFLUENCE OF THE INSIDE DIAMETER OF THE SEPARATION COMPARTMENT ON THE DIMENSIONLESS SEPARATION NUMBER

Parameter	Inside diameter (d_i , mm)		
	0.45	0.20	0.15
Driving current (I , μA)	80	25	25
Sample load (n_A^{\max} , nmole)	87.5	23.5	16.6
(n_B^{\max} , nmole)	87.5	23.5	16.6
Resolution time (t_{res} , sec)	1081	1030	703.7
Separation number (S_{theor})	0.100	0.100	0.100
($S_{A,exp}$)	0.098	0.088	0.091

Sample: A = formate (-0.05 M); B = glycolate (-0.05 M)
 $pH^{sample} = 2.41$. Operational system: Table 2.1, system 2.

The dimensionless separation number seems to be a reliable quantity for describing the current efficiency, as it is independent of operating conditions such as the electric driving current and column geometry. Table 2.6 gives the observed experimental efficiencies for the same sample under different operating conditions. From these results it follows that, although differences in the separation numbers occur, the efficiency is not significantly different. In our theoretical approach, Part 1 Chapter 2, we introduced relative mobilities to suppress the influence of temperature effects. Comparing literature data on ionic mobilities^{9,10}, it must be concluded that these temperature effects are only partially eliminated in this way, as many non-linear effects occur. Moreover, when considering temperature effects, the dissociation constants

should also be corrected. Mathematical iteration procedures to involve temperature corrections for various physico-chemical parameters can be introduced into the transient state model with a probable consequent, but small, increase in accuracy. There is however, a lack of reliable data on physico-chemical parameters and the present model seems sufficient reliable, the predicted parameters being confirmed experimentally.

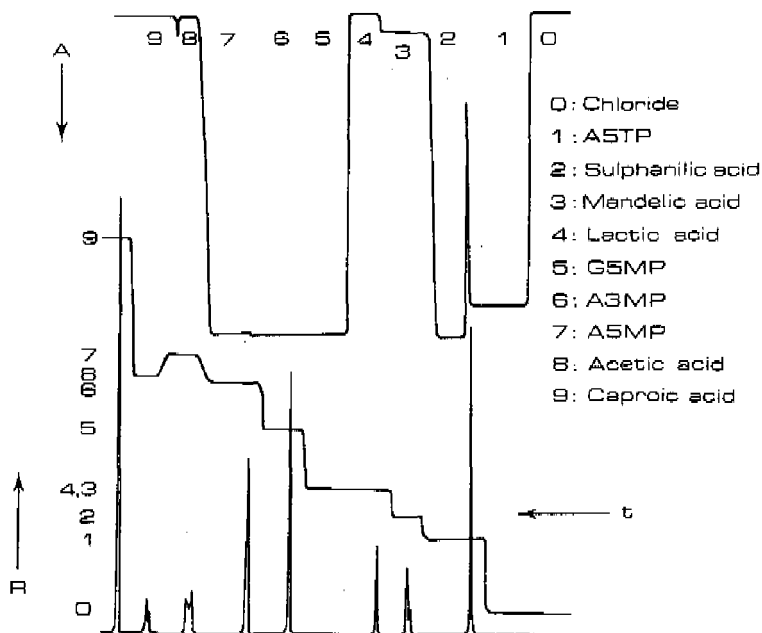


Fig. 2.7 Isotachophoretic state configurations.
 Operational system: Table 2.1 system no 2, $pH^L = 3.95$
 R = increasing resistance. A = UV absorption 254 nm.

From the theoretical formulations, it follows that the steady state effective separand mobilities can be only used as an indication for experimental separability. Constituents that have almost equal steady state mobilities can sometimes be separated quite efficiently. Moreover, it should be emphasized that the effective steady state

mobilities are only indicative for the steady state migration configuration; enforced isotachophoretic configurations¹⁴, in which a more mobile separand migrates behind a less mobile separand, can be perfectly stable with respects to time. An example of the possible configurations is shown in Fig. 2.7. Several separands confirm that generally constituents in isotachopheresis are migrating in order of decreasing effective separand mobilities.

TABLE 2.7
COMPARISON OF ZONE CHARACTERISTICS

Parameter	Trans = computerized transient-state model; X3 = computerized steady-state model ¹⁴						
	Chloride zone, experimental	Mandelate zone			Lactate zone		
		Trans	X3	Exp.	Trans	X3	Exp.
pK	-2	3.37			3.86		
$m \cdot 10^{-5} \text{ (cm}^2/\text{Vsec)}$	-77	-28.1			-33.9		
pH	3.95	4.21	4.22	4.25	4.27	4.28	4.29
E^L/E^X	1.00	0.319	0.320	0.322	0.318	0.319	0.322
$\bar{C}_X^X \text{ (mm)}$	-10.00	-6.47	-6.34		-7.16	-7.06	
$\frac{-\text{mandelate zone}}{n}$							
$\frac{-\text{lactate}}{n}$		0.956	0.960	0.974			
$\frac{-\text{mandelate zone}}{n}$							
$\frac{-\text{lactate}}{n}$							
$\frac{-\text{lactate zone}}{n}$					1.027	1.017	1.010
$\frac{-\text{lactate}}{n}$							
$\frac{-\text{mixed zone}}{n}$							
$\frac{-\text{mandelate}}{n}$	1.027						
$\frac{-\text{mixed zone}}{n}$							
$\frac{-\text{lactate}}{n}$							

The constituents lactic and mandelic acid, Fig. 2.7 no 3 and 4, however show virtually no difference in effective mobilities, as for their isotachophoretic migration the same electric gradient seems to be necessary (Fig. 2.6 and Table 2.7). From the linear conductance trace it appears that this pair has not resolved during the separation process. The UV trace, however, clearly indicates that mandelic acid has been resolved from lactic acid and that the former migrates in front of the latter. The transient state model reveals that the pH of the mixed zone, from which the pure zones are formed, is just below the critical pH of 4.32 at which no separation occurs. At the pH of the leading electrolyte mandelic acid will be

resolved in front of lactic acid.

From the data in Table 2.7 it follows that the experimental and theoretical zone characteristics are in good agreement. The minor differences between the transient state and the steady state results, have already been mentioned. The occurrence of a lactate ion in the resolved mandelic acid zone will cause a 2.6% deviation from the critical value of unity for the ratio of effective constituent mobilities. Mandelate ions, in the resolved lactic acid zone, would lead to a difference of 1%. From the UV trace it follows that these deviations are large enough to guarantee a satisfactory separation. The theoretical calculations show a larger difference and for the ratio of effective mobilities in the mixed zone a 2.6% deviation from unity was calculated. The experimental separation confirms that this deviation is sufficient to obtain resolution. It must be emphasized, however, that these small deviations result in a low efficiency and column overloading can easily occur. Fig. 2.7 nevertheless indicates clearly that isotachopherograms in which only one detection system is used must be interpreted with great care. The same, of course, applies when only UV detection is used. From the UV trace in Fig. 2.7 it would be concluded that the nucleotides G5MP and A5MP have not been resolved. The conductance trace however, clearly confirms the separation of the two separands. On most occasions small amounts of impurities, with either UV-absorbing or non UV-absorbing properties, will indicate the separation boundary.

The separand A5MP and acetate, constituents 7 and 8, are migrating in an enforced isotachophoretic configuration. The effective mobility of the acetate constituent in its proper zone is higher than that of the nucleotide A5MP in its proper zone, as indicated in Fig. 2.7 by the lower resistance of zone 8 in comparison with zone 7. For the relative effective mobilities it follows

$$\frac{\overset{-}{m}_{\text{Acetate}}}{\overset{-}{m}_{\text{Chloride}}} = 0.212 \quad \text{and} \quad \frac{\overset{-}{m}_{\text{A5MP}}}{\overset{-}{m}_{\text{Chloride}}} = 0.198$$

The 7% deviation from unity of the mobility ratio allows a satisfactory separation between the two separands. The reason for the stability can be found in the difference in pH values of the two resolved zones. Using the appropriate relationships it follows that the pH of the acetate zone is 4.57. A nucleotide ion, lost owing to the convection or diffusion from its proper zone into the acetate zone, will migrate there with a higher effective mobility than the acetate constituent. In the nucleotide zone the pH is 4.32, so any acetate ion in the nucleotide zone will migrate with a considerably lower velocity than the nucleotide. Hence the self-sharpening capabilities of the separation boundary allow the enforced isotachophoretic configuration to be stable with respect to time. The transient state model predicts even in this case, the separation configuration correctly. It should be noticed however, that enforced isotachophoretic configurations will not be encountered very frequently in common practice.

2.3. CONCLUSIONS

From both our previous theoretical considerations, Part I Chapter 3, and the experimental evaluation presented here, it follows that through optimization a considerable increase in current efficiency and load capacity and a decrease in time for resolution can be obtained. We restricted our theoretical and experimental considerations mainly to two separand samples but the same optimization rationales hold, be it to a lesser extent, for multicomponent samples⁸.

In optimization procedures three rationales should be followed:

- i The electrical driving current should be maximized during the separation process.
- ii The mobility of the counter constituent should be minimized.
- iii A low pH of both sample and leading electrolyte should be used for anionic separations. In case of cationic separations a high pH will be preferable.

Extreme pH's where the proton or hydroxyl ion concentrations have a deleterious influence on the transference number should be avoided. The pH at which no separation occurs can be calculated and hence can be avoided.

It must be emphasized that the result of any optimization procedure depends on the nature of the sample and calculations of isotachophoretic steady state characteristics are only indicative for separability. For very complex mixtures in which multicomponent information must be obtained, optimization can sometimes be elaborate and difficult. As a result analyses in more than one operational system are inevitable.

REFERENCES

1. F. Mikkers, F. Everaerts and J. Peek, *J. Chromatogr.*, 168 (1979) 293.
2. F. Kohlrausch, *Ann. Phys. Chem.*, 62 (1897) 14.
3. J. Hinckley, *J. Chromatogr.*, 109 (1975) 283.
4. P. Bocek, M. Deml and J. Janak, *J. Chromatogr.*, 106 (1975) 283.
5. F. Everaerts, J. Beckers and Th. Verheggen, *Isotachophoresis*, *J. Chromatogr. Libr.*, Vol. 6, Elsevier, Amsterdam-Oxford-New York, 1976.
6. D. Kaniansky and F. Everaerts, *J. Chromatogr.*, 148 (1978) 441.
7. P. Bocek, I. Miedziak, M. Deml and J. Janak, *J. Chromatogr.*, 137 (1977) 83.
8. J. Peek, *Graduation report*, Eindhoven University of Technology, Eindhoven (The Netherlands) 1977.
9. Landolt-Börnstein, *Zahlenwerte und Funktionen*, Springer, Berlin-Göttingen-Heidelberg, 1960, II-7.
10. R. Weast (Editor), *Handbook of Chemistry and Physics*, Chemical Rubber Co., Cleveland, Ohio, 49th edn. 1977.
11. D. Perrin, *Dissociation constants of organic acids and bases in aqueous solution*, Butterworths, London, 1965.
12. H. Miyazaki and K. Kato, *J. Chromatogr.*, 119 (1976) 369.

13. L. Arlinger, *J. Chromatogr.*, 91 (1974) 785.
14. J. Beckers, *Thesis*, Eindhoven University of Technology, Eindhoven (The Netherlands) 1973.

CHAPTER 3

Column coupling in isotachopheresis

A two dimensional electrophoretic instrument is described that allow the application of large sample loads, without appreciable increase in time of analysis. The instrument is fully automatized and can be used for micro-preparative and two dimensional separations.

3.0. INTRODUCTION

Separands are often present within a sample together with numerous other substances in which there is no interest. As long as the separand concentration predominates that of the interfering solutes qualitative and quantitative determination of the separand will cause only minor problems. Unfortunately this is generally not the case and according to our theoretical considerations, Part 1 Chapter 3, such samples have a deleterious impact on both the time for resolution and the maximal allowable sample load.

There are several approaches to alleviate this problem. First of all, sample pretreatment procedures, such as solvent extraction with or without extract concentration, can be used for either removal of interfering substances or selective enrichment of separands. Being general procedures they can be used successfully in isotach-

phoresis¹. Any sample pretreatment procedure, however, is sensitive for quantitative inaccuracy and as a result recovery studies have to be applied.

A somewhat more elegant method is the use of selective detection systems of high sensitivity, as they allow quantitative determinations at a low sample load. In this respect the UV-absorbance detector can be applied quite successfully, using the "UV-spike" method²⁻⁶. In this method the separand migrates in a very small zone, stacked between two non UV-absorbing spacers and the integrated peak area or the peak-height is used for quantitation.

Not considering selective detection systems, the quantitative aspects in isotachopheresis are directly related with the zone volume of the separand. With decreasing zone volume the quantitative reliability decreases. Moreover, for a fast responding detection system, such as the conductimeter, the volume of the detector is important. Due to the presence of a zone profile, a finite thickness of the transition boundaries and the presence of convective instabilities, theoretical calculations on the minimal detectable amount or the minimal required zone volume are rather academic⁴. For accurate quantitative determinations the zone volume should be maximized whereas the detector volume should be minimized. It should be noted that neither dilution of the leading electrolyte nor reduction of the diameter of the separation compartment, carried out as a uniform operation, will work advantageous since the maximal sample load is proportional with the concentration of leading electrolyte as well as the column hold-up volume. Moreover, a low concentration of the leading electrolyte, lower than 1 mM, will have a restricted pH applicability and detection systems of very small inner diameters, smaller than 0.1 mm, are difficult to realize.

According to theory the time-based zone length is linearly related with the sample load and inversely proportional to the driving current and the transference number. The latter quantity is invariable for a given separand in an optimized electrolyte system, whereas the

driving current has a limited degree of freedom. For a large time-based zone length a low driving current is favourable, whereas the separation process requires a maximized driving current. The maximal value during separation is governed by power dissipation and thermostating and the minimal value during detection is governed by the required sharpness of the transition boundaries. As a result time current programming can be useful as long as the resulting transient temperature regimes can be avoided.

The most straightforward method for increasing the actual or time-based zone length is by increasing the sample load. As mixed zones have to be avoided a larger column volume will be necessary and there are several possibilities to realize this.

Generally the length of the separation compartment can be elongated without much difficulty. This method has only limited practical applicability since both the time of analysis and the voltage drop over a column of uniform dimensions are proportional with its length. It will suffice for those analytical problems that require only a doubling of the sample load. When the sample load must be increased by at least one order of magnitude elongation of the separation compartment will fail due to the long time of analysis and the resulting unworkably high endvoltage. These disadvantages can be solved to some extent by using a separation compartment of non-uniform dimensions, e.g. conical compartments⁷, non uniform concentration distributions⁸ and time-current programming.

The second method that has been proven to be useful is counterflow of electrolyte⁹⁻¹⁴. An inherent drawback of counter flow of electrolyte is that its flow profile not only has a disturbing effect on the zone boundaries⁹ but also reduces the current efficiency of the separation process, introducing antiseperative velocity distributions in the mixed zones. As a result relatively large differences in the effective mobilities of the separands are necessary. The major benefit of counterflow of electrolyte compared with elongation of the separation compartment is the low

end-voltage and its versatility, especially when it is fully automatized⁹. If counterflow is not applied during detection the reproducibility of the analysis is comparable with that of analysis without it. Counterflow of electrolyte during detection is possible but its reliability has not been investigated yet and probably requires an accurate control system.

The use of continuous sampling systems^{15,16}, with or without counterflow of electrolyte does not provide a direct way of increasing the maximal sample load, but rather a large sample volume. The major drawback of counterflow of electrolyte is its decreased efficiency and the resulting long time of analysis.

3.1. COLUMN COUPLING

A more general solution to the problem of maximal allowable sample load is given by the use of two separation compartments with different inner diameters as shown schematically in Fig. 3.1. The first separation compartment has a relatively large volume, necessary for the resolution of a high sample load. Its large inner diameter allows the use of a high driving current. Only the separand zones of interest are allowed to migrate into the second separation compartment, where they can be analyzed further at a lower driving current. Hence by selective switching

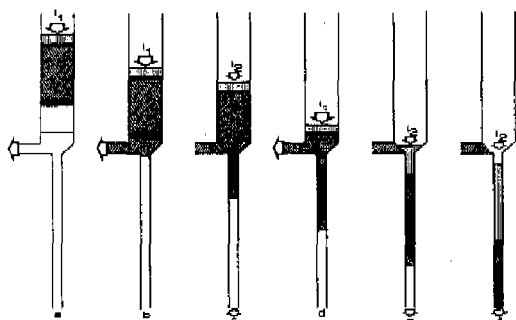


Fig. 3.1. Column Coupling

a, b, d: pre-separation mode, c, e, f: separation mode.

interfering substances can be removed from the isotachophoretic sample train.

The ultimate capabilities of the coupled column system can be evaluated by comparing its time of resolution, for a given sample, with that of a conventional instrument. As for the separation of a sample only the time-current integral is important, the required amount of coulombs Q is the same for both instruments.

For the coupled column system it follows that,

$$Q = I_1 t_1 + I_1 dt + I_2 t_2 \quad (3.1)$$

where I_1 is the driving current in the pre-separation compartment during the time t_1 and dt is the time an interfering zone needs to pass the bifurcation. I_2 and t_2 are respectively the driving current and time in the final separation compartment. For a conventional instrument it follows that,

$$Q = t_3 I_2 \quad (3.2)$$

where t_3 is the resolution time in the conventional instrument. It should be emphasized that for a correct comparison the inner diameter of the final separation capillary in the coupled column system is chosen to be equal of the conventional equipment.

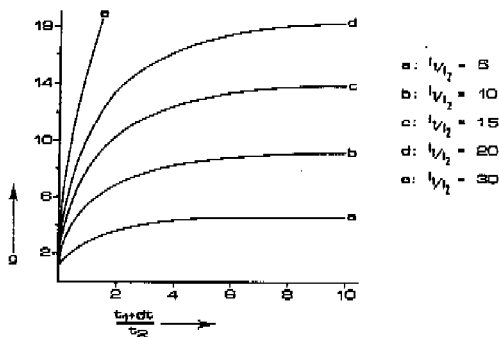


Fig. 3.2 The relative gain in time for resolution.

For the absolute profit in time for resolution t_g we find:

$$t_g = t_3 - (t_1 + dt + t_2) \quad (3.3)$$

or

$$t_g = (t_1 + dt) \left\{ \frac{I_1}{I_2} - 1 \right\} \quad (3.4)$$

The relative gain, g , is given by the ratio of the resolution time in the conventional equipment and that of the coupled column system. It follows that

$$g = \frac{\frac{I_1}{I_2} \left\{ \frac{t_1 + dt}{t_2} \right\} + 1}{\left\{ \frac{t_1 + dt}{t_2} \right\} + 1} \quad (3.5)$$

In Fig. 3.2 the relative gain has been plotted as a function of the ratio of the pre-separation time and the separation time. It follows that whenever $t_1 + dt$ is large in comparison with t_2 a constant relative gain is obtained and that a large benefit can be found in maximizing the ratio of the driving currents. The maximal value of I_1 is governed by power dissipation and the effectivity of thermostating, whereas the value of I_2 can not be chosen arbitrarily low since at very low driving currents considerable remixing of the separands during trapping can occur.

Instrumentation

The coupled column system essentially consists of three sections, Fig. 3.3:

- the pre-separation compartment
- the bifurcation block
- the separation compartment

The pre-separation compartment has the larger inner diameter resulting in a large column volume and allows the use of a high sample load and a high electric driving current. In order to alleviate the deleterious effects of relatively high power dissipations, this PTFE capillary can be thermostatted. A vertical orientation with downward

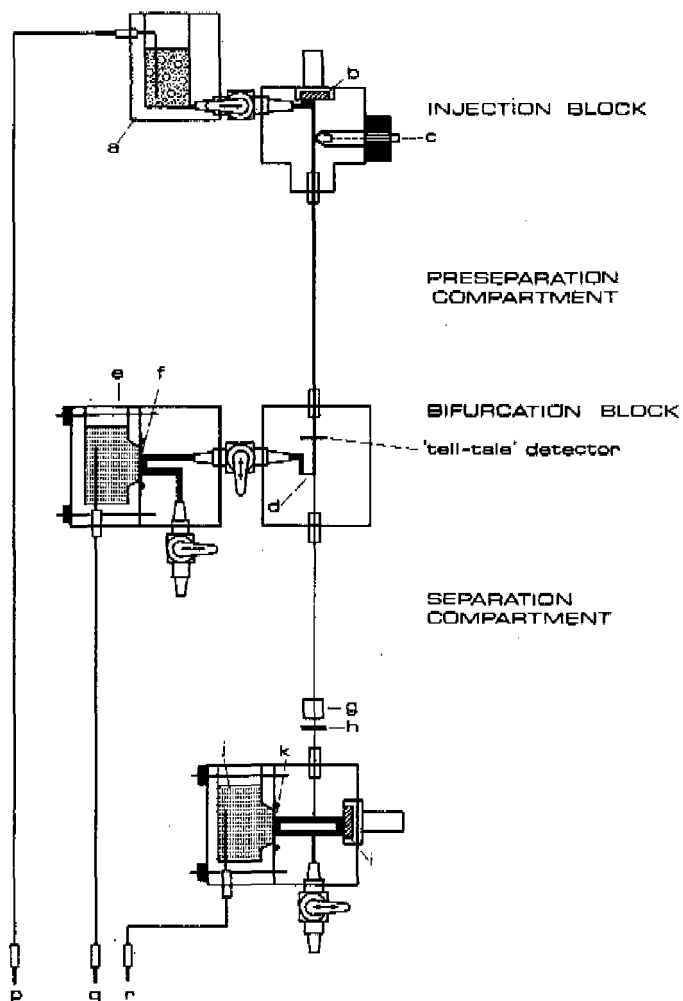


Fig. 3.3 The coupled column system.

a: terminating electrode compartment, b: septum, c: drain, d: flat channel, e: counter electrode compartment preseparation mode, f: membrane, g: UV detector, h: conductimeter, i: septum, j: counter electrode separation mode, k: membrane, p,q,r: leads to power supply.

migration of the separands has proven to give the most gravitationally stable configuration. The length and/or its inner diameter can be varied, though inner diameters larger than 1.2 mm are not generally applicable, since they require the use of relatively low current densities and the use of viscous electrolytes to prevent gravitational settling.

The separation compartment has a smaller inner diameter and due to its favourable thermal behaviour¹⁷ no thermostating is necessary. Moreover, its anticonvective wall-effect¹⁷ guarantees an orientation independent stable performance. All electrode compartments and detection systems are of the conventional type and have been described in detail elsewhere⁹.

Fig. 3.3 shows the bifurcation block in which the two separation compartments are coupled in an "in-line" configuration. The bifurcation block, made of acrylic, contains three different channels. The wide bore with an inner diameter of 0.8 mm, contains a conductimetric detection system, the "tell-tale" detector, and can be connected with the pre-separation compartment. A second boring with a small inner diameter, e.g. 0.2 mm, lies in line with the wide boring and forms the connection to the separation compartment. The connection with the counter electrode of the pre-separation mode, Fig. 3.3-e, is formed by a flat channel, width 1 mm and height 0.05 mm, and is perpendicular to the "in-line" separation compartment borings.

In the pre-separation mode the electrode compartments *a* and *e* are used and the sample is separated at a high driving current. The sample zones migrate toward the branching of in the bifurcation block. Using the electrode compartment *e* not relevant zones are allowed to vent, whereas separand zones can be trapped into the separation compartment using the counter electrode *j*.

The dimensions of the flat channel are chosen as to minimize diffusional and disturbing effects and allow optimal trapping. Though the flat channel has only a gap width of 0.05 mm still high driving currents in the

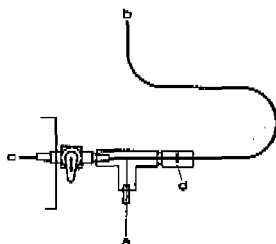


Fig. 3.4 The out of line bifurcation.

a: separation capillary, b: preseparation capillary,
c: vent, d: tell-tale detector.

preseparation mode can be used due to the effective heat removal of the flat channel. In the preseparation boring of the bifurcation block a conductimetric detection system, the "tell-tale" detector, is mounted. The separand zones, passing this detector, will need a definite time to cover the distance between the point of detection and the branching off. For a given electrolyte system and driving current this time the delay time t_d is invariable and can easily be measured. As a result this detector can be used to decide at which moment the instrument should be switched from the preseparation mode to the separation mode.

Another construction for coupling the two separation compartments is shown in Fig. 3.4. In this case the two separation compartments are not in-line. The bifurcation

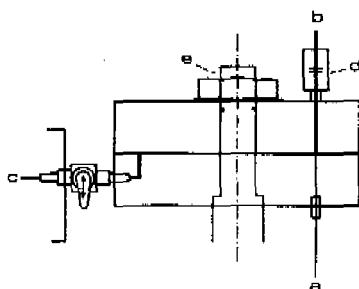


Fig. 3.5 The trapping valve.

a: separation capillary, b: preseparation capillary,
c: vent, d: tell-tale detector, e: adjusting-nut.

block consists of an acrylic T-piece with a large boring of 0.8 mm and perpendicular to this the small boring of 0.2 mm. The "tell-tale" detector is mounted separately. Though this type of coupling has proven to work satisfactorily the in line configuration has to be preferred, since the latter prevents gravitational settling.

The third possibility for coupling is the use of a disk-type valve instead of the bifurcation block, Fig. 3.5. Again a conductimeter is used to control the switching of the valve. Since the trapping volume can be varied using a disk with multiple borings, this configuration seems particular applicable for micropreparative work and off-column techniques.

Essential for optimal functioning of the coupled column system is that the two counter electrode compartments can be connected with the power supply separately. In the preseparation mode the electrode compartment of the separation capillary must be detached from the power supply and no leak current through the separation compartment should occur. In the trapping and separation mode the counter electrode of the preseparation compartment must be detached from the power supply, whereas the electrode of the separation compartment must be connected. During trapping and the final separation no leak current should occur through the preseparation electrode compartment and since this compartment can be at relatively high voltage it requires a perfect electric insulation. It should be emphasized that even a small current leak during trapping will result in incomplete and irreproducible trapping. Any current leak during detection will have a deleterious effect on the time-based zonelength. In the coupled column system this galvanic separation of the two electrode compartments is realized by the use of vacuum high voltage relays (Kilovac Corp. St. Barabara, Cal. USA). To prevent any current leakage through the "tell-tale" detector this detection system is mechanically disconnected in the final separation mode.

Automation of the coupled column system

Though the coupled column system can be operated manually its automated operation is more convenient. The basic operations for automatic handling are shown in Fig. 3.6

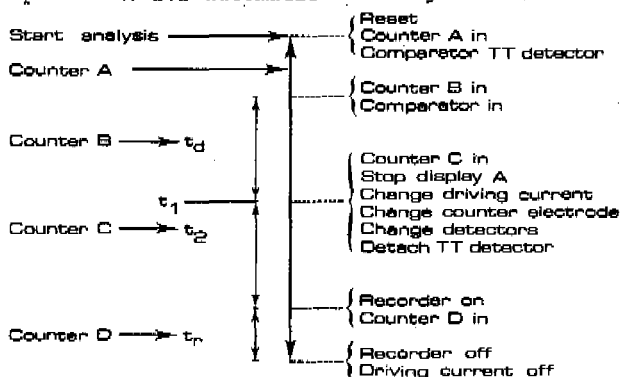


Fig. 3.6 Automation procedure.

t_1 is the preseparation time, t_d is the delay time, t_2 is the final separation time, t_r is the recording time.

Before the analysis is started the driving current for the preseparation compartment, I_1 , and the final separation, I_2 should be chosen. Various times, the delay time t_d , the separation time t_2 and the recording time can be stored in the memory of three counters. The output level of the "tell-tale" conductimeter is fed to a level comparator. The conductivity level of the selected zone must be chosen for the level comparator.

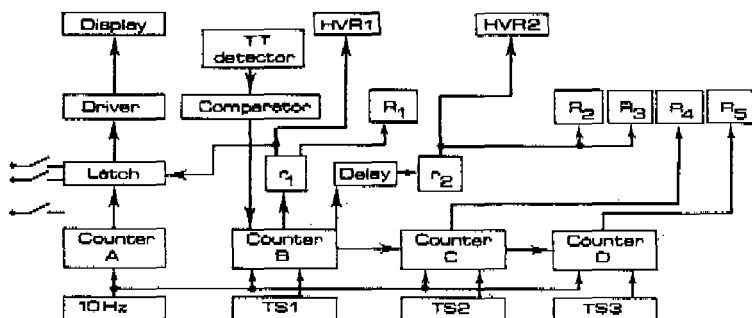


Fig. 3.7 Scheme of the electronic process control.

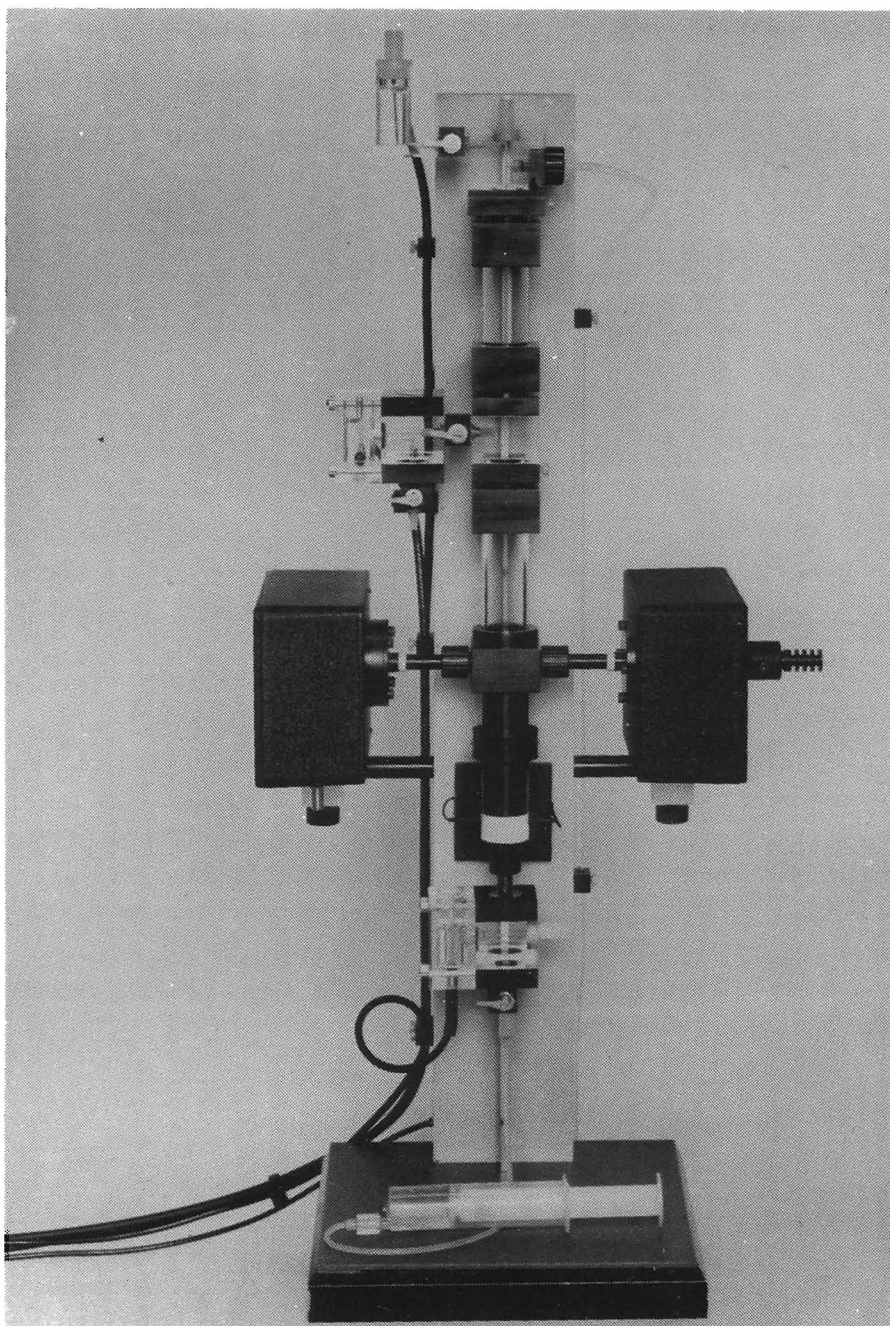


Fig. 3.8 Photograph of the coupled column instrument.

As soon as the analysis is started the counter A is activated in combination with the display. The various times can be measured with this counter. As soon as the signal derived from the "tell-tale" detector matches the chosen value in the level comparator, counter B is activated. In the memory of this counter the delay time t_d is stored. After the delay time the following operations are started simultaneously; the latch is activated and the display of counter A is stopped, the driving current is changed from its value I_1 to I_2 via the relays $R1$, counter C is activated and the separation compartment is attached to the current-stabilized power supply via the high voltage relay $HVR1$.

After 100 msec the counter electrode of the pre-separation compartment is detached via the second high voltage relay $HVR2$. Simultaneously, the "tell-tale" detector is mechanically, i.e. motor driven, disconnected by means of the relay $R2$. Moreover the conductimeter is switched from the "tell-tale" detector to the detector of the separation compartment, via relay $R3$. The display of counter A can be reactivated manually through the latch. After the final separation time, stored in counter C, has passed the paper transport of the recorder is started via relay $R4$. Simultaneously the counter D is activated. After t_p seconds, the recording time, the recorder is stopped and the driving current I_2 is switched off. The equipment is now ready for a new run and resetting.

3.2. EXPERIMENTAL PERFORMANCE

One of the most important features of the coupled column system is that it allows the analysis of samples in which an interfering constituent is present at a relatively high concentration. In Fig. 3.9 an example is shown of the analysis of ascorbic acid in a natural orange juice performed with the conventional instrument. The apparatus was equipped with a PTFE separation capillary with an inner diameter of 0.2 mm and the electrolyte systems and operational conditions are summarized in Table 3.1.

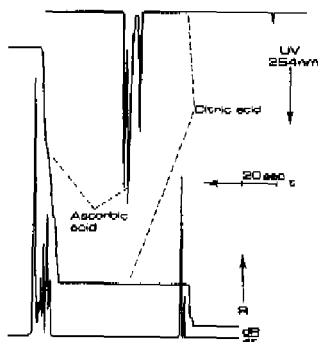


Fig. 3.9 Isotachopheretic separation of orange juice. Operational conditions Table 3.1, Conventional equipment. Sample load; 0.75 μ l, 1/10 diluted.

TABLE 3.1

ELECTROLYTE SYSTEMS AND OPERATIONAL CONDITIONS

	preseparation compartment	separation compartment	terminating compartment
Anion	Chloride	Chloride	MES
Concentration	0.01 M	0.01 M	0.005 M
Counter const.	HIST	HIST	TRIS
pH	6.02	6.02	6.4
Additive	0.2% HEC	0.2% HEC	--
Driving current	250 μ A	25 μ A	
UV		254 nm	

In the conventional equipment, the separation compartment conditions of the coupled column system were used.

Even when the conventional equipment was operated at its full load capacity, only the citrate zone, the interfering constituent, could be measured with sufficient accuracy. The separand of interest, ascorbic acid, is present as a small zone and the sample load should be at least one order of magnitude higher for an accurate determination and this is far beyond the capabilities of the conventional equipment. The same orange juice in its undiluted form was analyzed with the coupled column system at a much

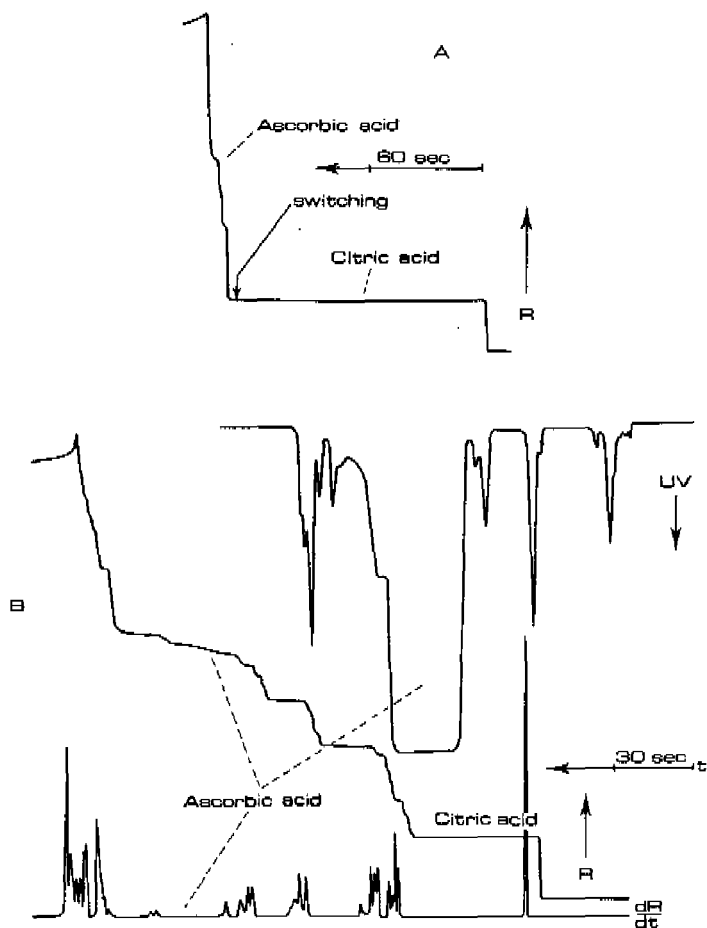


Fig. 3.10 Isotachopheric analysis of orange juice with the coupled column system.

A. Detection trace from the bell-tale detector in the pre-separation mode.

B. Detection traces in the separation mode.

Operational conditions: Table 3.1, Sample load: 1 μ l.

higher sample load. The pre-separation compartment with an inner diameter of 0.8 mm was coupled with a separation capillary i.d. 0.2 mm, using the off-line bifurcation. Again the operational conditions of Table 3.1 were used. The result, as obtained from the conductimetric tell-tale detector, mounted in the pre-separation compartment, is shown in Fig. 3.10 A. The leading boundary of the citrate zone passed the tell tale detector after 8 minutes. The swamping amount of citrate was allowed to pass the bifurcation and approximately 4.5 sec before the next zone boundary reached the bifurcation the system was switched in its separation mode. Only a small amount of the citrate was allowed to migrate into the separation capillary together with all the following separands. The result is shown in Fig. 3.10 B. The total time of analysis was about 15 min. Full qualitative and quantitative information could be obtained from both the conductivity and the UV detector. Using the calibration data the ascorbate content proved to be 586 mg/l.

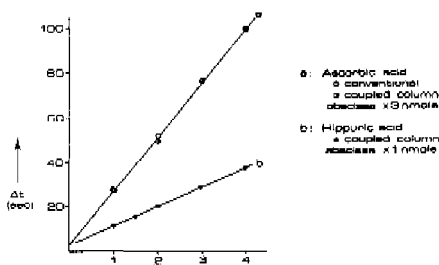


Fig. 3.11 Calibration data.

An essential requirement for the coupled column system is that the separand zones must be trapped quantitatively into the final separation capillary and that its results should be consistent with those obtained with the conventional equipment. In a series of experiments, the calibration characteristics of the coupled column system were evaluated using ascorbic acid and hippuric acid. The latter sample consisted of 5×10^{-4} M hippuric acid in 0.2 M NaCl solution, whereas the former contained only ascorbic acid. Again the operational conditions of Table 3.1

were used. Due to the swamping amount of chloride the hippuric acid sample could not be analyzed with the conventional equipment. From the calibration graphs of Fig. 3.11 it follows that the quantitative characteristics of the coupled column system are comparable with that of the conventional equipment. It should be noted that the calibration lines do not pass the origin. This is the result of the fact that some impurities were present in the electrolyte systems and is not related with trapping. The use of the coupled column system requires the application of ultrapure electrolyte systems. In fact the purity of the electrolyte systems can be limiting factor for realizing even higher relative gains.

A second benefit of the coupled column system is that it allows the use of different electrolyte systems in the pre-separation compartment and in the separation compartment.

TABLE 3.2

ELECTROLYTE SYSTEMS AND OPERATIONAL CONDITIONS

	pre-separation compartment	separation compartment	terminating compartment
Anion	Chloride	Chloride	Glutamate
Concentration	0.01 M	0.01 M	0.007 M
Counter const.	HIST	BALA	HIST
pH	6.02	3.00	6
Additive	0.2% HEC	0.2% HEC	--
Driving current	250 μ A	25 μ A	

The analysis in the conventional equipment was performed at $\text{pH}^L = 6.02$, at a driving current of 25 μ A.

In Fig. 3.12 A the separation of some acids is shown in the conventional instrument. At $\text{pH}^L = 6.02$ the sequence of the separand zones is; sulphate, formate, citrate, acetate, phosphate + lactate. The separands lactate and phosphate can not be separated at this pH. Using the coupled column system the pre-separation compartment was filled with the leading electrolyte at pH 6, whereas the final separation

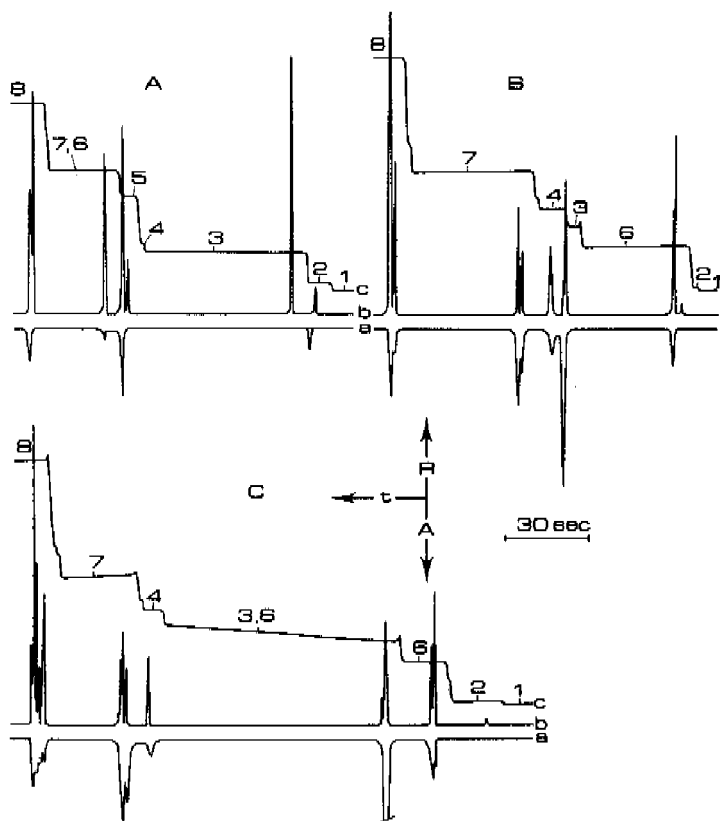


Fig. 3.12 The use of different electrolyte systems in the coupled column system.

1 = chloride, 2 = sulphate, 3 = formate, 4 = citrate, 5 = acetate, 6 = phosphate, 7 = lactate, 8 = glutamate.

R = increasing resistance, A = UV at 254 nm, t = time

A: Separation at $\text{pH}^L = 6$ in the conventional equipment, sample load 1 μl .

B: Separation with the coupled column system. Preseparation compartment $\text{pH}^L = 6$, separation compartment $\text{pH}^L = 3$. Sample load 3 μl ., selective trapping.

C: As B, complete trapping. Sample load 1.5 μl .

compartment was filled with the leading electrolyte at pH 6, whereas the final separation compartment was filled with the leading electrolyte at pH 3, Table 3.2. At pH 3 the sequence of the separand zones is: sulphate, phosphate, formate, citrate and lactate. In Fig. 3.12B the result is shown when two different electrolyte systems are used in the coupled column system. Formate was allowed to pass the bifurcation and therefore only a small formate zone is present in the final separation. The separands phosphate and lactate are now completely resolved. Acetate, constituent no 5, is not visible anymore as it has a smaller effective mobility than the terminating constituent at this pH. It should be emphasized that in using these two different electrolytes a total rearrangement of the separation configuration has occurred. This, of course, will have not always a favourable effect on the maximal allowable sample load as can be seen from the separation in Fig. 3.12C. In this case a lower sample load was applied and all the separand zones were trapped into the final separation compartment. From the separation it follows that the mixed zone between the relatively large amount of formate and phosphate has not been resolved.

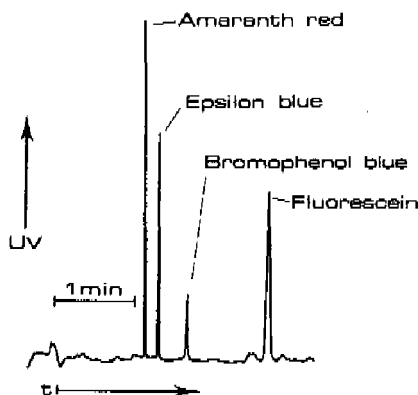


Fig. 3.13 Zone electrophoretic separation with the coupled column system.

Therefore the choice of electrolyte systems and the moment of column switching is extremely important when different electrolyte systems are used in the coupled column instrument.

Another field of application of the coupled column system is that it can be used for the combination of different electrophoretic principles.

TABLE 3.3

ELECTROLYTE SYSTEMS FOR DISCONTINUOUS ELECTROPHORESIS

	preseparation compartment	separation compartment	terminating compartment
Anion	Chloride	MES	MES
Concentration	0.01 M	0.005 M	0.005 M
Counter const.	HIST	HIST	HIST
pH	6.02	6.5	6.5
Additive	0.2 % HEC	0.2 % HEC	
Driving current	250 μ A	50 μ A	

In discontinuous electrophoresis isotachophoretically stacked zones are zone electrophoretically eluted by choosing the appropriate electrolyte and experimental conditions¹⁹. With the coupled column system the electrolyte conditions can be found rather easily: in the preseparation capillary a isotachophoretic leading-terminating electrolyte system has to be applied, whereas in the final separation capillary a zone electrophoretic electrolyte system must be used. Fig. 3.13 shows the zone electrophoretic separation of some anionic dyes, analyzed with the operational system of Table 3.3. The isotachophoretically migrating separands were trapped into the zone-electrophoretic electrolyte system, filling the final separation compartment. As can be seen from Fig. 3.13 a good separation is obtained and the result is at least comparable with the zone electrophoretic separations shown in Part 2 chapter 1.

Due to the fact that the migration configuration has not changed the isotachophoretic separation functioned as a almost ideal injection for the zone electrophoretic analysis.

3.3. CONCLUSIONS

Column coupling in isotachopheresis alleviates the problems that are encountered analyzing samples that contain ionic solutes at large concentration differences. Using a two dimensional system interfering ionic solutes can be removed from the isotachophoretically migrating sample by selective column switching. In comparison with conventional equipment the coupled column instrument allows a high sample load without a considerable increase in the analysis time. As the instrument comprises two separation compartments different electrolyte systems can be applied and combinations of different electrophoretic principles are allowed.

REFERENCES

1. B. Gustavsson and A. Baldesten, *J.Chromatogr.*, 165 (1979), 83.
2. L. Arlinger, *J.Chromatogr.*, 91 (1974) 785.
3. M. Svoboda and J. Vacik, *J.Chromatogr.*, 119 (1976) 339.
4. J. Wielders, *Thesis*, Eindhoven University of Technology, Eindhoven (The Netherlands) 1978.
5. U. Moberg and S. Hjalmarsson, *J.Chromatogr.*, 181 (1980) 147.
6. F.Mikkers and S. Ringoir, *Biochem. Biolog. Appl. Isotachopheresis*, A. Adam and C.Schots (Eds), Elsevier, Amsterdam (1980) 76.
7. F. Everaerts, Th. Verheggen and F.Mikkers, *J. Chromatogr.*, 169 (1979) 21.
8. P. Bocek, M. Deml and J. Janak, *J. Chromatogr.*, 156 (1978) 323.
9. F. Everaerts, J. Beckers and Th. Verheggen, *Isotachopheresis*, *J.Chromatogr. Libr. Vol. 6*, Elsevier, Amsterdam-Oxford-New York, 1976.
10. W. Preetz and H. Pfeifer, *Talanta*, 14 (1967) 143.
11. F. Everaerts, J. Vacik, Th. Verheggen and J. Zuska, *J. Chromatogr.*, 49 (1970) 262.

12. J.v.d. Venne, *Graduation report*, Eindhoven University of Technology, Eindhoven (The Netherlands) 1975.
13. J. Vacik and J. Zuska, *J. Chromatogr.*, 91 (1974) 795.
14. J. Akiyama and T. Mizuno, *Bunseki Kagaku*, 24 (1975) 728.
15. Z. Ryslavy, P. Bocek, M. Deml and J. Janak, *J. Chromatogr.*, 147 (1978) 446.
16. Z. Ryslavy, P. Bocek, M. Deml and J. Janak, *J. Chromatogr.*, 147 (1978) 369.
17. Th. Verheggen, F. Mikkers and F. Everaerts, *J. Chromatogr.*, 132 (1977) 205.
18. Th. Verheggen, F. Mikkers, D. Kroonenberg and F. Everaerts, *Biochem. Biolog. Appl. Isotachophoresis*, A. Adam and C. Schots (Eds), Elsevier, Amsterdam (1980) 41.
19. L. Ornstein, *Ann. N.Y. Acad. Sci.*, 121 (1964) 321.

CHAPTER 4

Separation of uremic metabolites

Uremic blood sera contain, in comparison with normal sera a large excess of low molecular weight anionic solutes, that are only partially removed by hemodialysis. Investigations on Middle Molecule fractions with gas chromatography, isotachopheresis and liquid chromatography could not substantiate the Middle Molecule hypothesis.

4.0. INTRODUCTION

One of the main functions of the kidneys in man is the excretion of metabolic waste products. They are one of the most important operating units in maintaining the favourable chemical environment of the body fluid system. The kidneys can be affected selectively by diseases that cause either gradual or sudden impairment of function. In terminal chronic renal failure life cannot be sustained without some substitution for renal function. Though transplantation is probably the most optimal solution, patients with chronic renal failure generally have to be submitted to intermittent hemodialysis or other dialysis and ultra-

filtration procedures. The patients show a complex of symptoms, usually called "the uremic syndrome" or "uremia". Many of these symptoms are related to a disturbance in the homeostatic or regenerative function of the kidneys, which results in retention of metabolic products and in disorders of hormonal and metabolic function.

Until the early 1960's, dialysis activities were limited to the treatment of acute renal failure. But when the problem of repeated access to the blood circulation was solved by Scribner¹, regular dialysis treatment of terminal renal failure became possible. By removing, be it partially, the accumulating waste products, the clinical manifestations of uremia can be alleviated and many of the patients can persevere life in an "acceptable" way. Adequate dialysis implies the removal, or even retention, of the right substances in the right way and to the right extent. Though this may seem to be a medical-technical problem, it is obvious that analytical chemistry can provide important "diagnostic" tools.

With the increasing refinement in analytical chemistry the number of chemical substances, that have been proven to accumulate in chronic renal failure, has grown vastly²⁻⁵. Nevertheless it has not been possible to attribute the broad spectrum of uremic symptoms to the accumulation of known chemical substances. This can be due to the fact that the criteria for a uremic toxin are not uniform, whereas in addition antagonistic, additive and synergistic effects may play an important role. The search for uremic toxins has been highly specific, assessing the possible toxicity of single known substances. The importance of various inorganic substances, such as sodium, potassium, magnesium, trace elements, phosphate and even water is well documented⁷⁻¹³. But even in the absence of gross abnormalities in water and electrolyte metabolism many uremic symptoms occur in patients with terminal renal failure.

Numerous organic substances are known to accumulate in chronic renal failure, varying from very simple mole-

cules, e.g. urea, to complex molecules like β_2 -microglobulin. There are indications that many of the retained components can act as cell toxins and enzyme inhibitors or may cause abnormal membrane transport in tissue and cells⁵. Many authors have investigated the role of lower molecular weight substances, such as guanidines, guanidino acids, amino acids, amines, phenolic acids, polyols etc.^{2,4,14-18}. Though in many cases appreciably increased concentrations in the body fluids were found, the relationship between the uremic symptoms and the increased concentration levels generally failed. In this respect it should be emphasized that most of these studies aimed at a specific accumulant or a specific class of accumulants. It seems that for an adequate assessment of their significance a multifactorial approach is necessary. In 1965 Scribner¹⁹ suggested that with more permeable dialysis membranes certain accumulating substances could be more efficiently removed. This suggestion stems from the clinical finding that patients on long term peritoneal dialysis were doing well, in spite of the relatively high serum concentrations of creatinine, uric acid and urea. It proved that not only the permeability was important for the efficiency of dialysis, but also the membrane surface area and the number of hours of dialysis per week. In the resulting *Square-Meter-Hour* hypothesis these parameters were related²⁰. The original suggestion however postulated the presence of unknown, but pathophysiologically important molecules with a molecular weight intermediate to that of rather small accumulating substances, i.e. molw. < 500, and large solutes such as lipoproteins, polypeptides and proteins. In 1972 the name m^2 -hr hypothesis was changed to *Middle Molecule* hypothesis²¹. Since the proposal of the middle molecule hypothesis, large surface-area dialyzers have been increasingly used to reduce dialysis time. Babb and Scribner²² developed the concept of the dialysis index to facilitate quantitation and prescription of dialysis therapy.

Though there was some clinical evidence for the

existence of middle molecules, their role in uremic toxicity remains controversial. Nowadays the middle molecule hypothesis comprises serum solutes with a molecular weight range of 500 to 2000. In dialysis patients such molecules may accumulate to a greater extent than small molecules, due to their relative low permeability across the dialysis membrane.

Obviously many investigators have tried to analyze, identify and isolate middle molecules. Most groups have used gelfiltration for separation and identification of compounds in the middle molecular weight range and used UV-detection²²⁻³⁶. Only few investigators claimed to have isolated or identified a specific solute of the required molecular weight³⁷⁻⁴⁰. Generally the results of gelfiltration analysis are taken as a quantitative measure for accumulation and elimination of middle molecules. Moreover middle molecular weight fractions of gelfiltration showed in vitro toxicity effects, such as inhibition of glucose utilization⁴¹, inhibition of phagocytic activity and inhibition of activity of a number of enzymes^{43-44,14,37}. Though many investigators emphasize the importance of middle molecules it should be noted that no convincing analytical demonstration of their presence has been given. As such the middle molecule hypothesis is still a hypothesis that remains to be proven.

In recent years however some research groups have followed a screening approach to the problem, in which chemical multicomponent analyses of biological fluids, derived from uremic patients, play an important role. The obvious drawback of such an approach is the extraordinary complexity of such fluids. Many methodological choices have to be made as the accumulating solutes can be very different; volatile-non volatile, low molecular weight-high molecular weight, ionic-non ionic. As a result various analytical techniques have to be used. Analytical chemistry has been successful in the development of techniques that permit separation, identification, quantification and isolation of many metabolites in biological

fluids . The choice which techniques have to be applied is in practice further limited by financial and manpower facilities. In our screening approach four different techniques are used: *Isotachophoresis, gas chromatography, liquid chromatography and mass-spectrometry*. For identification of solutes and to increase the differentiating capabilities the various techniques can be combined. The results of such a multifactorial approach will have its spin off in several ways. They should decrease our ignorance² on which accumulating solutes are important and will increase the knowledge on metabolism and homeostasis.

For the analysis of ionic solutes only few analytical techniques are available. Isotachophoresis is compatible with the basic requirements for screening approach procedures; multicomponent information, rapid completion, reliability and low cost. Moreover, the flexibility of the technique offers a vast spectrum of possibilities for detailed studies. Therefore isotachophoresis will provide useful information on the occurrence of ionic solutes in uremic biological fluids.

4.1. EXPERIMENTAL

Isotachophoresis was performed using the equipment developed by Everaerts et al.⁴⁵. The separation compartment consisted of a polytetrafluoro-ethylene capillary with an inner diameter of 0.2 mm and an outer diameter of 0.4 mm. The direct and constant electric driving current was taken from a Brandenburg (Thornton Heath, UK) high voltage power supply. Separated zones were detected by measuring the electric conductance as well as the UV-absorbance at 254 nm. Electrolyte systems and other operational conditions are summarized in Table 4.1. To increase the experimental performance 0.2% hydroxyethyl-cellulose was used as a viscous additive. The electrolyte system 3 of Table 4.1 is of a non-conventional type as two counter constituents are used. The leading electrolyte was prepared by dissolving TRISHCl buffer in

TABLE 4.1
ELECTROLYTE SYSTEMS AND OPERATIONAL CONDITIONS

Parameter	System no.		
	1	2	3
pH	3.50	6.02	8.10
Leading constituent	Cl ⁻	Cl ⁻	Cl ⁻
Concentration (M)	0.01	0.01	0.01
Counter constituent	BALA	HIST	TRIS/NH ₄ ⁺
Terminating constituent	CAPROIC	HEPES	OH ⁻
Concentration (M)	0.01	0.01	~
Additive	0.2% HEC	0.2% HEC	0.2% HEC
Driving current	25 μA	20 μA	30 μA

water at a concentration of 0.01 M. The desired pH was obtained by the addition of ammonia. The use of two counter constituents allows a large pH difference between the leading and the terminating electrolyte. As a result hydroxyl ions can be used as the terminator. A solution of barium-hydroxide, pH 10.5, was used as the terminating electrolyte and the precipitate of barium-carbonate, due to the carbon-dioxide content of the water, was removed by filtration. The performance characteristics of this electrolyte system are better than those of conventional electrolyte systems, in which generally an amino acid of doubtful purity is used. Separation times were generally less than twenty minutes and samples were introduced using a microliter syringe.

In the screening approach also high resolution gas chromatographic separations were performed following the procedure of Schoots⁴⁶. In the GC-procedure sample pretreatment comprised ultrafiltration, evaporation and derivatization. For identification mass-spectrometry was used^{46,47}. High performance liquid chromatographic separations were done in the reversed phase mode using a buffered water-methanol gradient⁴⁸. Serum samples were ultrafiltered before application. Gelfiltration was performed on Sephadex G-15 in an ammonium acetate buffer⁴⁹. The eluate was fractionated and

lyophilized. Relevant fractions were reanalyzed by isotachopheresis, gas chromatography and liquid chromatography.

If the removal of high molecular weight substances was required an ultrafiltration procedure was used. Pressure ultrafiltration was carried out in a micro-cell⁵⁰ using membranes of the required molecular weight cut-off. All membranes were carefully soaked in distilled water before use. In additional experiments cone-type ultrafiltration filters, that can be used in a centrifuge, were applied. All membranes, including the cone type, were purchased from Amicon (Oosterhout, The Netherlands). For removal of proteins the filters XM50, PM30 and CF25, with nominal mol. wt. cut-off of respectively 50.000, 30.000 and 25.000 were used.

Phagocytosis was studied by a modified method of Baehner at the analytical laboratory of the Nephrological division of the University Hospital of Ghent (Belgium)⁴². The burst of the metabolic activity, that is normally associated with phagocytosis was measured directly by ¹⁴CO₂ generated from glucose-1-¹⁴C by the hexose monophosphate shunt. Whole blood, collected from normal persons, was incubated with glucose-1-¹⁴C. Phagocytosis was initiated by the addition of polystyrene latex beads or zymosan at 37°C for 1 hour. ¹⁴CO₂ was trapped on a filter and counted with liquid scintillation. Inhibition of phagocytosis by uremic ultrafiltrate, gelfiltration fractions, normal urine and appropriate reference samples was studied.

Blood samples of uremic patients, before and after hemodialysis, ultrafiltrates and urines were obtained from the Nephrological Division of the University Hospital of Ghent (Belgium). Patients had different etiologies and were subjected to several dialysis strategies. All samples were stored at -20°C until use.

4.2. RESULTS AND DISCUSSION

Applying isotachopheresis as a screening approach much information must be obtained in a relatively short

time of analysis. We therefore limited the time of analysis to 20 minutes at moderate current densities. Concerning the multicomponent information a methodological choice has to be made between anionic and cationic separations. Preliminary experiments showed that cationic profiling of uremic sera gave only minor differences in comparison with normal sera. On the other hand, anionic separations showed more deviating results. So we confined our investigations mainly to the anionic separation mode. Anionic separands will have sufficient electrophoretic mobility, provided the pH of the leading electrolyte is sufficiently high. For the anionic profiling of uremic sera, Fig. 4.1, an electrolyte system at a high pH was used. The operational conditions for this electrolyte system are given in Table 4.1, system 3.

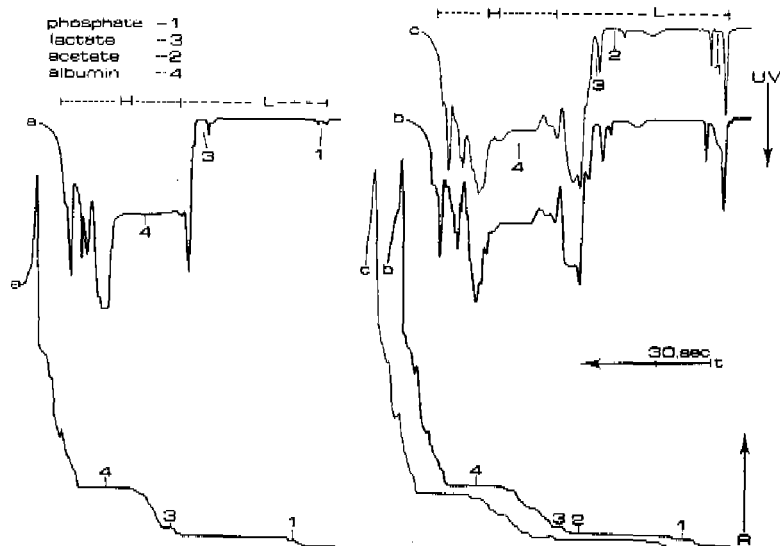


Fig. 4.1 Isotachopheretic serum analyses at high pH
 a: normal serum, b: uremic serum pre dialysis, c: uremic serum post dialysis. Injected volume: 0.2 μ l.
 UV: UV absorption at 254 nm, R = increasing resistance,
 t: time, H: High molecular weight region, L: Low molecular weight region.

Fig. 4.1 shows the analytical results when 0.2 μ l of normal, uremic pre and uremic postdialysis. Sera were injected. The uremic samples were obtained from a male patient, age 63 with chronic glomerulonephritis, on intermittent hemodialysis from January 1977. Dialysis was performed with a poly-acrylonitrile membrane three times per week for 4 h. in a RP6 (Rhône Poulenc, France) open system⁵¹. Due to the swamping amount of chloride and the relatively high protein content only a low sample load can be applied. The differences between the uremic and the normal sera are evident. The protein region in Fig. 4.1 indicated with H, in which albumin is the most abundant solute, shows only minor differences. They can be due to the proteins or to low concentrations of some amino acids, peptides, purines and pyrimidines, with fairly high pK_a values⁵². The major differences however occur in the lower molecular weight region and many of the accumulating solutes have UV absorption at 254 nm. The somewhat poor differentiation in this region is the analytical price for the successful attempt to stack as much anionic solutes as possible. The large zone between lactate and phosphate is mainly carbonate, originating from the electrolyte system and the sample. Comparing the analyses before and after hemodialysis, it follows that the accumulating solutes have been removed only partially. Moreover acetate, originating from the dialysate, is clearly visible. Though this electrolyte system seems very attractive for studying proteins in uremia it should be recognized that only moderate differentiation is obtained. This differentiation can be increased by the use of spacers⁵³, but probably more interesting separations will be obtained with isoelectric focusing.

More differentiation can be obtained when the pH of the leading electrolyte is lowered. The electrolyte system at pH = 6, which covers a large spectrum of anionic solutes, is given in Table 4.1. It should be noted that many of the proteins, peptides, amino-acids, purines and pyrimidines, will not migrate isotachophoretically in this

electrolyte system. Generally, anionic solutes with pK_a values higher than that of the terminator, pK_a (HEPES) = 7.5, will not be stacked. As some solutes are immobilized at this pH, a higher sample load can be applied. Uremic sera, however, can show appreciable fluctuations and therefore it is wise to work well below the maximal allowable sample load. In Fig. 4.2 the separations of uremic sera are compared with the result of a normal serum. Obviously the normal serum differs significantly from the uremic sera before and after hemodialysis. Several accumulating solutes have been identified⁵⁴. From the UV-detect-

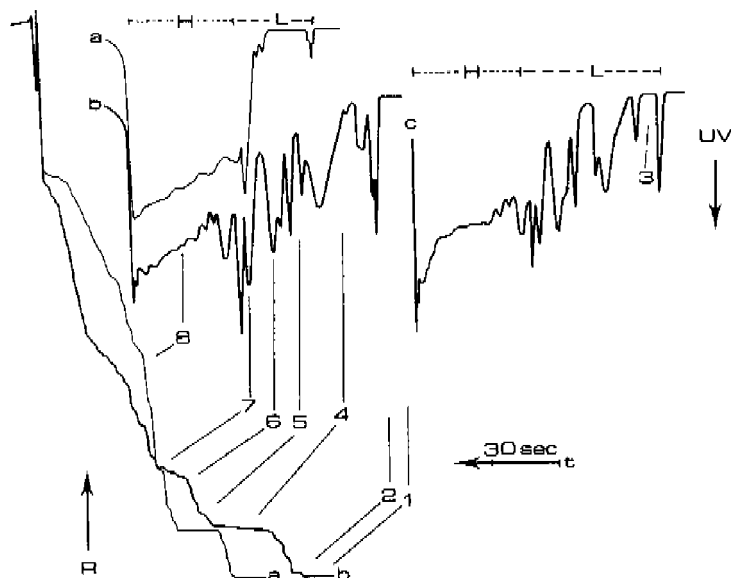


Fig. 4.2 Anionic profiling of uremic and normal sera at pH 6.

a: normal serum, 0.3 μ l, b: uremic pre dialysis, 0.3 μ l,
c: uremic post dialysis, 0.3 μ l.

1 = chloride, 2 = sulphate, 3 = acetate, 4 = phosphate + lactate, 5 = β -OH-butyrate, 6 = hippurate, 7 = urate, 8 = albumin.

R: increasing resistance. UV: UV-absorption 254 nm,
t: time.

tion traces it follows that the major differences between the uremic and the normal sera occur in the more mobile part of the isotachopherogram, indicated in Fig. 4.2 by L. In this part the anionic low molecular weight substances with relatively low pK_a values, i.e. $pK_a < 5.5$, will migrate. Comparing the UV-traces before and after hemodialysis it follows that the accumulating solutes have been removed only partially. Moreover, acetate, originating from the dialysate, is clearly visible in the uremic serum after hemodialysis. In the second part of the isotachopherogram, in Fig. 4.2 indicated by H, anionic solutes with a rather low effective mobility will migrate. This part of the isotachopherogram is mainly occupied by albumin, as only few low molecular weight substances have pK_a values between 5.5 and 7.5. Using an ultrafiltration step the H region can be easily removed from the isotachopherogram⁵⁵. From the separation profiles it follows that the differences between the normal and the uremic sera are much less pronounced in this part. The minor differences can be caused by the occurrence of albumin-heparin complex in the post-treatment samples. It has been shown that by the formation of such complexes not only the mobility of albumin, or other proteins, can be increased, but also that in this way protein binding of low molecular weight solutes, can be reduced⁵⁶. In fact the increased mobility of the albumin zone is characteristic for the post-treatment samples.

As the excess of low molecular weight substances is a characteristic difference between normal and uremic samples, it is advantageous to describe this difference in a single parameter. This is most conveniently done by taking the quotient of the two zone-lengths, H and L. The transition point between the albumin-zone and the lower molecular weight region is characteristic for all separations, done until now, and therefore this point is used for determining the two zone-lengths. It should be emphasized that the HL ratio does not provide direct quantitative information. The HL-ratio for normal sera always is signifi-

cantly higher than unity, indicating a relatively small content of the anionic low molecular weight solutes. For uremic sera the pre dialysis values are generally smaller than unity, due to the excess of the accumulating solutes. As acetate is metabolized rather quickly after hemodialysis^{57,58}, the HL-ratio should be corrected for this zone-length⁵⁴. In order to study the relevance of this ratio a patient was screened during several weeks of hemodialysis. The patient (female, age 38, chronic glomerulonephritis), was since August 1975 on intermittent hemodialysis. Dialysis was performed with a RP6 (Rhône Poulenc, France) open system three times per week for 4 h. The strong similarity of the separation profiles indicated that the patient was well stabilized and gave a fairly constant response to intermittent hemodialysis⁵⁴. In Table 4.2 the measured HL-ratios have been summarized.

TABLE 4.2

HL-RATIOS: NORMAL-, PRE- AND POST-DIALYSIS VALUES

Serum	HL-ratio									mean	cv%
Normal	1.10	1.25	1.22	1.17	1.18					1.18	5
Uremic pré	0.86	0.91	0.91	0.79	0.86	0.84	0.77	0.72	0.83	0.83	8
Uremic post	1.19	1.15	0.94	0.90	1.10	1.03	0.98	1.00	1.06	1.06	10
c.v. coefficient of variation											

Post dialysis values, corrected for the acetate contents, were slightly larger than unity, suggesting a correction towards the normal value.

As can be expected patients with chronic renal failure do not form a homogeneous group. Figure 4.3 gives some separation profiles of different patients before hemodialysis. Patients with a very large excess of anionic lower molecular weight solutes will have a low ratio, e.g. HL = 0.68. As can be seen the separation profiles can be very different. The example with HL = 1.19 is hardly deviating from normal. The samples show as well differences in the lower molecular weight part, L, as in the higher molecular weight part, H. The differences in the latter part, however, are much less pronounced. In Fig. 4.3 also the

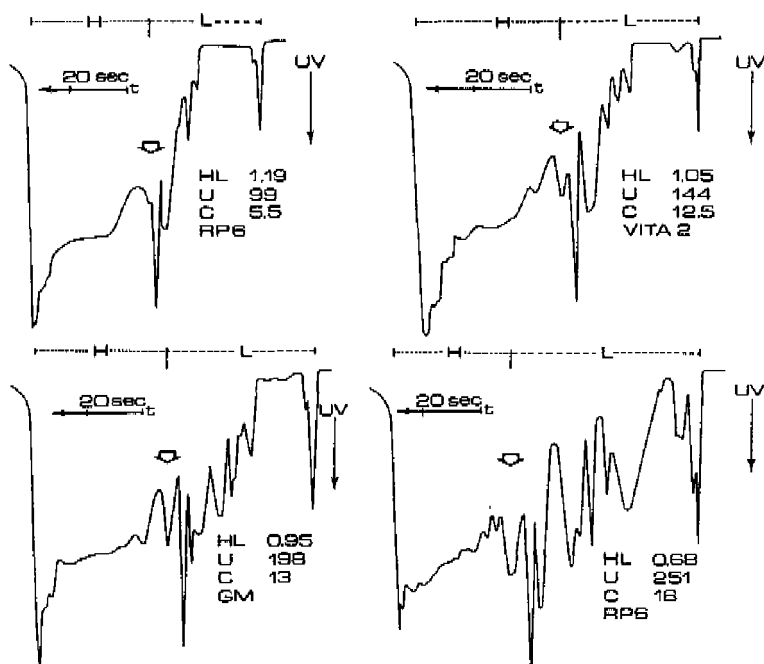


Fig. 4.3 UV-separation profiles of different patients. Operational system 2, Table 4.1, injected volume 0.3 μ l serum. HL: HL-ratio, U: urea (mg/100 ml), C: creatinine (mg/100 ml), RP6: Polyacrylonitrile, 1.0 m^2 , Rhône Poulenc (France), VITA 2: Cuprophane, 1.2 m^2 , Belleo Spa (Italy), G.M.: Cuprophane, 1.5 m^2 , Ab. Gambro (Sweden).

urea and creatinine concentrations and membranes of the dialyzer are given.

A HL ratio, which is close to normal, hardly improves by dialysis whereas the effect on low HL ratios can be appreciable. From Fig. 4.2 it follows that not only the concentration levels of the various accumulating solutes can differ but also the accumulating solutes can be different. The separation profiles of Fig. 4.2 are some representative examples, taken from a group of 27 different patients.

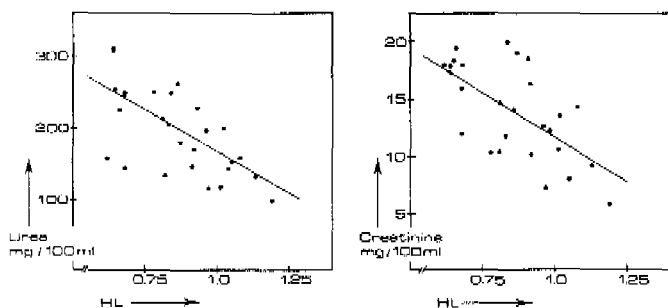


Fig. 4.4 HL-ratios versus urea and creatinine concentrations, pre dialysis values.

From the sera of these patients the HL-ratios, creatinine and urea concentrations were determined. In Fig. 4.3 the pre dialysis values are compared. As well the urea concentration as the creatinine concentration proved to be significantly correlated to the HL-ratio on the 95% probability level. From both the Figs. 4.3 and 4.4 it can be concluded that uremic patients form a rather heterogenic group. This heterogeneity can be the result of the impairment of renal function, secondary complications, differences in biological parameters, such as age and body weight, differences in dialysis treatment, in diet and way of living, renal restfunction etc. An adequate assessment of all these factors will require a large and more selected group of patients. All HL-ratios improved after hemodialysis but no significant correlation was found any more for the urea and creatinine concentrations with the HL ratio.

Whereas the electrolyte system at pH 6 can be used for a fast screening approach, more differentiation is obtained at low pH. The operational system for anionic separations at pH 3.5 is given in Table 4.1. Fig. 4.5 gives the separation profiles of a normal and a pre dialysis sample.

Whereas in the normal serum profile, lactate and phosphate are the most abundant solutes (constituents 5 and 17), many other anionic solutes are present in the uremic serum.

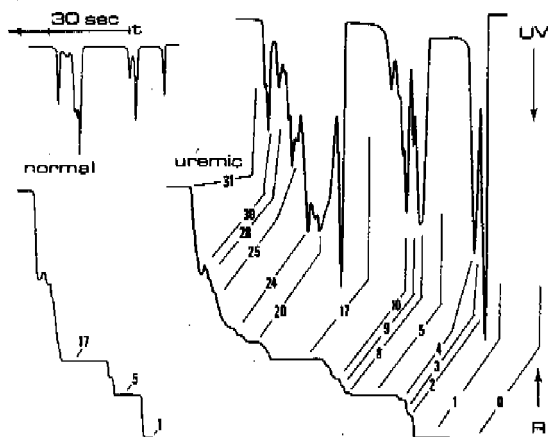


Fig. 4.5 Anionic separation at low pH of a normal and a uremic serum pre dialysis.

Operational system. Table 4.1 system 1. Injected volume 0.8 μ l. R: increasing resistance, UV: UV-absorption 254 nm, t: time, Constituents: Table 4.2

Caproate was used as the terminating ion and therefore generally only anionic solutes with a pK_a values smaller than that of caproic acid, $pK_a = 4.8$, will migrate isotachophoretically. As many of the solutes do not migrate at this low pH, the sample load can be increased in comparison with the analyses at pH 6. Several solutes have been identified^{54,57} and are given in Table 4.2.

TABLE 4.2
ANIONIC UREMIC SOLUTES, FIGS. 4.5 AND 4.6

t: tentatively			
no	constituent	no	constituent
0	chloride	17	lactate
1	sulphate	19	β -OH-butyrate
2	ATP	20	hippurate
3	pyruvate	21	nicotinate (t)
4	indoxylsulphate	24	ascorbate
5	phosphate	25	succinate
8	ADP (t)	28	glutathion (t)
9	citrate	30	acetate
10	orotate	32	caproate

The concentration levels of the various accumulating solutes again can show appreciable differences, but many of them are present just below the mM. range. For a quantitative determination the UV-spike method or the coupled column system, Part 2 Chapter 3, has to be used. In Fig. 4.6 the separation profile of the uremic serum after hemodialysis is given. In comparison with the predialysis sample the excess of solutes, as analyzed by isotachopheresis, has been reduced for approximately 60%.

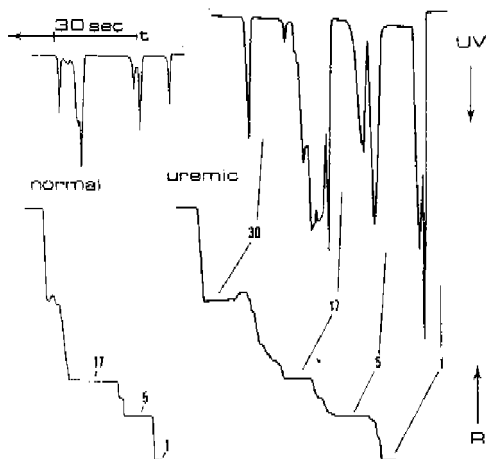


Fig. 4.6 Anionic separation at pH 3.5 of a normal and a uremic serum after hemodialysis.

Operational system, Table 4.1 system 1, Injected volume 0.8 μ l. R: increasing resistance, UV: UV-absorption 254 nm, t: time, constituents: Table 4.2.

Nevertheless the uremic serum after hemodialysis still differs considerably from the normal one. Moreover, acetate, originating the dialysate, is clearly visible and can be determined without problem⁵⁴. This operational electrolyte system additionally has been used for the separation of normal and uremic urines. Normal urine and serum give completely different separation profiles⁵⁵ as a result of the selective and concentrating capabilities of the normally functioning kidneys. In case of renal refunction, the separation

profiles of uremic urine and uremic serum show a large similarity. Almost each solute, which is present in the uremic sera, proved also to be present in the uremic urines, though individual concentration differences do exist. Uremic urine, that was produced during hemodialysis or shortly after it can contain an appreciable acetate concentration.

From all the isotachophoretic separations shown it follows that the excess of relatively low molecular weight solutes is characteristic for uremic serum samples. Pre-dialysis and post dialysis serum samples have also been investigated with gas-chromatography⁴⁶ and liquid chromatography⁴⁸. Representative chromatograms are shown in the Figs. 4.7 and 4.8.

In the gaschromatographic procedure high molecular weight solutes were removed by pressure ultrafiltration through membrane filters with a mol. wt. cut-off at 50.000. Ultrafiltrates were evaporated to dryness and derivatized to silyl derivatives to enable gaschromatographic analysis. Separations were performed on glass capillary columns, coated with SE-30⁴⁶. The method proved to be reliable, reproducible and relatively fast. Solutes that were separated and detected by this method are related to carbohydrate metabolism, such as aldoses, aldonic acids and polyols. Also other organic acids and some nitrogen containing compounds were detected. Some thirty solutes have been identified in combination with mass-spectrometry⁴⁷. From the chromatograms of Fig. 4.7 it follows that the differences in concentration of various solutes are large. A group of ten patients showed similar profiles, though individual differences did occur. Profiles from pre and post dialysis serum show that hemodialysis results in a significant decrease of the concentration of many solutes. Comparison of the separation profiles of different patients re-emphasized the heterogeneity of the uremic patient group. In the liquid chromatographic procedure⁴⁸ proteins were removed from serum using Amicon CF 25 ultrafiltration filters with a mol. wt. cut-off at 25.000. Analyses

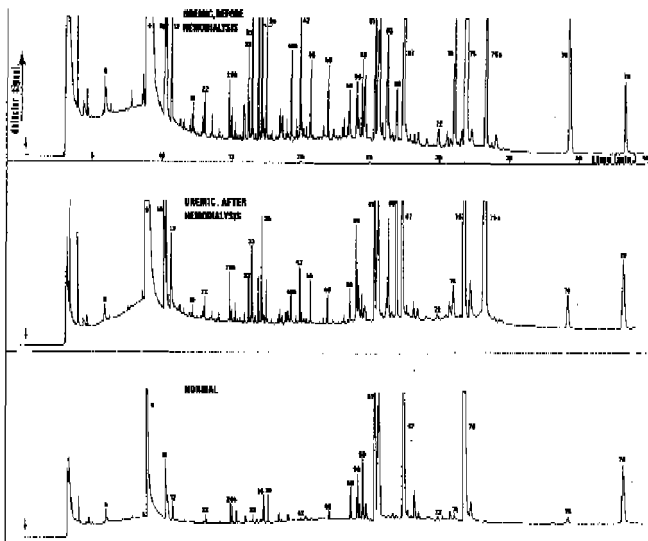


Fig. 4.7 Gaschromatographic profiles of ultrafiltered serum from an uremic patient before and after hemodialysis and from a pool of non-uremic sera.

9: urea, 10: phosphoric acid, 11: glycerol, 18: tartronic acid, 22: threonine, 26b: homoserine, 30: Δ -pyrrolidone-5-carboxylic acid, 32: threitol, 33: erythritol, 35: erythroic acid, 40a: tartronic acid, 49: arabinitol, 55: arabinonic acid, 58: citric acid, 58: fructose 61: galactose, 66: glucono-1,4-lactone, 67: α -D-glucose, 72: mannitol, 75: β -D-glucose, 76a: gluconic acid, 78: myo-inositol.

were done in the reversed phase mode, C_{18} chemically modified silica, using a buffered water methanol gradient. Elution was achieved with a 60-minute linear gradient programmed from 0.05 M aqueous ammonium formate, pH 4, to methanol. The column effluent was monitored with UV detection at 254 nm, and several peaks were collected and identified with off-line mass-spectrometry. From Fig. 4.8 the differences between the normal and the uremic sera can be seen. In the normal serum uric acid, hippuric acid and hypoxanthine are the most abundant solutes. The uremic sera, how-

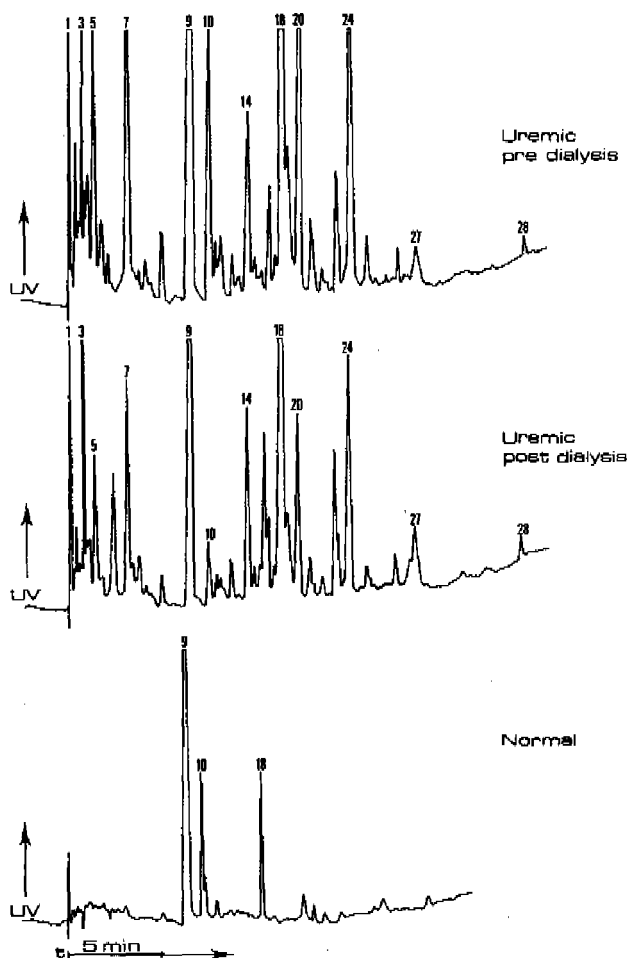


Fig. 4.8 High performance liquid chromatography profiles of ultrafiltered serum from an uremic patient before and after hemodialysis and from a pool of non uremic sera.

UV: UV-absorbance 254 nm, t: time

1 = Ascorbic acid

9 = uric acid, 10 = hypoxanthine, 18 = hippuric acid.

however, contain numerous other solutes with UV-absorbing properties at 254 nm. Some of them are given in the legend of Fig. 4.8. Other UV-absorbing solutes probably belong to the class of purines, pyrimidines, phenolic and indolic acids^{59,60}.

From all the separations shown, it follows that the excess of relatively low molecular weight substances is characteristic for the uremic state. According to the middle molecule hypothesis^{20,21} solutes in the molecular weight range of 500-2000 should accumulate in uremic serum. The allocation of this molecular weight range is mainly based on gelchromatographic results. The relation between retention volume and molecular weight for these substances is however rather poor³², as many non size related retention mechanisms dominate⁶¹. Zimmerman reanalyzed middle molecular weight gelfiltration fractions and ion-exchange reprocessed subfractions with isotachopheresis⁴⁰. Both the gelfiltration fractions and the subfractions proved to contain several UV-absorbing solutes of rather high effective mobilities. The applied electrolyte system is almost equal to the system 1 of Table 4.1 at pH 3.5. The authors suggest that the separated solutes are peptides with a molecular weight of approximately 1000. This is however rather unlikely as such peptides only can be analyzed as anionic constituents by isotachopheresis at a high pH of the leading electrolyte. At low pH they will migrate as cations or will not migrate at all. The mobilities and UV-absorbing properties indicate that the analysed solutes belong to the class of low molecular weight organic acids, with fairly low pK_a values. Possible candidates probably can be found amongst the substituted hippuric- and benzoic acids or nucleotides.

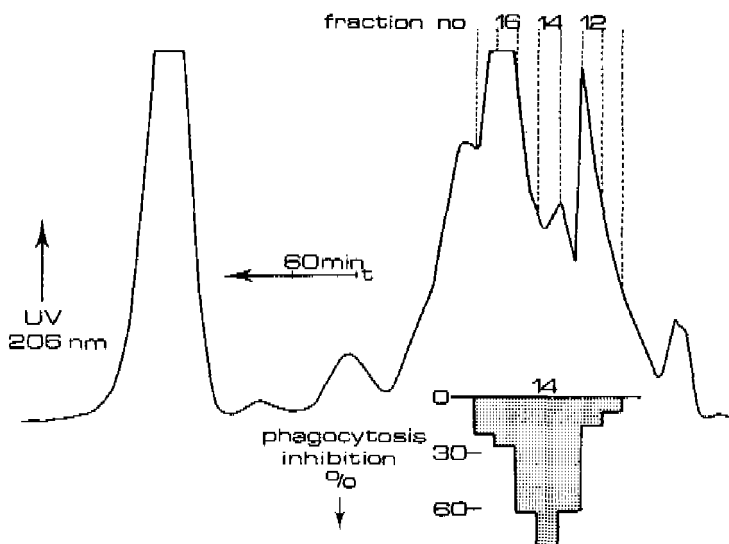
In order to obtain more detailed information on middle molecules gelchromatographic fractions were analyzed with isotachopheresis, high performance liquid chromatography and high resolution gas chromatography⁶². Lyophilized gelchromatographic fractions from ultrafiltered mal serum, normal urine and several uremic ultrafiltrates

were investigated. The operational conditions for gelchromatography are given in Table 4.3

TABLE 4.3
OPERATIONAL CONDITIONS FOR GELCHROMATOGRAPHY

Column	length 60 cm, i.d. 1.6 cm
Gel	Sephadex G-15
Eluent	0.3 M NH ₄ Acetate
Flow	15 ml/h
Detection	UV: 206 nm, 280 nm
Fractions	5 ml
Sample load	uremic ultrafiltrate: 5 ml normal serum: 2 ml normal urine: 2 ml

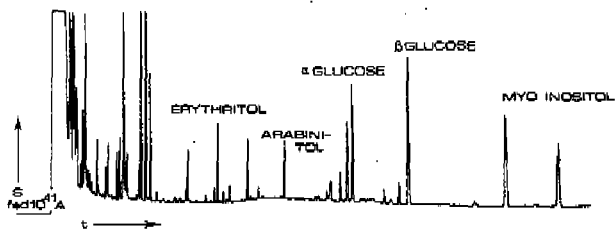
The ammonium acetate eluent was chosen as it is easily removed during lyophilization. Each fraction was divided in three parts which were, after lyophilization, used for analysis and the measurement of phagocytosis inhibition. In Fig. 4.9 the gelchromatogram and the fractions are given. Middle molecules are supposed to eluate in fractions 11-15. The fractions of the ultrafiltered normal serum showed no significant inhibition of phagocytosis, whereas the middle molecule fractions gave considerable inhibition. All fractions of the first part of the gelchromatogram, i.e. fraction no. 3-18 in Fig. 4.9, were analyzed with isotachopheresis, gas chromatography and liquid chromatography. It proved that almost the entire spectrum of accumulating low molecular weight solutes, that normally are found in uremic ultrafiltrate, eluate in the middle molecular weight region. In Fig. 4.9 the distribution of some identified solutes is given. Moreover numerous solutes, that have not yet been identified were present. Some representative results are shown in Fig. 4.10. All the identified solutes have rather low molecular weight, but nevertheless eluate in the middle molecule region. Though some separation has occurred Figs. 4.9 and 4.10 emphasize the fact that gelchromatography cannot be used as a size discriminating separation technique for solutes of intermediate molecular weight



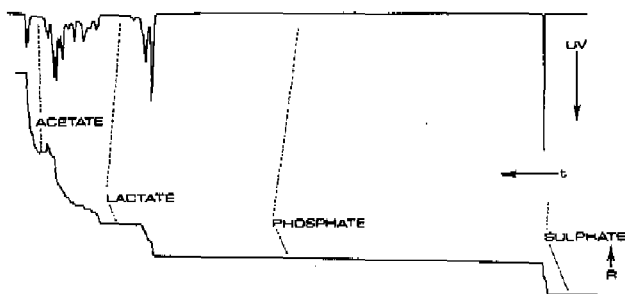
sodium			⊙	⊙	⊙	⊙
creatinine		⊙	⊙			
urea		⊙				
acetate			⊙	⊙	⊙	⊙
lactate				⊙	⊙	
gluconate					⊙	
aspartate				⊙	⊙	
phosphate						⊙
serine					⊙	
threonine					⊙	
glucose			⊙	⊙	⊙	
fructose				⊙		
galactose					⊙	
glucitol				⊙		
arabinitol				⊙		
erythritol				⊙	⊙	
myo-inositol				⊙		

Fig. 1.9 Gelchromatographic separation of uremic ultrafiltrate. The fractions were analyzed by gas chromatography, liquid chromatography and isotachophoresis and tested for inhibition of phagocytosis. The distribution of various solutes is shown: ⊙ high concentration, ○ low concentration. The analyses of fractions 13 and 14 are shown in Fig. 4.10.

GAS CHROMATOGRAPHY FRACTION NO 14



ISOTACHOPHORESIS FRACTION NO 13, ANIONS PM 3.5



LIQUID CHROMATOGRAPHY FRACTION NO 13

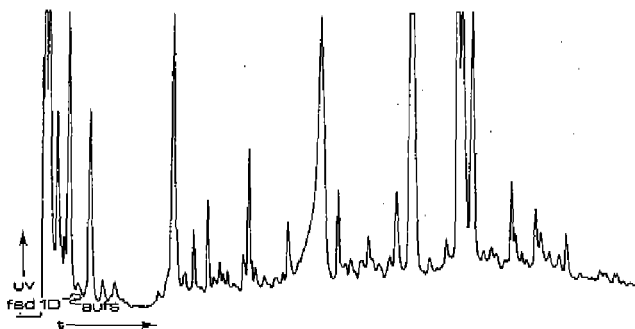


Fig. 4.10 Analysis of a middle molecule fraction with gas chromatography, liquid chromatography and isotachopheresis.

4.3. CONCLUSIONS

Isotachopheresis provides multicomponent information of uremic serum samples in a relatively short time of analysis. Due to the minimal sample pretreatment and standardized experimental conditions the results have good reproducibility (and a high reliability).

In anionic separations appreciable differences are found between uremic and normal sera, whereas in cationic separations only minor differences occur. Differentiation can be increased by choosing appropriate electrolyte systems. Anionic separations at a high pH of the leading electrolyte will include the analysis of proteins. Due to the relatively high protein contents of serum only a low sample load can be applied. Anionic profiling at pH = 6 will involve the analysis of albumin and the low molecular weight anionic solutes. Uremic sera show a large excess of low molecular weight solutes in comparison with normal sera. For isotachopheresis this can be expressed in the ratio of high molecular weight solutes to low molecular weight anionic solutes: the HL-ratio. Uremic sera show HL-ratios that are smaller than normal sera, dialysis increases the HL-ratio. Uremic patients form a heterogenic group, when the accumulating solutes are measured with isotachopheresis, gas chromatography and high performance liquid chromatography. Several solutes have been identified and proved to have a rather low molecular weight.

Investigations on middle molecule fractions, obtained with gel chromatography, showed that these fractions contain numerous solutes of low molecular weight. As a result the significance of the determination of "middle molecules", having molecular weights between 500 and 2000, by gelchromatography is highly questionable.

REFERENCES

1. W. Quinton, D. Dillard and B. Scribner, *Trans. Amer. Soc. Artif. Intern. Organs*, 6 (1960) 104.
2. G. Schreiner, *Kidney Int.*, 7 (1975) 270.

3. S. Giovanetti and G. Barsotti, *Nephron*, 14 (1975) 123.
4. J. Bergström and P. Fürst, in *Replacement of renal function by dialysis*, W. Drukker (Ed.), M. Nijhoff. Publ., The Hague-Boston-London, 1979, 334.
5. J. Grantham, F. Whithier and D. Diederich, in *Physiology of membrane disorders*, T. Andreoli (Ed.), Plenum Publ. Co., 1978, 955.
6. J. Bergström and P. Fürst, *Kidney Int.*, 15 (1978) 9.
7. J. Knochel, *Clin. Nephrol.*, 7 (1977) 131.
8. E. Slatopolski, *Clin. Nephrol.*, 7 (1977) 138.
9. S. Indrapasit, G. Alexander and H. Gonick, *J. Chron. Dis.*, 27 (1974) 135.
10. S. Massry and M. Seelig, *Clin. Nephrol.*, 7 (1977) 147.
11. F. Singer, J. Bethane and S. Massry, *Clin. Nephrol.*, 7 (1977) 154.
12. R. Friedler, A. Koffler and K. Kurokawa, *Clin. Nephrol.*, 7 (1977) 163.
13. R. Kunau and J. Stein, *Clin. Nephrol.*, 7 (1977) 173.
14. T. Yamada and S. Nakagawa, *Trans. Amer. Soc. Artif. Intern. Organs*, 12 (1976) 155.
15. G. von Karnassiolis and H. Cramer, *Nier. u. Hochdruckkrankh.*, 21 (1978) 62.
16. R. Porter, W. Cathcart-Rake, S. Wan, F. Withier and J. Grantham, *J. Lab. Clin. Med.*, 85 (1975) 723.
17. J. Condon and A. Asatoor, *Clin. Chim. Acta*, 32 (1971) 333.
18. J. Bergström, P. Fürst, L. Honie and E. Vinnars, *Clin. Sci. Molec. Med.*, 54 (1978) 51.
19. B. Scribner, *Trans. Amer. Soc. Artif. Intern. Organs*, 11 (1965) 29.
20. A. Babb, R. Popovich, T. Christopher and B. Scribner, *Trans. Amer. Soc. Artif. Intern. Organs*, 17 (1971) 81.
21. A. Babb, P. Farrell, D. Uvelli and B. Scribner, *Trans. Amer. Soc. Artif. Intern. Organs*, 18 (1972) 98.
22. A. Babb, H. Strand, D. Uvelli, D. Milutinovic and B. Scribner, *Kidney Int.*, 5 (1975) 23.
23. R. Dzúrik, P. Bozek, J. Reznicek and A. Bornikova, *Proc. Eur. Dial. Transpl. Assoc.*, 10 (1973) 263.

24. N. Man, B. Terlain, J. Paris, G. Werner, A. Sausse and J. Funck-Brentano, *Trans. Amer. Soc. Artif. Intern. Organs*, 19 (1973) 320.
25. L. Migone, P. Dall'aglio and C. Buzio, *Clin. Nephrol.*, 3 (1975) 82.
26. P. Dall'aglio, C. Buzio, V. Cambi, L. Arisi and L. Migone, *Proc. Eur. Dial. Transpl. Assoc.*, 9 (1972) 409.
27. J. Funck-Brentano, N. Man, A. Saussé, G. Cueille, J. Zinfroff, T. Bruecke, P. Jungers and J. Billon, *Kidney Int.*, 7 (1975) 352.
28. P. Fürst, J. Bergström, A. Gordon and L. Zimmerman, *Kidney Int.*, 7 (1975) 272.
29. J. Bergström and P. Fürst, *Clin. Nephrol.*, 5 (1976) 143.
30. B. Scribner and A. Babb, *Kidney Int.*, 7 (1975) 349.
31. P. Fürst, L. Zimmerman and J. Bergström, *Clin. Nephrol.*, 5 (1976) 178.
32. G. Cueille, *J. Chromatogr.*, 146 (1978) 55.
33. S. Ringoir, R. de Smet and I. Becaus, in *Aktuelle Probleme der Dialyse Verfahren und Nieren Insuffizienz*, P. von Dittricht (Ed.), Verlag Crl Bindernagel, 1977, 128.
34. J. Funck-Brentano, G. Cueille and N. Man, *Kidney Int.*, 13 (1978) 31.
35. J. Bergström and P. Fürst, *Dial. Transplant.*, 7 (1978) 346.
36. L. Henderson, *Nephron.*, 22 (1978) 146.
37. B. Lamberts, H. Branner, H. Ocks, P. Spellenberg and R. Heintz, *Clin. Nephrol.*, 6 (1976) 465.
38. W. Lutz, *Acta. Med. Pol.*, 17 (1976) 137.
39. P. Fürst, L. Zimmerman and J. Bergström, *Clin. Nephrol.*, 5 (1976) 178.
40. L. Zimmerman, A. Baldenstein, J. Bergström and P. Fürst, *Clin. Nephrol.*, 13 (1980) 183.
41. R. Dzurik, V. Hupkova and J. Holomann, *Int. Urol. Nephrol.*, 3 (1971) 409.

42. S. Ringoir, N. van Landschoot and R. de Smet, *Clin. Nephrol.*, 13 (1980) 109.
43. W. Lutz, K. Markiewicz and L. Klyszejko, *Acta Med. Pol.*, 15 (1974) 97.
44. J. F. Cloix, G. Cueille and J. Funck-Brentano, *Biomed.*, 25 (1976) 215.
45. F. Everaerts, J. Beckers and Th. Verheggen, *Isotachophoresis*, J. Chromatogr. Lib. Vol. VI, Elsevier, Amsterdam-Oxford-New York, 1976.
46. A. Schoots, F. Mikkers, C. Cramers and S. Ringoir, *J. Schromatogr.*, 164 (1979) 1.
47. A. Schoots and P. Leclercq, *Biomed. Mass. Spectrom.*, 6 (1979) 502.
48. A. Schoots, F. Mikkers, H. Claessens and S. Ringoir, in prep.
49. S. Ringoir, R. de Smet and I. Bécaus, *Int. J. Artif. Organs*, 1 (1978) 218.
50. R. Bachner, D. Nathan and M. Karnovsky, *J. Clin. Invest.*, 49 (1970) 865.
51. F. Mikkers, Th. Verheggen and S. Ringoir, *Protides Biol. Fluids*, 27 (1979) 727.
52. F. Oerlemans, Th. Verheggen, F. Mikkers, F. Everaerts and C. de Bruyn, in *Purine Metabolism in Man-III*, Part B. A Rapad (Ed.), Plenum Publ. Co. 1980, 441.
53. P. Delmotte, in *Biochemical and Biomedical Applications of Isotachophoresis*, A. Adam (Ed.), Elsevier, Amsterdam 1980, 58.
54. F. Mikkers, S. Ringoir and R. de Smet, *J. Chromatogr.*, 162 (1979) 341.
55. F. Mikkers and S. Ringoir, in *Biochemical and Biomedical Applications of Isotachophoresis*, A. Dam (Ed.), Elsevier, Amsterdam, 1980, 97.
56. F. Mikkers, Th. Verheggen and F. Everaerts, in prep.
57. F. Lundquist, *Natura*, 193 (1962) 579.
58. T. v. Noorden, Graduation Report, Eindhoven University of Technology, Eindhoven (The Netherlands), 1980.
59. F. Senftleber, A. Halline, H. Veening and D. Dayton, *Clin. Chem.*, 22 (1976) 1522.

60. R. Hartwick, *Thesis*, University of Rhode Island, USA, 1978.
61. Th. Hafkenscheid, Graduation report, Eindhoven University of Technology, Eindhoven (The Netherlands), 1977.
62. F. Mikkers, A. Schoots, S. Ringoir and R. de Smet
Kidney Int., submitted.
63. S. Ringoir, personal communication.

CHAPTER 5

Determination of valproic acid in human serum

An isotachopheretic procedure for the determination of the anticonvulsant valproic acid in serum is given. The procedure requires only micro liter amounts of sample and no sample pretreatment is necessary. Quantitative determinations can be done at the therapeutic level within fifteen minutes. Results are compared with a routine gaschromatographic procedure.

5.0. INTRODUCTION

Sodium valproate is known as a useful anticonvulsant drug in primary generalized epilepsy¹. The concentration of the anticonvulsant in serum is of importance for the correct treatment of epileptic patients, especially in establishing the pharmacotherapy. Optimal therapeutic serum concentrations are known to be approximately 60 µg/ml.

Several gaschromatographic procedures have been described²⁻⁹, each with its own advantages and limitations.

A disadvantage, common to all gaschromatographic procedures, is the treatment of the sample prior to chromatography. Dependent on the specific procedure, solvent extraction, derivatisation and evaporation have to be used.

Isotachopheresis¹⁰ requires no sample pretreatment and only minute amounts of sample are necessary for an accurate determination. Since valproate is an ionic solute and its therapeutic concentration level is just below the millimolar range, it is possible to determine it directly by analytical isotachopheresis.

5.1. EXPERIMENTAL

All chemicals were of analytical grade or additionally purified by conventional methods. Sodium valproate was obtained from Labaz (Maassluis, The Netherlands). Test- and reference sera were obtained from a hospital dispensary (Apotheek Haagse Ziekenhuizen, Den Haag, The Netherlands). In addition to valproic acid the testsera contained phenobarbital, phenytoin, ethosuximide, primidone, clonazepam, carbamazepine and 10,11-epoxycarbamazepine. Serum samples were taken from venous blood; after clotting and centrifugation the sera were stored at -20°C until use.

Gaschromatography

For the gaschromatographic determinations a Packard Becker 421 chromatograph was used. Separations were performed in a glass column 1.5 m x 4 mm I.D., packed with 5% FFAP on Chromosorb WHP, 80-100 mesh (Free Fatty Acid Phase, Chrompack, Middelburg, The Netherlands). The injection temperature was 160°C , whereas the oven temperature was kept isothermal at 150°C . Nitrogen was the carrier gas and FID detection at 175°C was used. Cyclohexanecarbonic acid was applied as the internal standard.

Isotachopheresis

For the isotachopheretic separations the coupled column system, Part 2 Chapter 3, was used. The inner diameter

of the preseparation compartment was 0.8 mm. At a leading ion concentration of 0.01 M an electrical driving current of 377 μ A was used. The valproate zone was trapped into the analytical column, which had an inner diameter of 0.2 mm. The electric driving current in the analytical column was 10 μ A. The electrolyte systems and other operational conditions are given in Table 5.1.

TABLE 5.1
ELECTROLYTE SYSTEMS AND OPERATIONAL CONDITIONS

	preseparation compartment	separation compartment	terminating compartment
Anion	Chloride	Chloride	MES
Concentration	0.01 M	0.005 M	0.005 M
Counter Const.	EACA	EACA	TRIS
pH	5.00	5.00	6.50
Additive	0.3% HEC	0.3% HEC	--
Current Density	0.075 A/cm ²	0.0318 A/cm ²	
Temperature	22°C	ambient.	
UV	--	254 nm	

The constant electric driving current was taken from a modified Brandenburg power supply (Thornton Heath, UK). The voltage varied between 1 and 15 kV. Serum samples were injected directly, using a microliter syringe. Separated zones were detected by measuring the electric conductance as well as the UV absorption at 254 nm.

5.2. RESULTS AND DISCUSSION

One of the major advantages of isotachopheresis is that ionic solutes often can be analyzed without sample pretreatment. Therapeutic levels of valproate in serum, however, differ at least two orders of magnitude from the physiological chloride concentration. Due to this unfavourable sampling ratio, the electrolyte system will have a rather low current efficiency¹². Hence, for a reliable determination, a large column volume must be available, resulting in a large time of analysis. Most of these pro-

blems can be solved using a coupled system. This system not only allows the use of high sample load, but also the use of different electrolyte concentrations, e.g. Table 5.1. For the determination of valproate the concentration of the leading ion in the pre-separation compartment was 0.01 M. At a high driving current serum samples were separated in approximately 6 minutes. The swamping amount of chloride was allowed to pass the bifurcation with the analytical column. The valproate zone was trapped into the analytical column, which contained the leading ion at a concentration of 0.005 M. Figure 1 shows a representative result when 3 μ l of a patient serum was injected. The total time of analysis was less than 15 minutes. Since trapping was started two seconds before the valproate zone

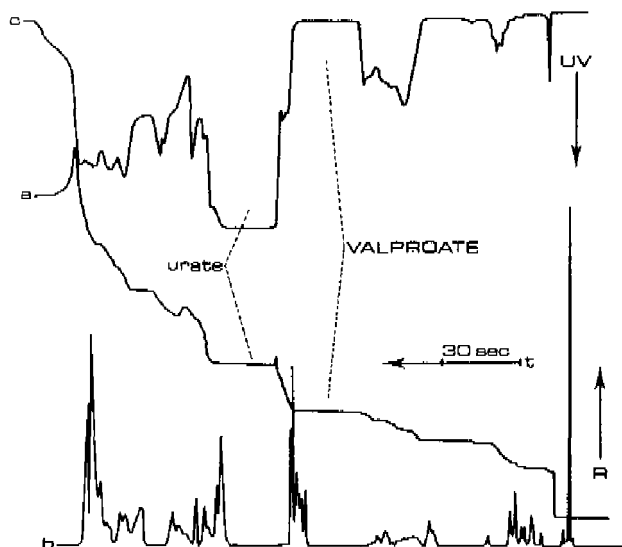


Fig. 5.1 Isotachopheretic separation of a patient serum. UV = UV absorption at 254 nm; R = increasing resistance; t = increasing time. Injected volume: 3.0 μ l of serum. a. Conductimetric trace; b. differentiated conductimetric trace; c. UV trace, 254 nm.

reached the bifurcation point, some other solutes have been analyzed additionally. The valproate zone, however, easily can be localized in both the UV trace, Fig. 5.1c, and the conductimetric trace, Fig. 5.1a. From the separation in Fig. 5.1 it follows that uric acid could have been used as the terminating ion, instead of morpholine-ethanesulfonic acid. As a result a lower end-voltage would have been obtained allowing a further optimization of the time for analysis.

For the quantitative analyses, the characteristics of the calibration line, i.e. zone-length versus amount of valproic acid, were determined. The calibration points were measured with standard valproate solutions in water and in serum. Additionally several testsera, containing various other drugs were analyzed. A good linear relation was found with a correlation coefficient of 0.99914 ($n = 26$). The response was found to be 6.12 ng/sec and the mean error per point was 3.8 ng in the detection range of 50-500 ng. The additional other drugs did not interfere. The gaschromatographic procedure yielded also a good calibration line, with a correlation coefficient of 0.99969. In the detection range of 2-20 ng the mean error per point was 0.1 ng. Using these calibration data, valproic acid concentration levels were determined in the sera of twenty patients. The isotachophoretic results were compared with the gaschromatographic results. As can be seen from Fig. 5.3 there is a good relation. The experimental slope deviates only one percent from the ideal value of unity. A positive intercept of 4.9 ng valproic acid, however, is present. The group mean was 62.1 $\mu\text{g/ml}$ for the isotachophoretic determinations and 57.8 $\mu\text{g/ml}$ for the gaschromatographic determinations. The origine of the systematic deviation is still under investigation. The results of four different testsera, bovine sera, were for both methods in good agreement with the expected values.

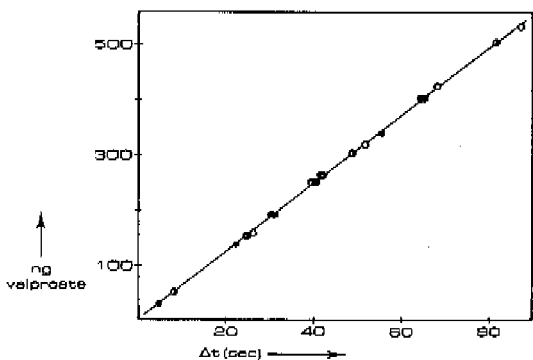


Fig. 5.2 The calibration graph for isotachophoretic valproate determinations. ○ standard solution in water
◐ standard solution in serum
● test sera.

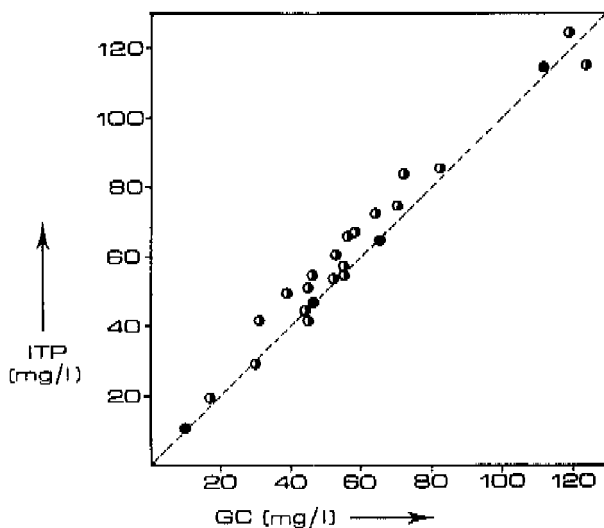


Fig. 5.3 Comparison of gas chromatographic and isotachophoretic results. ○ patient sera
● test sera.

5.3. CONCLUSIONS

Valproate in serum can be determined quantitatively by isotachphoresis. The procedure requires no sample pretreatment and only 3 μ l of serum is necessary for the analysis. Results agree reasonably well with gaschromatographic results, though a systematic deviation exists.

REFERENCES

1. R. Pinder, R. Brogden, T. Speight and G. Avery, *Drugs*, 13 (1977) 81.
2. C. Jakobs, M. Bojash and F. Hanefeld, *J. Chromatogr.*, 146 (1978) 494.
3. S. Willox and S. Foote, *J. Chromatogr.*, 151 (1978) 67.
4. D. Berry and L. Clarke, *J. Chromatogr.*, 156 (1978) 301.
5. J. Libeer, G. Scharpé, P. Schepens and R. Verkerk, *J. Chromatogr.*, 160 (1978) 285.
6. O. Gyllenhaul and A. Albinsson, *J. Chromatogr.*, 161 (1978) 343.
7. G. Chabert, P. Bondon, M. Revol and J. Plasse, in "Recent developments in Chromatography and Electrophoresis". Chromatography Symposia Series, Vol. 1, Eds. A. Frigerio and L. Renoz, Elsevier, Amsterdam-Oxford-New York, (1979) 123.
8. J. Lebeer, P. Schepens and L. Lakiere, in "Recent Developments in Chromatography and Electrophoresis". Chromatography Symposia Series, Vol. 1, Eds. A. Frigerio and L. Renoz, Elsevier, Amsterdam-Oxford-New York, (1979) 163.
9. I. Dijkhuis and E. Vervloet, *Pharm. Weekbl.*, 109 (1974) 42.
10. F. Everaerts, J. Beckers and Th. Verheggen, *Isotachophoresis: Theory, Instrumentation and Application*. Elsevier, Amsterdam-Oxford-New York, (1967).
11. F. Everaerts, Th. Verheggen and F. Mikkers, *J. Chromatogr.*, 169 (1979) 21.
12. F. Mikkers, F. Everaerts and J. Peek, *J. Chromatogr.*, 168 (1979) 293.

CHAPTER 6

Determination of uric acid in human serum

An operational system is described for the isotachophoretic determination of urate in serum. Results show a good agreement with a standard enzymatic procedure. For the isotachophoretic determination only 3 μ l of serum is required and the sample can be analysed without any pretreatment.

6.0. INTRODUCTION

Uric acid is the end-product of purine catabolism in man. An abnormal concentration of uric acid in the body fluids may be indicative for a number of disturbances. An increased serum concentration, hyperuricemia, is seen in primary gout: although there is a normal excretion rate, uric acid is overproduced or it is underexcreted¹. In secondary gout, hyperuricemia might result either from increased nucleic acid turn-over e.g. hematologic disorders, or from decreased renal excretion of uric acid induced by drugs or dietary factors. Also in a number of genetic disorders, such as glycogen storage disease, Down's syndrome

and psoriasis, hyperuricemia is a common feature^{2,1}.

The methods currently in use to assay uric acid in serum are based on either chemical or enzymatic oxidation to allantoin. The enzymatic procedure seems to be the method of choice because of its sensitivity, accuracy and specificity^{3,4}. Analytical techniques such as high performance liquid chromatography and isotachopheresis can be applied for the determination of various metabolites in biological fluids. Methods using HPLC have been reported for urate in serum⁵ and urine⁶. Isotachopheresis has been employed in the analysis of nucleotides in muscle extracts⁷ and urinary purines and pyrimidines, including uric acid⁸.

Unlike other available methods, such as the colorimetric⁹ and the enzymatic^{3,4} methods, the determination of uric acid by HPLC and isotachopheresis is much less hampered by interfering substances, such as drugs and biological metabolites. In contrast to HPLC, where generally the proteins have to be removed by an appropriate sample pretreatment, isotachopheresis requires no sample pretreatment. Moreover the ratio of free to protein urate can be determined conveniently using a simple ultrafiltration procedure.

6.1. EXPERIMENTAL

In this study the isotachopheretic coupled column system, Part 2 Chapter 3, was used. This system is of special interest for the analysis of biological samples. In such samples separands are often present in a relatively low concentration and the concentration of other solutes can differ by an order of magnitude. This is the case in serum, for example, where the chloride concentration can exceed the concentration of uric acid by a factor of up to 500. In such mixtures the analysis time, required to obtain sufficient information, is rather large because a high sample load must be applied. The coupled column system alleviates this problem. The system comprised a pre-separation capillary with an inner diameter of 0.8 mm and a final separation capillary with an inner diameter of 0.2 mm. The

driving current was taken from a Brandenburg, (Thornton Heath, UK) power supply and separated zones were detected using conductimetric and UV-detection systems¹⁰. Electrolyte systems and additional operational conditions are summarized in Table 6.1.

The enzymatic determinations of serum uric acid were performed in the laboratory of the Department of Neurology (University Hospital, Nijmegen) with an ABA 100 bichromatic analyzer (Abbot, UK). The determination of uric acid is based on the successive action of three purified enzymes which are added to the reaction mixture: uricase, catalase and aldehyde dehydrogenase⁴. The formation of NADPH from NADP⁺ in the latter reaction, measured at both 340 and 380 nm) is used for the quantification of uric acid.

TABLE 6.1
ELECTROLYTE SYSTEMS AND OPERATIONAL CONDITIONS

	preparation compartment	separation compartment	terminating compartment
Anion	Chloride	Chloride	MES
Concentration	0.01 M	0.01 M	0.005 M
Counter Const.	EACA	EACA	TRIS
pH	5.00	5.00	6.5
Additive	0.25% HEC	0.25% HEC	--
Driving current	250 μ A	20 μ A	

Serum was prepared from venous blood after clotting, 2h at room temperature, and centrifugation for 10 min at 1000 g at 4 °C. The samples were stored at - 20 °C until use. All chemicals used were of analytical grade or purified by conventional methods. Ultrafiltration CF 25 centriflow filters, nominal mol. wt. cut-off 25.000, were purchased from Amicon (Oosterhout, The Netherlands).

6.2. RESULTS AND DISCUSSION

Physiological uric acid serum concentrations normally range between 0.15 and 0.45 mM. The calibration line for uric acid in the given operational system proved to be

linear and had a response of 0.0474 nmole urate per sec. The identity of uric acid was confirmed in several ways. In Fig. 6.1 an experiment is shown which demonstrates that the uric acid zone is completely abolished by pre-incubation of the sample with purified uricase¹¹. Moreover injection of an additional amount of uric acid increased the zone-length of the urate zone, whereas its isotachophoretic mobility, as measured by the conductimetric step height, remained constant.

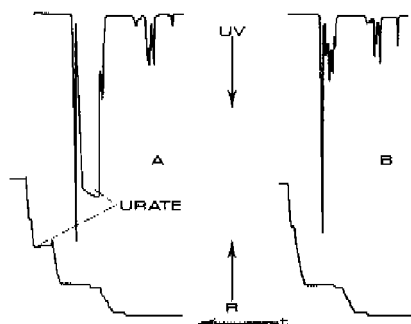


Fig. 6.1 Effect of incubation of serum with purified uricase.

A. Serum ultrafiltrate before incubation,

B. Serum ultrafiltrate after enzymatic incubation.

When standard solutions of uric acid were added to serum, extensively dialysed against 0.9% NaCl solution, the isotachophoretic analyses yielded recoveries of 99.0 - 100.5%. From this it can be concluded that the uric acid protein binding is broken during the isotachophoretic analysis. Some serum samples showed turbidity, as judged from visual inspection. Those samples were rapidly passed through a Millipore filter, Millex[®], 0.22 μ m. The recovery of uric acid was not affected by this procedure.

Serum samples from six healthy controls were assayed for uric acid using the isotachophoretic and the enzymatic procedure. The samples were used either directly or after ultrafiltration. The serum uric acid values obtained with the enzymatic and the isotachophoretic procedure showed

an acceptable correlation with a correlation coefficient of 0.980. The uric acid determinations in the ultrafiltered samples showed also an acceptable correlation, correlation coefficient 0.976, but the group mean of the enzymatic method was somewhat lower than that of the isotachophoretic method. The precision of both methods for a repeatedly tested sample was better than 2%. The isotachophoretic and the enzymatic procedures showed day-to-day variations of less than 2% and 6% respectively.

TABLE 6.2
ISOTACHOPHORETIC AND ENZYMATIC RESULTS FROM SIX CONTROLS

No	Isotachopheresis			Enzymatic		
	NF	UF	Bound	NF	UF	Bound
	μM	μM	%	μM	μM	%
1	374	329	12	390	303	22
2	392	282	28	383	283	26
3	294	224	24	292	233	20
4	483	415	14	483	400	17
5	361	298	17	375	317	15
6	463	385	17	498	365	27
mean	395	332	19	403	317	21

NF is non ultrafiltered, UF is ultrafiltered.

The recoveries were not affected by the use of the CF-25 ultra filter membranes; recoveries of standard solution using the ultrafiltration membrane were 99.4%. From the table 6.2 it follows that protein binding varies between twelve and twenty-eight percent. The physiological significance of urate binding to plasma protein binding is still disputed. Reversible interactions between urate and serum albumin, low-density-lipoprotein, β_2 -macroglobulins and α_1, α_2 globulins have been reported^{12,13}. Percentages of 20-40% of bound urate have been described under different conditions of temperature, ionic strength, buffers, etc.^{12,13,14}. Our values agree with these data. Reduced binding capacity of plasma proteins might lead to higher levels of free uric acid; in patients with gout

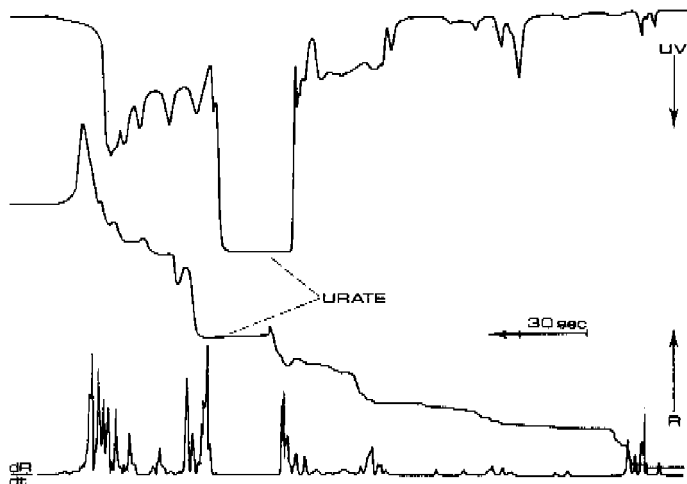


Fig. 6.2 Isotachopheretic separation of a hyperuricemic serum. R = increasing resistance, UV = UV transmission at 280 nm, t = time, $\frac{dR}{dt}$ = differential of the linear conductimetric trace.

such a decreased binding capacity has been reported¹⁵. It has also been shown that several drugs, such as salicylates, phenylbutazone and probenecid, reduce urate binding *in vitro*¹⁶. It should be stressed however, that all these studies, including our own were done under non-physiological conditions. Therefore, no conclusion can be drawn regarding the physiological significance, especially because some *in vivo* measurements have shown that at 37 °C the percentage of urate bound is small¹⁷.

TABLE 6.3

THE EFFECT OF HOMOGENTISIC ACID ON THE URIC ACID DETERMINATION

Addition	Isotachopheresis	Enzymatic
None	348 μ M	348 μ M
0.5 g/l homogentisic	348 μ M	364 μ M
5.0 g/l homogentisic	346 μ M	676 μ M

Several metabolites can interfere with the enzymatic method for the determination of uric acid in serum. An example is homogentisic acid, a compound which occurs in increased quantities in urine of patients with alkaptonuria, in inborn error of amino acid metabolism^{18,19}. It interferes with the enzymatic uric acid determination at 340 nm by giving lower values than those actually present. Even when unphysiologically high amounts of homogentisic acid were added to serum samples, no effect on the isotachopheretic determinations was seen. Increased levels however were found with the enzymatic procedure carried out with the bichromatic (340 and 380 nm) analyzed ABA-100. No attempts were done to elucidate this experimentally, but the differences might be attributed to the use of the bichromatic analyzer, in contrast to a monochromatic determination at 340 nm only⁴.

TABLE 6.4

SERUM URIC ACID CONCENTRATIONS IN PATIENTS RECEIVING VARIOUS DRUGS

Diagnosis	Medication	Uric Acid μM	
		Enzymatic	Isotachopheresis
Gout (male, age 63)	Zyloric	286	299
Rheumatoid arthritis with hyperuricemia (female, age 68)	Hygroton, Selokene, Penicillinamide, Indocid Seresta	620	647
Rheumatoid arthritis with hyperuricemia (female, age 44)	Baktrimel, Primitison, Torecon	356	366

Serum uric acid values in three initially hyperuricemic rheumatologic patients, who were treated with a number of drugs, were in close agreement when determined with both procedures. None of the drugs seemed to interfere with the uric acid determination both procedures.

6.3. CONCLUSIONS

The isotachophoretic procedure for the determination of uric acid in serum is quantitative, reliable and reproducible. In contrast to the general practice in HPLC there is no need for deproteinisation of the serum samples. Once the electrolyte system has been optimized for the isotachophoretic determination, analyses can be done with a low day-to-day variation. At present the isotachophoretic method is more accurate than the enzymatic method, although the latter is faster when automated.

REFERENCES

1. J.B. Wyngaarden and W.N. Kelly, in *The metabolic consequences of inherited disease*, New York, 1978, 916.
2. D. Newcombe, *Inherited Biochemical Disorders and uric acid metabolism*, Univers. Park Press, Baltimore, USA, 1975.
3. L. Liddle, J.E. Seegmiller and L. Laster, *J. Lab. Clin. Med.*, 54 (1959) 903.
4. R. Haeckel, *J. Clin. Chem. Biochem.*, 14 (1976) 101.
5. W. Saunwhite, L. Pachlan, D. Wenke and P. Kissinger, *Clin. Chem.*, 21 (1975) 1427.
6. J. Millner and A. Perkins, *Anal. Biochem.*, 88 (1979) 560.
7. D. Gower and R. Woledge, *Sci. Tools*, 24 (1977) 17.
8. A. Sahota, H. Simmonds and R. Payne, *J. Pharm. Methods*, 2 (1979) 303.
9. N. Kageyama, *Clin. Chim. Acta*, 31 (1971) 421.
10. F. Everaerts, J. Beckers and Th. Verheggen, *Isotachopheresis*, J. Chromatogr. Libr. Vol. 6, Elsevier, Amsterdam-Oxford-New York, 1976.
11. F. Oerlemans, Th. Verheggen, F. Mikkers, F. Everaerts and C. de Bruyn, *Adv. Exp. Med. Biol.*, 122 (1980).
12. J. Alvsaker, *Scan. J. Clin. Lab. Invest.*, 18 (1966) 227.
13. J. Alvsaker, *Scan. J. Clin. Lab. Invest.*, 17 (1965) 467.

14. P. Farrel, R. Popovich and A. Babb, *Biochem. Biophys. Acta*, 243 (1971) 49.
15. J. Klinenberg and I. Kippen, *J. Lab. Clin. Med.*, 75 (1970) 503.
16. R. Bluestone, I. Kippen, J. Klinenberg and M. Whitehouse, *J. Lab. Clin. Med.*, 76 (1970) 85.
17. A. Postlethwaite, R. Gutman and M. Kelley, *Metabolism*, 23 (1974) 771.
18. T. Verheggen, F. Mikkers, F. Everaerts, P. Oerlemans and Ch. de Bruyn, *J. Chromatogr.*, 182 (1980) 317.

Abbreviations of chemical substances

A3MP	adenosine 3'-monophosphate
A5MP	adenosine 5'-monophosphate
ATP	adenosine 5'-triphosphate
BALA	β -alanine
CREAT	creatinine
EACA	ϵ -aminocaproic acid
HEC	hydroxyethyl cellulose (Polysciences Inc; Warrington Pa, USA, Cat. no 5568)
HEPES	N-2-hydroxyethylpiperazine-N'-2-ethanesulfo- nic acid
HIST	L-histidine
GABA	γ -amino-n-butyric acid
G5MP	guanosine 5'-monophosphate
MES	2(N-morpholino)ethane sulfonic acid
MM	middle molecule
MOWIOL	polyvinylalcohol (N 8-88 Hoechst A.G., Frank- furt, GFR)
TRIS	tris(hydroxymethyl)aminomethane
U	Urea

Symbols

	linescript ↓ superscript ↓ subscript ↓	designation
A	o	ionic species, constituent
A	o	UV absorption
A	o	zone indicator
A	o	constituent indicator
a	o	constant
α	o	degree of dissociation
α	o	constant
B	o	ionic species, constituent

	linescript		
	↓	superscript	
		↓	subscript
B	o		zone indicator
B	o		constituent indicator
b	o		constant
β	o		constant
C	o		load capacity
C	o		ionic species, constituent
C	o		zone indicator
C	o		constituent indicator
c	o		constant
c	o		subspecies concentration (geq. cm^{-3})
\bar{c}	o		constituent concentration (mole. cm^{-3})
γ	o		constant
D	o		diffusion coefficient ($\text{cm}^2 \cdot \text{sec}^{-1}$)
d	o		diameter (cm)
Δl	o		sampling width (cm)
Δt	o		time-based zone length (sec)
δ	o		zone width (cm)
E	o		electric field strength (V. cm^{-1})
F	o		constant of Faraday (C. geq^{-1})
ϕ	o		sampling ratio
g	o		relative gain in time
H	o		high molecular weight region
H	o		height equivalent to a theoretical plate (cm)
HL	o		HL ratio
I	o		electric driving current (A)
I	o		ionic species, constituent
I	o		zone indicator
I	o		constituent indicator
i	o		constituent
i	o		constituent indicator
J	o		electric current density (A. cm^{-2})

	linescript		
	↓	superscript	
		↓	subscript
		↓	
J	o		ionic species, constituent
J	o		zone indicator
J		o	constituent indicator
j	o		constituent
j		o	constituent indicator
K	o		equilibrium constant
		o	zone indicator
k	o		constant
κ	o		specific conductance ($\Omega^{-1} \cdot \text{cm}^{-1}$)
L	o		column length (cm)
L	o		low molecular weight region
L	o		leading constituent
L		o	zone indicator
L		o	constituent indicator
ℓ	o		zone length
M		o	mixed zone indicator
MO		o	mixed zone indicator
m	o		ionic mobility ($\text{cm}^2 \cdot \text{V}^{-1} \cdot \text{sec}^{-1}$)
\bar{m}	o		effective mobility ($\text{cm}^2 \cdot \text{V}^{-1} \cdot \text{sec}^{-1}$)
N	o		number of theoretical plates
n	o		amount
n	o		sample load (mole)
n	o		subspecies
O	o		cross-sectional area (cm^2)
pH	o		pH
pI	o		isoelectric point
pK	o		negative logarithm of the pro- tolysis constant
Π	o		product function
Q	o		amount of electric charge (C)
R	o		Resolution
R	o		resistance (Ω)
r	o		relative mobility
\bar{r}	o		relative effective mobility

	linescript		
	↓	superscript	
		↓	subscript
ρ	o		relative leading concentration
S	o		separation number
S	o		separand
S	o	o	zone indicator
S	o	o	constituent indicator
Σ	o		summation
σ	o		standard deviation
T	o		transference number
T	o		terminating constituent
T	o	o	zone indicator
T	o	o	constituent indicator
t	o		time (sec)
t _{det}	o		time of detection (sec)
t _g	o		gain in time (sec)
t _{gr}	o		time-based centre of gravity
t _r	o		retention time (sec)
t _{res}	o		time of resolution (sec)
t _{stop}	o		time of detection (sec)
UV	o		Uv absorption
v	o		migration velocity (cm.sec ⁻¹)
x	o		place coordinate
x _{det}	o		length of detection (cm)
x _{max}	o		maximal migrated distance (cm)
x _{min}	o		minimal migrated distance (cm)
x _{res}	o		length of resolution (cm)
z	o		valency
w	o		Kohlrausch function
*	o		indicator sampling compartment
**	o		indicator terminator compartment

Summary

Electrophoresis can be used as a method for achieving separation of ionic solutes in solution and is based on the differential migration of the separands in an electric field. This thesis describes the theoretical, experimental and instrumental developments of zone electrophoresis and isotachophoresis in narrow bore tubes.

Electrophoresis inherently involves the local change of electrolyte constituent concentrations. This changing of concentrations is not an arbitrary process, but is a strongly regulated one, governed by the Kohlrausch regulating functions. This Kohlrausch concept has been applied to zone electrophoresis and isotachophoresis and allows a fundamental understanding of the capabilities of both analytical techniques.

In zone electrophoresis the effect of electrophoretic migration on the concentration distributions is evaluated, using a non-diffusional model. It follows that the sample constituents, that have an effective mobility larger than that of the carrier constituent, migrate with concentration distributions that are diffuse at the front and sharp at the rear of the zone. The reversed holds for sample constituents that have an effective mobility lower than that of the carrier constituent. As a result of the regulating functions no independent retention behaviour can exist in zone electrophoresis. In an experimental approach to high performance zone electrophoresis it is shown that non migrational dispersion can be well controlled by the use of narrow bore tubes. The measured concentration distributions conform with theory and their asymmetry can only be suppressed by the application of very small amounts of sample. High performance zone electrophoretic separations, using UV absorbance and conductimetric detection, are shown. The theoretical and practical limitations of zone electrophoresis are indicated.

The initial stage of zone electrophoresis is essentially not different from moving boundary electrophoresis or the separation process in isotachopheresis. The latter is elucidated using a transient-state model for monovalent weakly ionic constituents. The influence of operational parameters, such as pH, electric driving current, sample load and counter constituent, is described in terms of time of resolution, load capacity and current efficiency. Theoretically and experimentally it is shown that optimization procedures in isotachopheresis are governed by three rationales: the pH, the counter constituent and the electric driving current. For anionic separations a low pH of both the leading electrolyte and the sample will favour resolution, whereas for cationic separations a high pH will be preferable. The deleterious effects of extreme values of pH are discussed. The counter constituents should have a low mobility and the electric driving current should be maximized. Steady-state configurations, in which the sample constituents are not migrating in order of mobility, are shown and discussed.

The time-based zone length is in isotachopheresis directly related to the amount of sample. To avoid column-overloading only a limited sample load can be applied in conventional instruments. A new two-dimensional, fully automated, electrophoretic instrument is described, which allows the application of high sample loads, two dimensional separations and feasibility for micro-preparative applications.

Both the theoretical concepts and instrumental developments were applied to several biomedical research topics. In the search for uremic toxins, isotachopheresis was used for the determination of ionic solutes in the body fluids of patients with terminal chronic renal failure. It is shown that uremic patients form a rather heterogenic group and that hemodialysis removes only partially the accumulating metabolic products from the body fluids of patients with chronic renal failure. The existence of toxic molecules with intermediate molecular weight, the so-called middle molecules, which are supposed to accumulate in chronic renal failure, could not be substantiated with isotachopheresis, gas chro-

matography or high performance liquid chromatography. The middle molecular weight fractions, as obtained with gel chromatography, proved to contain numerous solutes of rather low molecular weight.

Isotachophoresis was successfully applied for the direct determination of the anticonvulsant drug valproate in serum and for the determination of uric acid in serum.

Samenvatting

Electroforese wordt veelal toegepast als analytische scheidingsmethodiek voor ionogene stoffen. Dit proefschrift beschrijft zowel de theoretische achtergronden als de instrumentele ontwikkelingen van zone electroforese en isotachoforese in capillaire kolommen.

Gedurende een electroforetisch proces treden, plaatselijk, veranderingen in de electrolyet concentratie(s) op. Dit proces verloopt niet willekeurig, maar zeer stringent gereguleerd, hetgeen beschreven kan worden met behulp van de zgn. Kohlrausch functies. Hierdoor kan een inzicht verkregen worden in de analytische mogelijkheden van zowel zone electroforese als isotachoforese.

Uitgaande van een zone electroforetisch model, waarin de invloed van diffusie verwaarloosd wordt, blijken asymmetrische concentratieverdelingen op te kunnen treden. Ionogene componenten, met een effectieve mobiliteit groter dan die van de drager, blijken een asymmetrische concentratieverdeling te hebben, die aan de voorkant diffuus is terwijl de achterkant scherp blijft. Mutatis mutandis geldt voor ionogene componenten met een kleinere effectieve mobiliteit dan die van de drager. Doordat het zone electroforetische proces zeer stringent gereguleerd verloopt, wordt het retentiegedrag van vrijwel iedere ionogene component beïnvloed door de aanwezigheid van andere. Dispersie kan in zone electroforese geminimaliseerd worden door deze techniek uit te voeren in capillaire kolommen. De experimenteel gemeten concentratieverdelingen bevestigen de juistheid van de theoretische berekeningen. De asymmetrie van de verdelingen kan slechts onderdrukt worden door het inbrengen van zeer geringe hoeveelheden monster. Zone electroforetische scheidingen, waarbij gebruik gemaakt wordt van zowel conductometrische als UV-absorptie detectie, tonen de praktische en theoretische beperkingen van deze techniek.

Het scheidingsproces van zone electroforese en isotachoforese verlopen beide volgens het bewegende grensvlak principe. Het scheidingsproces van isotachoforese wordt beschreven in een mathematisch model, dat toepasbaar is bij de analyse van eenwaardige zwakke elektrolieten. Uit de modelbeschouwingen volgt dat de optimalisering van een isotachoforetisch scheidingsproces beheerst wordt door de pH van de elektrolieten, de aard van het tegenion en de toegepaste stroomsterkte. De invloed van deze, experimenteel belangrijke, parameters komt tot uitdrukking in de resolutietijd, de beladingscapaciteit en het stroomrendement. De resolutietijd is omgekeerd evenredig met de elektrische stroomsterkte, zodat deze laatste gemaximaliseerd dient te worden. Bij scheidingen van anionen worden de optimale condities verkregen bij een lage pH van zowel loopelectrolyet als monster. In het geval van de scheiding van cationen verdient een hoge pH de voorkeur. De tegenionen dienen altijd een kleine mobiliteit te bezitten. Zowel theoretisch als experimenteel wordt aangetoond, dat de ionogene componenten van een monster zich bij isotachoforese niet altijd rangschikken in volgorde van effectieve mobiliteit.

De hoeveelheid ingebrachte stof is bij isotachoforese direct gerelateerd aan de zone-lengte. Teneinde grote hoeveelheden van een monster te kunnen analyseren werd een nieuw tweedimensionaal instrument ontwikkeld. De voordelen van dit volledig geautomatiseerde instrument ten opzichte van conventionele apparatuur worden beschreven.

Zowel de theoretische inzichten als de instrumentele ontwikkelingen werden toegepast op diverse onderwerpen uit het biomedisch gelieerd onderzoek. Isotachoforese blijkt geschikt te zijn voor de analyse van ionogene stoffen in de lichaamsvloeistoffen van chronische nierpatienten. Uit de isotachoforetische analyses blijkt dat nierpatienten, wat betreft de accumulerende stoffen, een inhomogene groep vormen. De stoffen, die in de lichaamsvloeistoffen van chronische nierpatienten accumuleren, worden slechts ten dele door hemodialyse verwijderd. De " middle molecule " hypothese kon niet bevestigd worden

met behulp van isotachoforese, gaschromatografie of vloeistofchromatografie.

Isotachoforese werd met succes gebruikt voor de directe bepaling van het geneesmiddel valproïnezuur in het serum van patienten met epilepsie. De resultaten werden vergeleken met die van een standaard gaschromatografische analysemethode. De isotachoforetische bepaling van urinezuur in serum bleek goed in overeenstemming te zijn met de resultaten van een enzymatische bepalingsmethodiek.

Author's publications on electrophoresis

- F. Mikkers, *Graduation report*, Eindhoven University of technology, Eindhoven (The Netherlands), 1974
Isotachophoresis of proteins and the development of double isotachophoretic systems for discontinuous electrophoresis.
- F. Everaerts, M. Geurts, F. Mikkers and Th. Verheggen, *J. Chromatogr.*, 119 (1976) 129.
Analytical isotachophoresis.
- Th. Verheggen, F. Mikkers and F. Everaerts, *J. Chromatogr.*, 132 (1977) 205
Isotachophoresis in narrow bore tubes. Influence of the diameter of the separation compartment.
- F. Everaerts, F. Mikkers and Th. Verheggen, *Sep. Pur. Methods*, 6 (1979) 287
Isotachophoresis.
- F. Mikkers, F. Everaerts and J. Peek, *J. Chromatogr.*, 168 (1979) 293
Isotachophoresis: the concept of resolution, load capacity and separation efficiency. part I. Theory.
- F. Mikkers, F. Everaerts and J. Peek, *J. Chromatogr.*, 168 (1979) 317
Isotachophoresis: The concept of resolution, load capacity and separation efficiency. part II. Experimental evaluation.
- F. Mikkers, S. Ringoir and R. de Smet, *J. Chromatogr.*, 162 (1979) 341
Analytical isotachophoresis of uremic blood samples.
- A. Schoots, F. Mikkers, C. Cramers and S. Ringoir, *J. Chromatogr.*, 164 (1979) 1
Profiling of uremic serum by high resolution gas chromatography electron impact, chemical ionization mass spectrometry.
- F. Mikkers, F. Everaerts and Th. Verheggen, *J. Chromatogr.*, 169 (1979) 1.
Concentration distribution in free zone electrophoresis.
- F. Mikkers, F. Everaerts and Th. Verheggen, *J. Chromatogr.*, 169 (1979) 12
High performance zone electrophoresis.
- F. Everaerts, Th. Verheggen and F. Mikkers, *J. Chromatogr.*, 169 (1979) 21
Determination of substances at low concentration in complex mixtures by isotachophoresis with column coupling.
- F. Mikkers, Th. Verheggen and S. Ringoir, *Prot. Biol. Fluids*, 27 (1979) 727
Isotachophoresis of uremic metabolites.

F. Everaerts, F. Mikkers and Th. Verheggen, *Prot. Biol. Fluids*, 27 (1979) 723.

A new construction for column coupling

Th. Verheggen, F. Mikkers, D. Kroonenberg and F. Everaerts, *Biochem. Biol. Appl. Isotachophoresis*, A. Adam (Ed), Elsevier, Amsterdam 1980, 41.

A new construction for column coupling in isotachophoresis.

F. Everaerts, F. Mikkers, *Biochem. Biol. Appl. Isotachophoresis*, A. Adam (Ed), Elsevier, Amsterdam 1980, 1.

Isotachophoresis. A general introduction.

F. Oerlemans, Th. Verheggen, F. Mikkers, F. Everaerts and Ch. de Bruyn, *Biochem. Biol. Appl. Isotachophoresis*, A. Adam (Ed), Elsevier, Amsterdam 1980, 63.

Isotachophoretic separation of serum purines and pyrimidines.

F. Mikkers and S. Ringoir, *Biochem. Biol. Appl. Isotachophoresis*, A. Adam (Ed), Elsevier, Amsterdam 1980, 127.

Isotachophoresis of uremic metabolites.

F. Oerlemans, Th. Verheggen, F. Mikkers, F. Everaerts and Ch. de Bruyn, *Purine Metab. in man III, part B*, A. Rapado (Ed), Plenum Publ. Co., 1980, 429.

Analysis of serum purines and pyrimidines by isotachophoresis.

F. Oerlemans, Th. Verheggen, F. Mikkers, F. Everaerts and Ch. de Bruyn, *Purine Metab. in man III, part B*, A. Rapado (Ed), Plenum Publ. Co., 1980, 435.

Determination of uric acid in serum: Comparison of a standard enzymatic method and isotachophoresis.

F. Everaerts, F. Mikkers and Th. Verheggen, *Electrophoresis '79*, B. Radola (Ed), 1980, 255.

Enhancement of load capacity in isotachophoresis.

F. Mikkers, Th. Verheggen, F. Everaerts, J. Hulsman and C. Meyers, *J. Chromatogr.*, 182 (1980) 496.

Direct determination of valproate in serum by isotachophoresis. Comparison with a gas chromatographic method.

Th. Verheggen, F. Mikkers, F. Everaerts, F. Oerlemans and Ch. de Bruyn, *J. Chromatogr.*, 182 (1980) 317.

Determination of uric acid in serum using isotachophoresis.

F. Everaerts, J. Vacik, F. Mikkers and Th. Verheggen, *Chromatography*, E. Heftmann, Elsevier, Amsterdam, in press.

Electrophoresis.

F. Mikkers, A. Schoots, S. Ringoir and R. de Smet, in prep. *Investigations on gelchromatographic middle molecular weight fractions by isotachophoresis, gas chromatography and high performance liquid chromatography.*

F. Mikkers, F. Everaerts and Th. Verheggen, *Isotachophoresis 1980*, Elsevier, Amsterdam, in press.

Theoretical and practical aspects of isotachophoresis.

Th. Verheggen, F. Mikkers and F. Everaerts, *Isotachophoresis 1980*, Elsevier, Amsterdam, in press.

Column coupling and automation of isotachophoresis.

Ch. de Bruyn, F. Oerlemans, F. Mikkers, Th. Verheggen and F. Everaerts, *Isotachophoresis 1980*, Elsevier, Amsterdam in press.

The use of isotachophoresis for the study of inborn errors of purine metabolism in man.

K. Uyttendaele, F. Soetewy, H. Peeters, F. Everaerts, F. Mikkers and Th. Verheggen, *Isotachophoresis 1980*, Elsevier, Amsterdam, in press.

Magnetic fields and free flow double layer electrophoresis systems.

F. Mikkers, W. van Gils and W. Roos, *Isotachophoresis 1980*, Elsevier, Amsterdam, in press.

Sodium tripolyphosphate and sodium pyrophosphate for industrial use. Separation and quantification by isotachophoresis.

Acknowledgements

Though my memory plays me tricks, I am indebted to'

Frans, Theo, Jo, Ton, Evert, Gonnje, Piet, Ad, John, Arie, John, René, Harrie, Jan, Jan, Jos, Theo, Jetse, Math, Tum, Ad, Cees, Maarten, Niels, Peter, Gerard, Huub, Paul, Nico, Ad, José, Martin, Carel, Jack, Piet, Jan, Jan, Leo, Wim, Henk, Gius, Bèrt, Chris, Hans, Huib, Dick, Joop, Peter, Marjon, Tineke, Jaap, Wim, Eugène, Trudy, Arjenne, Frank, Chris, Cees, Hans, Jo, Wim, Jack, Severin, Rita, Archer, Ann, Anne, Paul, Huub, Jiri, Petr, Dusan, Josef, Mirko, Jiri, Eric, Ton, Herman, Jaap, Jaap, Frans, Frans, Ad, Ad and last but not least to Bea, as she typed the manuscript.

From all I learned something, from a few a learned a lot, only few may have the opportunity to teach me something in future.

Curriculum vitae

The author was born on november 16th 1947 in Valkenswaard, the Netherlands. After graduating from the "Gymnasium Augustinianum " he started his studies in chemical engineering at the Eindhoven University of Technology (Eindhoven, the Netherlands) in 1967. The graduation work was carried out at the Laboratory of Instrumental Analysis and he obtained his "ir" degree, cum laude, in 1974.

After a short but sharp career in military service, he rejoined the research group on electrophoresis at the Eindhoven University of Technology. In november 1976 the author started the research described in this thesis.

Mane de Tabula

STELLINGEN

1. De veronderstelling dat bij zone electroforese de beste scheidingscondities verkregen worden wanneer het verschil van de beweeglijkheden van de te scheiden monstercomponenten maximaal is *, lijkt aantrekkelijk maar is onjuist.
* R. Consden, A.H. Gordon en A.J.P. Martin, *Biochem. J.*, 40 (1946) 33.
2. Het scheidingsproces bij isotachoforese wordt bepaald door de condities in de mengzone(s). Getabelleerde isotachoforetische beweeglijkheden * geven slechts een indicatie of monstercomponenten al dan niet met behulp van isotachoforese gescheiden kunnen worden.
* F.M. Everaerts, J.L. Beckers en Th.P.E.M. Verheggen, *Isotachophoresis, J. Chromatogr. Libr.*, Vol. 6, Elsevier, Amsterdam-Oxford-New York, 1976.
3. Wanneer bij de verklaring van de kathodische drift bij iso-electrische focusering geen rekening gehouden wordt met het feit dat de absolute waarden van de electroforetische beweeglijkheden van protonen en hydroxylionen niet gelijk zijn *, dient deze verklaring in twijfel te worden getrokken.
* N.Y. Nguyen en A. Crambach, *Anal. Biochem.*, 82 (1977) 226.
B.A. der Lan en A. Crambach, *Electrophoresis*, 1 (1980) 23.
4. Chromatofocusering, als scheidingsmethodiek voor eiwitten, verdient meer aandacht.
L.A.AE. Sluyterman en O. Elgersma, *J.Chromatogr.*, 150 (1978) 17.
L.A.AE. Sluyterman en J. Wijdenes, *J.Chromatogr.*, 150 (1978) 31.
5. Het piekoppervlak uit een chromatogram, verkregen bij de gelchromatografische scheiding van uremisch serum, kan niet als kwantitatieve maat * dienen voor het voor-

komen van de zogenaamde "middle molecules" in uremisch serum.

* L. Migone, P. Dall'Aglio en C. Buzo, Clin. Nephrol., 3 (1975) 82.

J. Bergström en P. Fürst, Clin. Nephrol., 5 (1976) 144.

J.L. Funck Brentano, G.F. Cueille en N.K. Man, Kidney Internat., 13 (1978) 31.

6. De uitspraak van Bergström * dat de zogenaamde "middle molecules" bestaan en dat deze biologisch actief zijn, moet als triviaal beschouwd worden.

* J. Bergström, P. Fürst en L. Zimmerman, Clin. Nephrol., 11 (1979) 229.

7. Bij het gebruik van electro-osmotische vloeistofpompen dient men er rekening mee te houden, dat electro-osmose beïnvloed wordt door de aanwezigheid van oppervlakte-actieve stoffen.

* V. Pretorius, B.J. Hopkins en J.D. Schieke, J. Chromatogr., 99 (1974) 23.

Z. Ryslavy, P. Bocek, M. Deml en J. Janak, J. Chromatogr., 147 (1978) 446.

8. De toename van het gebruik van mini- en microcomputers in het analytische laboratorium en de daaraan blijkbaar inherente verslaving, zal leiden tot een vermindering van de inzet op het eigen, d.w.z. analytische, vakgebied.

9. De opmerking van Schumacher * dat het proefschrift van Everaerts ** uitmunt door het niet refereren naar Schumacher *** is niet juist.

* E. Schumacher en P. Ryser, Chimia, 30 (1976) 105.

** F.M. Everaerts, Proefschrift, Technische Hogeschool Eindhoven, 1968.

*** E. Schumacher en T. Studer, Helv. Chim. Acta, 18 (1964) 957.